

2004

Life Without GPR7, the Neuropeptide W1 Receptor: Regulation of Energy Homeostasis by GPR7 and its Endogenous Neuropeptide Ligands

Makoto Ishii

Follow this and additional works at: http://digitalcommons.rockefeller.edu/student_theses_and_dissertations

 Part of the [Life Sciences Commons](#)

Recommended Citation

Ishii, Makoto, "Life Without GPR7, the Neuropeptide W1 Receptor: Regulation of Energy Homeostasis by GPR7 and its Endogenous Neuropeptide Ligands" (2004). *Student Theses and Dissertations*. Paper 35.



**Life without GPR7, the Neuropeptide W_1 Receptor:
Regulation of Energy Homeostasis by GPR7 and
Its Endogenous Neuropeptide Ligands**

A thesis presented to the faculty of
the Rockefeller University
in partial fulfillment of the requirements for
the degree of Doctor of Philosophy

by

Makoto Ishii

The Rockefeller University

New York, New York

September 2004

Dedication

This thesis is dedicated to my parents and my brother. Their support has carried me throughout the years, and I continue to lean on them even now.

Acknowledgements

As with almost all endeavors of this nature, this was not a solo project. Jeff Friedman, my mentor and *sensei*, has been instrumental in shaping me as a researcher. He has given me a great deal of flexibility, more so than perhaps I deserve, to pursue any and all of my research interests while still keeping me grounded enough to see the big important pictures. I admire his intellect, his drive for finding new and exciting avenues in science, and his appreciation of the finer foods in life. I look forward to continuing to work together in the future and to sharing many more bottles of fine wine and sake together. It has also been an honor and a pleasure to work with the members of my thesis committee: Bob Darnell, Nat Heintz, and Brad Lowell, who have given me useful suggestions and comments throughout the process.

The lab is often a community, a family if you will, sometimes simply by name association, but at other times, as is in this case, a lively source of friendship, inspiration, motivation, and amusement. A major incentive to join the lab back in the summer of 2000 was the students in the lab at the time. My three *senpais* taught me a lot about the inner workings of life as a graduate student when I first joined the lab. Alex was always quick to give me advice and guidance on issues beyond the many protocols he taught me. Jason, the most senior student, also embraced me with his wise musings over a drink or two at the faculty club. A strong testament to my respect for his scientific skills and my friendship to him, Paul was the first one that I would seek for advice on setting up any experiment or if I wanted some amusing and friendly distractions to get me through the day. I would also like to thank him for providing me with the leptin treated samples used in this thesis. I also had one *kohai* during my time. Lisa Moy was a talented and motivated high school student, who assisted me for two summers doing anything that I asked of her no matter how mundane or messy. I hope that I was able to inspire her to look at a possible career in the life sciences. Many other lab members, past and

present, have also been extremely helpful during my time in the lab. First of all, thank you to Hong Fei for starting this project and for the initial work leading to the generation of the GPR7-/- mice. I would like to thank Silvia Novelli for being a close friend who has taught me the many ways of enjoying life the Italian way; Esra Asilmaz for showing me the difference between a Greek Cypriot and a Turkish one (which one was the “good” side again?); Dvora Shmulewitz for making sure that I always had someone that I could talk sports to; Javier Torrens for inspiring me to try to one day become as compassionate of a physician as he is; Zhu Chen for showing me the many artful ways of sighing; Jeremy Segal for all the deeds not fit for print in a public forum, although all of those deeds were done out in the public; Shirly Pinto for being a great conference buddy of mine, any conference I attend without her will be certainly lesser because of it; Jeff Defalco and Mike Eisenstein for many memorable nights in and out of the lab; Susan Korres and Alena Pithart for being helpful with any task or request that I have asked throughout my time here. I have also been blessed with wonderful bay-mates throughout my years in the lab, who have somehow managed to tolerate me, from the early days of Xiaoli Cai and Aaron Roseberry to the second incarnation with Florence “Super Flo” Massiera and Wolfgang “the original Herr Doktor” Liedtke to the final incarnation of Ratnendra “Anaconda 2 is worth seeing” Sharma and Hironobu “I need regulation height tennis nets” Hiyoshi. I would also like to thank the many new faces of the lab this past year or two. You have all been wonderful to me during my years in the lab.

Scientific research often branches outside of the immediate family extending outwards in many wonderful different directions. Masashi Yanagisawa, my old mentor when I was a young naïve college student, has continued to be a strong influence on me. Perhaps by accident or perhaps by some design, my thesis project led me to walk in the same paths as his. Many members of his laboratory have been very helpful to me throughout this time. Hirokazu Tanaka has always been quick to reply back to all of my questions about the ligands even when the data was very preliminary. Toshiyuki Motoike has been very helpful in providing me with all of my needs

during my short stay in Dallas. I am also grateful to him for allowing me to present the *Xenopus* melanophore data in this thesis. Michihiro Mieda is a talented and inspiring scientist who I learned everything I know about making sleep recordings in mice. I would also like to thank Shelley Dixon, Michele Kelly, Takeshi Sakurai, and everyone else that is and was a part of the Yanagisawa lab in Dallas and in Japan for all of their various assistances along the way. At Rockefeller University, I would like to thank the Gene Targeting Facility for their help with the ES cell work; Bruce McEwen and Russ Romeo for their help in setting up the behavior work; Fred Quimby and Tim Scase for the initial gross necropsy and histology analysis of the GPR7^{-/-} mice; Fred Quimby and his staff at LARC for being very helpful in accommodating all of my requests concerning animal work. Both the MD-PhD Program Office and the Rockefeller University Dean's Office have given me tremendous support and are definitely a significant factor in making student life here as pleasurable as an experience as possible. Without them, being a student here would not be the same. I would also like to gratefully acknowledge the generous funding from the NIH MSTP to the Tri-Institutional Cornell, Rockefeller, Sloan-Kettering MD-PhD program.

I would like to thank all of my friends and family for all of their support throughout the years. To all my fellow MD-PhD classmates and friends, Marianna Ruzinova, Sukhvinder Sahota, Svetlana Gorokhova, Genevieve Yuen, Abhinav Seth, and to everyone else too numerous to mention, thank you for your friendship. I would like to especially thank two very close friends, who started this same journey as I did in the summer of 1998, Howard Moskowitz and Richard Wang. We shared walls. We exchanged research ideas. We have bought dinners, although I am still waiting for one from Rich, which undoubtedly will come soon in a spectacular fashion. The trip, although only partially completed, was made much more enjoyable knowing that there were others traveling the same road. Finally, my warmest thank you to my family for always giving me the support I need to continue moving onwards.

Table of Contents

Dedication	<i>iii</i>
Acknowledgements	<i>iv-vi</i>
Table of Contents	<i>vii-ix</i>
Directory of Figures	<i>x-xii</i>
Directory of Tables	<i>xiii</i>
List of Publications	<i>xiv</i>

Abstract	1-2
-----------------	------------

Chapter 1	3-41	Introduction
	3	Obesity: Medical epidemic and its prevalence in society
	7	Early studies in obesity from lesions to mouse mutants
	11	Leptin: The start of the molecular genetics era of obesity
	14	Leptin receptor and the neural circuit of energy homeostasis
	20	Candidate obesity genes: Genetic versus pharmacological evidence
	24	Candidate gene search in the ventral medial nuclei of the hypothalamus
	32	GPR7 ligands – Neuropeptide B and Neuropeptide W
	41	Specific Aims

Chapter 2 42-64 Materials and Methods

Chapter 3 65-109 Results

65	Gene targeting strategy
66	Generation of GPR7 ^{-/-} mice
67	Effect of GPR7 disruption on body weight and composition
72	Metabolic defects: Food intake, metabolic rate, and locomotor activity
74	Plasma values in GPR7 ^{-/-} mice
76	Fasting-induced feeding response in GPR7 ^{-/-} mice
77	Glucoprivic feeding in GPR7 ^{-/-} mice – 2-deoxy-D-glucose
79	Hypothalamic neuropeptide levels in GPR7 ^{-/-} mice
81	Body weights and metabolic activity of ob/ob GPR7 ^{-/-} and Ay/a GPR7 ^{-/-} mice
84	Ligand activity and binding data to mouse GPR7
85	Tissue distribution of GPR7 and its ligands, NPB and NPW
89	Effects of feeding and metabolic states on the regulation of NPB, NPW, and GPR7
95	Behavioral analysis of GPR7 ^{-/-} mice
96	Sleep recordings – Investigating the potential role of GPR7 in sleep homeostasis
100	Circadian rhythm in GPR7 ^{-/-} mice
102	Anxiety of GPR7 ^{-/-} mice – Open field and elevated plus maze

108 Depression in GPR7-/- mice – Forced swim test

Chapter 4 110 **Discussion**

References 125

List of Figures

Figure 1	4	Obesity trend among US adults from 1991 to 2002
Figure 2	8	Rats with hypothalamic lesions
Figure 3	14	Leptin and its signaling pathway
Figure 4	15	Leptin receptor isoforms and receptor mutations in rodents
Figure 5	23	Genetic and pharmacological models of the hypothalamic pathways that regulate energy homeostasis
Figure 6	28	GTG causes obesity in mice and down-regulates hypothalamic GPR7 expression
Figure 7	29-30	Amino acid sequence alignments of GPR7 and GPR8
Figure 8	31	GPR7 mRNA distribution patterns in rat brain by <i>in situ</i> hybridization
Figure 9	33	Amino acid sequences of NPB and NPW
Figure 10	34	<i>In vitro</i> pharmacology of NPB and NPW
Figure 11	37	<i>In situ</i> hybridization of NPB and NPW mRNA on mouse brain sections
Figure 12	39	<i>In vitro</i> pharmacological effects of ICV injected NPB on food intake
Figure 13	66	Gene targeting strategy and confirmation of <i>GPR7</i> deletion
Figure 14	68	Body weight curves of male and female GPR7 mice
Figure 15	69	Gross necropsy of representative 52 week old male GPR7 mice
Figure 16	70	Body composition analysis of GPR7 mice

Figure 17	71	Increased fat acclimation in tissues and hepatic steatosis in older male GPR7 ^{-/-} mice
Figure 18	73	Food intake of adult male GPR7 ^{-/-} mice
Figure 19	73	Resting metabolic rate for adult GPR7 mice
Figure 20	74	Locomotor activity for adult GPR7 mice
Figure 21	75	Linear relationship between plasma leptin levels and body fat percentage in male GPR7 mice
Figure 22	76	Feeding response of adult male GPR7 mice after a 24 hour fast
Figure 23	78-79	Response to glucoprivation by 2-deoxy-D-glucose in male GPR7
Figure 24	80	Hypothalamic neuropeptide expression levels in 24 week old male GPR7 mice
Figure 25	81	Hypothalamic neuropeptide expression levels in 52 week old male GPR7 mice
Figure 26	82-83	Body weight curve for double knockout mice
Figure 27	83	Metabolic and locomotor activity of adult Ay/a GPR7 mice
Figure 28	85	Xenopus melanophore assay for ligand binding to mouse GPR7
Figure 29	87	Tissue distribution of GPR7, NPB, and NPW in mice
Figure 30	88	Hypothalamic NPB and NPW levels in adult GPR7 mice
Figure 31	90	Effects of 48 hour fasting and thirsting on hypothalamic NPB, NPW, and GPR7 gene expression levels
Figure 32	92	Change in body weight in adult male C57BL/6J mice after a 48 hour fast
Figure 33	92	Hypothalamic expression levels after a 48 hour fast

Figure 34	93	Stomach NPB and NPW expression levels after a 48 hour fast
Figure 35	94-95	Chronic subcutaneous leptin administration's effect on stomach NPB and NPW expression levels
Figure 36	98	Examples of EEG and EMG recordings of different sleep-wake states in adult mice
Figure 37	99	Time spent in each sleep state for adult male GPR7 mice by EEG recordings
Figure 38	101	Representative running wheel behavior actogram double plots for adult female GPR7 mice
Figure 39	104	Open field analysis of adult male GPR7 using an automated system
Figure 40	105	Open field analysis of adult female GPR7 using an automated system
Figure 41	106	Open field analysis of adult male GPR7 using a manual test apparatus
Figure 42	107	Elevated plus maze test on adult GPR7 mice
Figure 43	109	Forced swim test for depression analysis in adult male GPR7-/- mice
Figure 44	115	Regulation of energy homeostasis by proposed neuropeptide B and neuropeptide W signaling pathways from peripheral tissues to the central nervous system

List of Tables

Table 1	19	List of known factors regulating feeding behavior when centrally administered by ICV injections
Table 2	70	Percent body composition of male GPR7 mice
Table 3	75	Plasma values of 24 week and 52 week old GPR7 male and female mice
Table 4	99	Summary of baseline sleep recordings for male GPR7 ^{+/+} and GPR7 ^{-/-} mice
Table 5	100	tau (period) calculations for adult female GPR7 mice
Table 6	124	Summary of the known functional roles for GPR7 and its ligands (NPB and NPW)

Publications

Ishii, M., Fei, H., and Friedman, J. M. (2003). Targeted disruption of GPR7, the endogenous receptor for neuropeptides B and W, leads to metabolic defects and adult-onset obesity. *Proc. Natl. Acad. Sci. USA*, 100: 10540-10545.

Presentations

Ishii, M., Fei, H., and Friedman, J. M. “Metabolic Defects in Mice with a Targeted Disruption of a Hypothalamic Orphan G Protein-Coupled Receptor.” Keystone Symposia, Obesity: New Insights into Pathogenesis and Treatment, invited plenary talk and poster presentation, January 2003.

Ishii, M., Fei, H., and Friedman, J. M. “Metabolic Defects in Mice with a Targeted Disruption of a Hypothalamic Orphan G Protein-Coupled Receptor.” Society for Neuroscience 33rd Annual Meeting, poster presentation, November 2003

Ishii, M., Fei, H., and Friedman J. M. “The Role of GPR7 and its Endogenous Ligands NPB and NPW in Maintaining Energy Homeostasis and Other Physiological Functions.” Days of Molecular Medicine 2004: Integrative Physiology and Human Disease – Neurohormonal and Metabolic Pathways, invited oral presentation, March 2004.

Abstract

Classic lesion experiments from the 1940s have established the hypothalamus as playing an essential role in controlling energy homeostasis. Gold-thioglucose (GTG) induces lesions in the ventromedial nucleus of the hypothalamus (VMH) resulting in hyperphagia and obesity. To identify genes involved in the hypothalamic regulation of energy homeostasis, we employed a screen to search for genes that were dysregulated in GTG induced obese mice. In this screen, *GPR7*, the endogenous G protein-coupled receptor (GPCR) for the recently identified ligands neuropeptide B (NPB) and neuropeptide W (NPW), was found to be specifically down-regulated after GTG treatment.

The physiological role of *GPR7* was investigated by generating and analyzing mice with targeted disruption of *GPR7*. Male *GPR7*^{-/-} mice developed an adult-onset obesity syndrome that progressively worsened with age and was greatly exacerbated when animals were fed a high fat diet. Male *GPR7*^{-/-} mice were hyperphagic and had decreased energy expenditure and locomotor activity. These mice also had an abnormal response to fasting-induced feeding but not to glucoprivic-induced feeding suggesting that central response to glucose was normal. The hypothalamic RNA levels of

neuropeptide Y and proopiomelanocortin in male GPR7^{-/-} mice were more indicative of a lean state than a leptin deficient “starved” state. Furthermore, ob/ob GPR7^{-/-} and Ay/a GPR7^{-/-} double mutant male mice were heavier than normal ob/ob or Ay/a male mice suggesting that the obesity of GPR7^{-/-} mice is independent of leptin and melanocortin signaling. Interestingly, female GPR7^{-/-} mice did not show any significant weight increase or associated metabolic defects. Additionally, other behavioral paradigms were investigated in the GPR7^{-/-} mice. Baseline sleep-wake cycles, circadian rhythms, anxiety-like behaviors, and depression-like behaviors were all normal in GPR7^{-/-} mice. Therefore, these behavioral disorders can not account for the feeding disorders seen in GPR7^{-/-} mice.

In aggregate, these data strongly suggest a physiological role for GPR7 and its endogenous ligands, NPB and NPW, as a catabolic signaling pathway independent of leptin and melanocortin pathways. Future studies of GPR7, its ligands, and the GPR7 knockout mice will further elucidate the full range of physiological functions of this novel signaling pathway.

Chapter 1: Introduction

Obesity: Medical epidemic and its prevalence in society

While a comprehensive coverage of obesity as a medical epidemic in modern society is beyond the scope of this introduction, a brief overview of the topic is presented below. Obesity has become a major health problem since the late 20th century in the Western world. From 1980 to 1994, there was an increase in the prevalence of obesity (defined as a Body Mass Index or BMI over 30, where BMI is the weight of a person in kilograms divided by the height of a person in meters squared) from 14.5% to 22.5% in the US population (Taubes, 1998). This increasing obesity trend continues to rise as in 1999-2000 the-age adjusted prevalence of obesity was 30.5% with extreme obesity (BMI > 40) significantly increasing from 2.8% to 4.7% (Flegal et al., 2002). The latest Center for Disease Control (CDC) data strongly shows the increased prevalence of obesity throughout the US adult population from 1991 to 2002 (Figure 1). Furthermore, the obesity epidemic is spreading to other parts of the world such as Brazil and Africa that typically had low to practically no incidence of obesity (Kopelman, 2000).

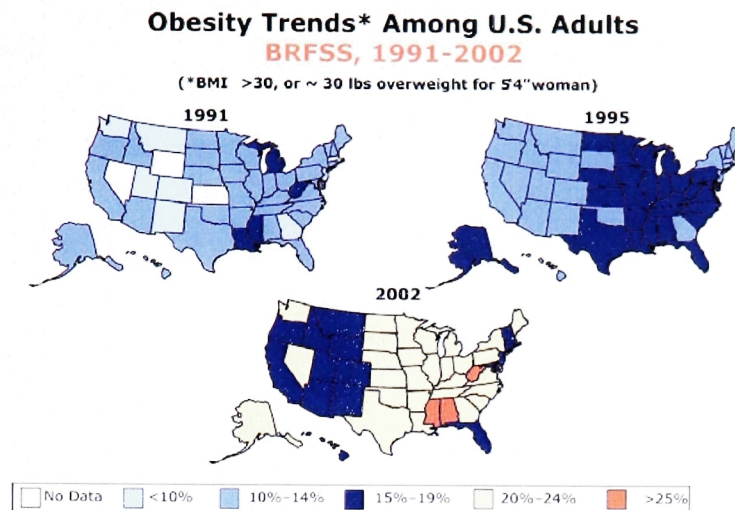


Figure 1) Obesity trends among US adults from 1991 to 2002. Source: CDC's Behavioral Risk Factor Surveillance System (BRFSS).

The medical cost associated with obesity and obesity-related conditions is rapidly rising. An increase in body weight (BMI) has been found to be associated with an increase risk factor for type 2 diabetes, hypertension, coronary heart disease, gallstones, dyslipidemia, osteoarthritis, sleep apnea, and some form of cancers (Kopelman, 2000). Obesity-related health issues are now approaching smoking as the number one cause of preventable mortality in the modern US society with 400,000 deaths compared to 435,000 deaths from smoking in the year 2000 (Mokdad et al., 2004). With the overwhelming clinical, epidemiological, and basic science data supporting obesity as a major health epidemic, the study of the causes of obesity and the development of safe and effective treatments for obesity are essential.

The causes of obesity have long been debated. While the popular press and companies promoting diet programs have advocated the need to lose weight by going on special diets or by simply eating less, often shifting the blame to an individual's lack-of-willpower, the problem is not so easily solved. Almost all dieters who lose weight rebound back to their original weight within months of starting their diet (Wadden, 1993). Gastric bypass or bariatric surgery has been found to be the most effective therapeutic option for morbidly obese patient with nearly all patients losing a significant amount of their body weight immediately after surgery (Fisher and Schauer, 2002). However, rebound weight gain is still a large concern even among these patients. The surgery often forces the patients to change their normal eating habits as it may actually reduce physical hunger as well as decreasing the stomach's physical capacity to hold food; however, binge-eating or grazing is still seen postoperatively especially among patients that had eating disorders prior to surgery (Kalarchian et al., 2002; Saunders, 2001; Saunders, 2004). Patients who have some rebounding in weight after bariatric surgery may constitute a significant portion of obese patients undergoing this operation.

Hence, long-term body weight is physiologically regulated by some rigid homeostatic controller despite even radical attempts to physically or psychologically change it. This idea has led to the "set point" theory. In this theory, energy stores and

therefore body weight are maintained at constant levels by long-term regulators that coordinates food intake and energy expenditure (Friedman and Leibel, 1992). Energy homeostasis can be considered as the balance between energy intake by food intake and energy expenditure by metabolic activity including physical activity and thermogenesis. This balance between energy intake and energy expenditure may be similar and related to other physiological homeostatic controls such as osmotic and thermal homeostasis.

Strong evidences for genetics playing a key role in regulating one's body weight are emerging from several studies. The classical "gold standard" for determining whether there is a genetic contribution of a known disease or disorder is by studying monozygotic twins who have been reared together, sharing the same environment, to those who have been reared apart, living in different environmental conditions. Studies have found that obesity, especially in terms of BMI, is strongly influenced by genetic factors for both monozygotic twins raised together or apart (Allison et al., 1996; Stunkard et al., 1986; Stunkard et al., 1990). Body mass index and body weight had similar heritability as height at 20 years of age and after a 25 year follow-up study on the same group (Stunkard et al., 1986). Furthermore, the heritability of obesity can be considered higher than many diseases and disorders commonly thought as having a genetic component including schizophrenia, breast cancer, and heart disease. Therefore, the

elucidation of the key genetic and physiological factors affecting energy homeostasis is essential for developing new therapeutic medical interventions.

Early studies in obesity from lesions to mouse mutants

Classic lesion experiments have placed specific regions of the brain namely the hypothalamus as playing a major role in maintaining energy homeostasis. As early as the 1940s and 1950s, it was known that lesions in certain hypothalamic nuclei caused either a rapid hyperphagia and obesity or hypophagia and starvation (Anand and Brobeck, 1951; Hetherington and Ranson, 1940). Hypothalamic lesions were induced in rodents either by electrical or chemical means such as by gold thioglucose (GTG) (Figure 2). Anatomical studies of these animals have shown that the region leading to hyperphagia after lesions was in the ventromedial nucleus of the hypothalamus (VMH). These nuclei were named the “satiety center.” The lateral hypothalamic (LH) nucleus corresponded to the region leading to hypophagia after lesions and was called the “feeding center.” However, the actual nature of the hypothalamic control of food intake was unclear.

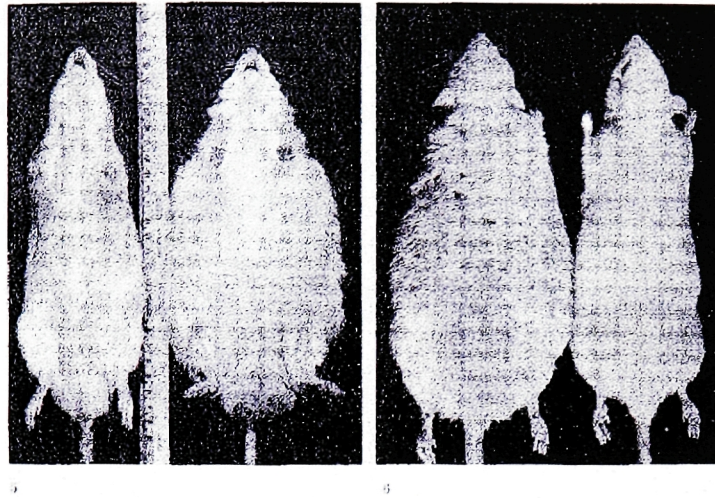


Fig. 5 Obese rat Rb-25, photographed at autopsy, 8 months after operation, and Rb-28, its control. Hypothalamic lesions were made at the age of 1½ months.

Fig. 6 Obese rat Rb-11, photographed at autopsy, 4½ months after operation, and Rb-13, the control. Hypothalamic lesions were made at the age of 7 weeks. Note the sparse hair and scabbled, scaly skin of the fat rat.

Figure 2) Rats with hypothalamic lesions as originally described by Hetherington and Ranson in their classic 1940 paper (Hetherington and Ranson, 1940).

Several theories on the maintenance of energy homeostasis emerged in the late 1940s and 1950s. The first proposed by Brobeck stated that feeding behavior was controlled by the normal body temperature of an animal (Brobeck, 1947). According to this thermostatic theory, “animals eat to keep warm, and stop eating to prevent hyperthermia.” The lipostatic theory was proposed by Kennedy to rebuke the thermostat theory (Kennedy, 1953). In this theory, a “chemical limiting factor” existed from the fat depot that would act as a signal to the hypothalamus. Therefore, this circulating metabolite from fat would be the primary controller of energy homeostasis and not body temperature. A third theory was soon proposed afterwards. Mayer hypothesized that

glucose was the main determinant of energy homeostasis (Mayer, 1953; Mayer, 1955; Mayer and Thomas, 1967). This glucostatic theory was based on the fact that glucose is the primary energy source for the CNS. Glucose stores in liver and skeletal muscle get depleted over the course of a day and was therefore theorized to be the main regulatory element in energy homeostasis (Mayer and Thomas, 1967).

In 1950, perhaps the strongest evidence for genetics controlling in part obesity was seen in Jackson Laboratories (Coleman, 1978; Ingalls et al., 1950). The *ob/ob* obese mice were first discovered as a spontaneous autosomal recessive mutation in a noninbred stock. The *ob* mutation was then placed on a C57BL/6J strain and resulted in marked obesity, hyperphagia, transient hyperglycemia, and elevated plasma insulin. This mutation also resulted in infertility in both sexes. In 1966, another mutation called diabetes (*db/db*) was discovered in a C57BL/KsJ mouse line (Hummel et al., 1966). Obesity, hyperphagia, and severe diabetes with marked hyperglycemia characterized the *db/db* mutants. While having a similar phenotype with the C57BL/6J *ob/ob* mice, the C57BL/Ks *db/db* mice's diabetes were more severe and had a less pronounced obesity. Another allele *db^{2J}/db^{2J}* arose in the Jackson Laboratories in the C57BL/6J strain. The phenotype of the *db^{2J}/db^{2J}* mutants and the C57BL/6J *ob/ob* were similar suggesting that they had mutations in the same pathway. When the *db^{2J}/db^{2J}* allele was placed on a

C57BL/Ks background, it showed the same phenotype as the original db/db mice. This established that db^{2J}/db^{2J} and the original db/db were the same genetic mutation and that the *ob* and *db* genes were probably two different genes affecting the same pathway.

Parabiosis experiments, where the circulatory system of two animals are joined, between ob/ob, db/db, and normal mice by Coleman and his colleagues suggested that the normal mice produced a satiety factor that was either lacking in the ob/ob mice or unresponsive in the db/db mice (Coleman and Hummel, 1969; Coleman, 1973). In these experiments, either ob/ob or db/db mice had their circulatory system joined with that of a normal mouse. For the case of the db/db parabiosis, the normal parabiont stopped eating, rapidly lost weight, became hypoglycemic and eventually died of starvation, while the db/db mice maintained its hyperphagia and obesity. However, the normal parabiont to an ob/ob mouse did not develop these effects and instead decreased the weight and food intake of the ob/ob mouse. Furthermore, when an ob/ob mouse was parabiosed to a db/db mouse, the initially hyperphagic and obese ob/ob mouse rapidly lost weight and eventually died of starvation. It was concluded that a defect in the ob/ob mice resulted in the lack of production of a satiety factor, while a defect in the db/db mice led to it being unable to respond to this satiety factor and perhaps producing an abnormally high level of the factor. Coleman suggested that a primary hypothalamic defect could be

involved in these mice in particular with the db/db mice. This hypothesis was bolstered by an earlier parabiosis study where VMH lesioned rats were parabiosed to normal rats and had a similar result to that of Coleman's parabiosis experiments with db/db mice (Hervey, 1959). The normal parabiont rat soon stopped eating and died of starvation, while the VMH lesioned rat maintained its hyperphagia and obesity. These db/db mice may have a defective "satiety center" analogous to those rodents with VMH lesions. The *ob* gene could be producing the factor that was first proposed in the lipostat theory by Kennedy in 1953. From the 1950s to early 1990s, most of the studies on obesity and energy homeostasis revolved around these themes using lesion experiments, the spontaneously arising obese mouse mutants, and animal physiology studies.

Leptin: The start of the molecular genetics era of obesity

In 1994, a basic molecular understanding of the energy homeostasis circuit was solved in part by the positional cloning of the *ob* gene leading to the discovery of leptin (Zhang et al., 1994). The immediate impact of this discovery is unquestionable. The identification of leptin and the subsequent cloning of the leptin receptor gene, *db*, by expression and positional cloning of the db/db mutant mice confirmed Kennedy's lipostat theory and Coleman's theories based on his earlier parabiosis experiments (Chen et al.,

1996; Chua et al., 1996; Lee et al., 1996; Tartaglia et al., 1995). *ob/ob* mutant mice had a single point mutation that changed an arginine to a stop codon leading to the absence of leptin production. Leptin is a 16 kDa circulating (167 amino acid) cytokine hormone produced primarily in the adipocytes but also in lower amounts in other tissues such as the placenta, skeletal muscle, and gastric epithelium (Bado et al., 1998; Masuzaki et al., 1997; Wang et al., 1998). The initial and subsequent data have shown that leptin is the afferent signal in a negative-feedback loop regulating the size of adipose tissue mass (Friedman and Halaas, 1998). Levels of leptin correlate with adipose tissue mass and decrease after a fall in body weight in both humans and mice (Maffei et al., 1995; McGregor et al., 1996).

Leptin has many pleiotropic effects when administered at pharmacological doses (Figure 3) (Ahima and Flier, 2000; Friedman and Halaas, 1998). When leptin is administered to *ob/ob* mice, most of the abnormalities seen in the *ob/ob* mice are corrected (Campfield et al., 1995; Halaas et al., 1995; Pelleymounter et al., 1995). The *ob/ob* mice decrease its food intake and increase its energy expenditure. Diabetes, infertility, fatty liver, and hypothermia are all reversed after leptin treatment (Ahima et al., 1996; Chehab et al., 1996; Halaas et al., 1997; Pelleymounter et al., 1995). The phenotypic abnormalities displayed by the *ob/ob* mice are similar to many of those seen

in starved animals. Therefore, decreased leptin might be signaling starvation in animals (Ahima et al., 1996). Injections into wildtype mice also lead to hypophagia and adipose tissue loss (Halaas et al., 1997; Halaas et al., 1995). However, the weight loss is strictly in adipose tissue and can not be caused solely by the decrease in food intake (Levin et al., 1996). Therefore, leptin must have a vital role in other complex metabolic pathways such as lipid metabolism. Leptin may also be playing a physiological role in regulating the onset of puberty. Female mice treated with leptin develop puberty faster and have a generally accelerated onset of reproductive cycle and capacity (Ahima et al., 1997; Chehab et al., 1997).

The main action of leptin is thought to occur in the central nervous system (CNS). Initial pharmacological studies with leptin showed that very low doses given as intracerebroventricular (ICV) injections (3ng/hour or 200 fmoles/hour) had the same effects as those of 100 to 1000 times higher doses given peripherally (Campfield et al., 1995; Halaas et al., 1997). This suggested that the leptin receptor might be located in the CNS, possibly in the same regions as seen in the classic lesion studies of the 1940s and 1950s. However, it remained possible that leptin might also directly affect adipose tissue, liver, and other peripheral organs in light of leptin's multi-faceted role.

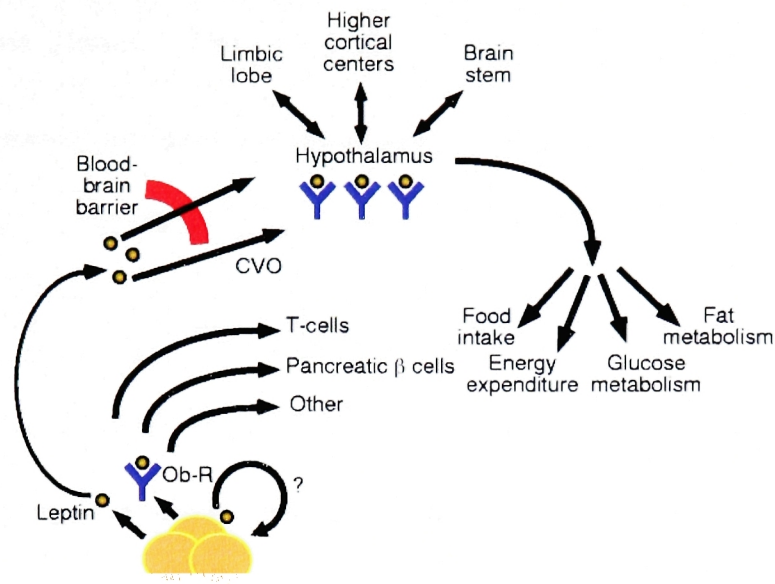


Figure 3) Leptin is an adipocyte derived hormone that is part of an afferent loop that regulates energy homeostasis and other physiological systems (Friedman and Halaas, 1998). The main site of action is believed to be the hypothalamus through the circumventricular organ (CVO); however, there remains the possibility that leptin may have direct actions on peripheral tissues such as T-cells as well.

Leptin receptor and the neural circuit of energy homeostasis

Expression cloning identified a receptor (Ob-R) with high affinity for leptin from mouse choroid plexus (Tartaglia et al., 1995). Positional cloning of the various db/db mutant mice and the fatty rat further validated that this was the endogenous receptor for leptin (Chen et al., 1996; Chua et al., 1996; Lee et al., 1996). Ob-R has at least five alternatively spliced isoforms Ob-R (a-e) and is a member of the class I cytokine receptor family, most closely related with IL-6 receptor, glycoprotein 130, leukemia inhibitory factor, and granulocyte-colony stimulating factor (Figure 4)

(Friedman and Halaas, 1998). All the isoforms of Ob-R have identical long extracellular domain for ligand binding but differ in the C-terminus. All isoforms of the leptin receptor except Ob-Re have a membrane spanning region. Ob-Rb, the long isoform, has a long cytoplasmic tail with consensus Jak-Stat binding motifs with three tyrosines that function as phosphorylation targets for SH-2 domain proteins. Other signaling pathways may also be involved as activation of Ob-Rb and possibly Ob-Ra can promote Jak-dependent, STAT-independent pathways such as MAP kinases.

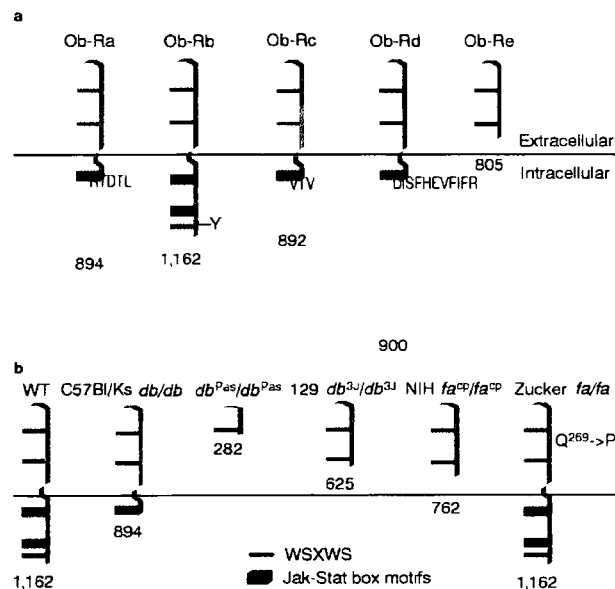


Figure 4) Leptin receptor isoforms and receptor mutations in rodents (Friedman and Halaas, 1998). A) The five known isoforms of the leptin receptor. There are possibly others. B) Ob-R mutations in rodent modes of obesity.

The various *db/db* mutations lead to a defect in all the isoforms of Ob-R except

C57BL/Ks db/db. The C57BL/Ks db/db mutant was found to have a premature stop codon leading to a defective Ob-Rb isoform while the other isoforms remained intact (Chen et al., 1996; Lee et al., 1996). Since the phenotype of C57BL/Ks db/db mice is indistinguishable from other strains of db/db mice, which have complete inactivity of all isoforms of Ob-R, Ob-Rb was considered the main signaling receptor critical for leptin function. The physiological roles that other Ob-R isoforms might have are presently unknown. Ob-Ra has a short tail that is missing many of the putative signaling domains possessed by Ob-Rb, but it can mediate signal transduction *in vitro* (Bjorbaek et al., 1997). Some researchers believe that short isoforms of the leptin receptor such as Ob-Ra might be involved in leptin transport into the CNS (Hileman et al., 2002; Uotani et al., 1999). Ob-Re, on the other hand, has been suggested to be a secreted soluble receptor that binds to leptin in the plasma (Lee et al., 1996; Liu et al., 1997).

While Ob-R is expressed in almost all known tissues, the hypothalamus has particularly high expression levels of Ob-Rb (Fei et al., 1997; Mercer et al., 1996; Tartaglia et al., 1995). This data with the pharmacological evidence suggest that leptin's main site of action may be in the hypothalamic area classically thought to regulate energy homeostasis. *In situ* hybridization studies have shown high Ob-Rb expression in the arcuate nucleus, dorsomedial hypothalamus (DMH), VMH, paraventricular nucleus

(PVN), and lateral hypothalamus (LH) (Elmqvist et al., 1998; Fei et al., 1997). Stat3 activation is seen after injection of leptin in the hypothalamus of all mice possessing an active Ob-Rb (Vaisse et al., 1996). Fos expression in the hypothalamus is also induced by peripheral leptin injections (Elias et al., 2000). Leptin signaling through Ob-R is negatively regulated by SHP-2, a phosphatase that decreases JAK2 phosphorylation, and SOCS-3 (Bjorbaek et al., 1998; Carpenter et al., 1998; Li and Friedman, 1999; Myers, 2004). The localization of leptin receptor in the hypothalamus, the pharmacological data showing a higher efficacy in ICV injections versus peripheral injections, and the activation of known signaling molecules in the hypothalamus strongly point to the hypothalamus as the main site of leptin's action. Furthermore, a brain specific deletion of the leptin receptor using the cre-lox system in mice has led to an identical, at least in regards to energy homeostasis, phenocopy to the db/db mutation (Cohen et al., 2001).

After the cloning of leptin and its receptor, a rapidly growing list of neurotransmitters, neuropeptides, and hormones and their receptors have been found to be involved in the hypothalamic regulation of energy homeostasis (Table 1) (Salton et al., 2000). While other peripheral signals such as insulin may have a role, leptin appears to be a central factor in the neural circuit in energy homeostasis (Schwartz et al., 2000). A broad overview of the known signaling pathways has leptin, synthesized in the adipose

tissue, acting on neurons in the arcuate nucleus with stimulation also of the VMH and dorsomedial nucleus. As mentioned above, lesions of the arcuate and VMH lead to obesity, while LH causes leanness. The arcuate neurons express Ob-R and either NPY/AgRP or POMC/CART coexpressing neurons (Cheung et al., 1997; Hahn et al., 1998; Kristensen et al., 1998). NPY is a potent anabolic/orexigenic molecule, while POMC expresses α -MSH, a strong catabolic/anorectic peptide affecting the melanocortin signaling pathway (Clark et al., 1984; Poggioli et al., 1986). AgRP is an endogenous orexigenic peptide inhibitor of melanocortin signaling (Ollmann et al., 1997). CART is a relatively recently identified anorectic peptide hormone regulated by leptin (Kristensen et al., 1998). From the arcuate nucleus, the signal is transmitted to other various hypothalamic nuclei, most notably the lateral hypothalamus (LH) and paraventricular nucleus (PVN). The paraventricular nuclei contain both NPY receptors and melanocortin receptors. In the PVN, stimulation of the melanocortin receptors by α -MSH results in a catabolic effect, while inhibition of the melanocortin receptors by AgRP results in an anabolic effect. The activation of NPY receptors in the PVN acts as an anabolic signal. With this dual regulation of energy homeostasis, the PVN may act as the integratory nuclei for the hypothalamic energy homeostasis pathway. In the LH, there are also melanocortin receptors and NPY receptors. The LH contains at least two

Table 1: List of some of the known factors (neurotransmitters and peptides) regulating feeding behavior when centrally administered by ICV injections. Leptin might regulate some or all of these signals. Nearly all known receptors in this pathway are GPCRs.

Stimulatory / Anabolic	Inhibitory / Catabolic
Neuropeptide Y (NPY)	α -Melanocyte-stimulating hormone (α -MSH)
Melanin-concentrating hormone (MCH)	Cocaine-amphetamine-related transcript (CART)
Galanin	Cholecystokinin (CCK)
Orexin a and b	Corticotropin-releasing factor (CRF)
Peptide YY	Glucagon-like peptide 1 (GLP-1)
Norepinephrine (α 2 receptor)	Galanin-like peptide (GALP)
Agouti-related protein (AgRP)	Bombesin
Ghrelin	Urocortin
Opioids	Serotonin
	Dopamine
	Histamine
	Neurotensin
	Amylin
	Calcitonin-gene related peptide (CGRP)
	Prolactin-releasing peptide (PrRP)
	Adrenomedullin
	Pituitary adenylate-cyclase activating polypeptide (PACAP)
	Interleukin-1 β
	Insulin
	Norepinephrine (β receptor)

neuronal cell populations involved in energy homeostasis, the melanin-concentrating hormone (MCH) containing neurons and the orexin containing neurons (Qu et al., 1996; Sakurai et al., 1998). Release of either peptide causes a stimulation of feeding response in rodents. This complex neural circuit is only beginning to be unfolded as more hormones, neurotransmitters, and peptides are implicated in this pathway at an

astounding pace.

Candidate obesity genes: Genetic versus pharmacological evidences

While at pharmacological doses several molecules have been found to stimulate or inhibit food intake and generally regulate aspects of energy homeostasis, it is not known whether this correlates to an actual endogenous physiological function. It may simply be due to some pharmacological “side-effect.” For finding an obesity drug, this may be sufficient. However, if one wants to find the true physiological pathway of energy homeostasis, this is insufficient. To try to delineate between a pharmacological role and a physiological role of these signaling molecules, knockout and transgenic mice of many of these molecules and their receptors have been made. Surprisingly, several of these transgenic and knockout animals show a different or no obvious or striking feeding-related phenotype. These includes NPY, AgRP, CRF, CCK, GLP-1, and ghrelin (Erickson et al., 1996a; Kopin et al., 1999; Muglia et al., 1995; Qian et al., 2002; Scrocchi et al., 2000; Sun et al., 2003). The initial lack of a phenotype in energy metabolism can be due to several reasons. These molecules may have redundant roles with other similar signaling mechanism, or there may be compensatory changes with a loss of one of these factors. One could expect that since energy homeostasis is vital to

life there could be several redundant mechanisms in the event that one of them fails. In a related manner, these signaling factors may only be essential under certain conditions such as during fasting or chronic stress that were not tested in the initial characterization of these transgenic and knockout mice.

Another approach to the analysis of these potential signaling molecules would be to state that any effects seen in energy homeostasis were purely pharmacological or secondary to their “true” physiological role. This might be the case with orexin. Orexin was initially identified as a neuropeptide that when centrally administered to rats caused a hyperphagic response (Sakurai et al., 1998). While orexin appears to still play a role in energy homeostasis, it may have a stronger role in vigilance and wakefulness as indicated by the narcoleptic phenotypes of the orexin knockout mice and the naturally occurring orexin receptor 2 mutant dogs (Chemelli et al., 1999; Lin et al., 1999). Likewise, CRF may pharmacologically be considered an anorectic peptide, but its main role may be more closely related to controlling stress and anxiety through stimulating glucocorticoid release (Muglia et al., 1995). Neither CRF nor its receptor knockout mice displayed a striking obesity phenotype (Bale et al., 2000; Kishimoto et al., 2000; Muglia et al., 1995; Smith et al., 1998).

While some studies have failed to find a large effect from monogenic manipulations in mice, knockout and transgenic studies have been “successful” in showing a physiological role in many other molecules including the melanocortin receptors, POMC, MCH, and serotonin receptors (Huszar et al., 1997; Nonogaki et al., 1998; Shimada et al., 1998; Yaswen et al., 1999). All of these mice showed a phenotype as expected from earlier pharmacological studies. Final validation for some of these factors has come from the identification of monogenic obesity syndromes in morbidly obese human patients (Farooqi and O’Rahilly, 2004).

Additional gene targeting and transgenic studies might also help to identify physiological roles for each newly identified gene such as with Cidea and bombesin receptor subtype 3 (Ohki-Hamazaki et al., 1997; Zhou et al., 2003). The immediate mechanism leading to the obesity phenotype for these animals is often unknown. Many genes that were initially not directly linked to obesity have been found to give rise to an obese animal when manipulated or knocked-out such as with syndecan-3, a cell surface heparan sulfate proteoglycan (Reizes et al., 2001). A relatively recent genetic and a pharmacological model of the neural circuit modulating energy homeostasis are shown below (Figure 5A and B). The picture of the neural circuit of energy homeostasis is a complex and rapidly changing one.

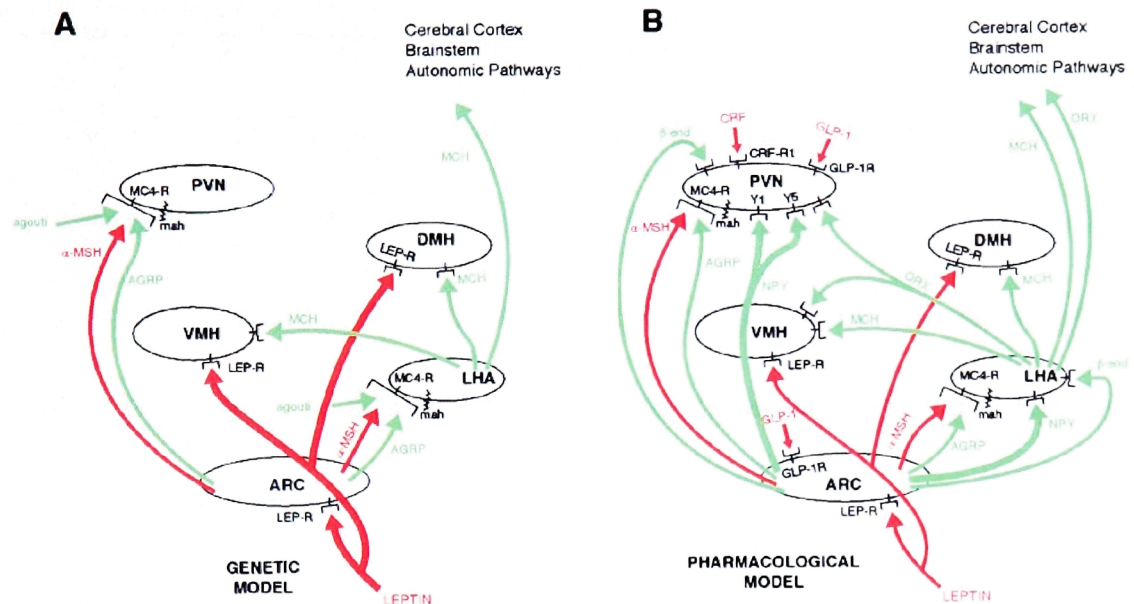


Figure 5: Models, One Based on Genetic and the Other on Pharmacological Data, of the Hypothalamic Pathways that Regulate Energy Balance (Salton et al., 2000). Two models are presented, one consistent with genetic (A) and the other with pharmacological (B) data. The caliber of the arrows is proportionate to the impact that the anorexigenic (dark/red) or orexigenic (light/green) pathways have on feeding and/or metabolism. Pathways that appear to have a lesser impact on energy metabolism have been left out for the sake of simplicity. The melanocortin, MCH, and leptin pathways have been implicated by genetic and pharmacological studies as being critical regulators of energy homeostasis and so are depicted in both panels. Major contributions of NPY, orexin, -endorphin, CRF, and GLP-1 to the control of energy balance are not supported by genetic analyses, and so these pathways are shown only in (B). Abbreviations: AGRP, agouti-related peptide; -MSH, -melanocyte-stimulating hormone; ARC, arcuate nucleus; -end, -endorphin; CRF, corticotropin-releasing factor; CRF-R1, CRF receptor 1; DMH, dorsomedial hypothalamus; GLP-1, glucagon-like peptide 1; GLP-1R, GLP-1 receptor; Lep-R, leptin receptor; LHA, lateral hypothalamic area; mah, mahogany; MC4-R, melanocortin 4 receptor; MCH, melanin-concentrating hormone; NPY, neuropeptide Y; ORX, orexin/hypocretin; PVN, paraventricular nucleus; VMH, ventromedial hypothalamus; Y1, NPY receptor 1; Y5, NPY receptor 5.

It must be noted that besides central regulation of energy homeostasis, a large body of work, too numerous to detail here, is currently being conducted on peripheral mechanisms involved in energy homeostasis. These include the study of genes involved in diabetes/glucose metabolism, adipogenesis, thermogenesis, and lipid metabolism (Havel, 2004; Lowell and Bachman, 2003; Nandi et al., 2004; Rangwala and Lazar, 2000). Of course, many, if not all, of these peripheral modulators of energy homeostasis are also closely intertwined with the central neural circuit.

Obesity research has advanced remarkably from the original theories postulated in the 1950s to the cloning of leptin and the numerous other candidate obesity genes. However, these recent advances have only left us with more questions as we try to understand this complex pathway and identify new targets in order to develop better therapeutics for perhaps the worst medical epidemic of our current time.

Candidate gene search in the ventral medial nuclei of the hypothalamus

We were interested in identifying new genes that are involved in the energy homeostatic pathway. The current literature suggested that the hypothalamus plays a key role. Therefore, a screen for hypothalamic genes regulating and regulated by the energy homeostatic pathway was developed. Gold thioglucose (GTG) was chosen to

chemically ablate these neurons. Genes in the neurons affected by GTG treatment were hypothesized to play a possible catabolic role in energy homeostasis.

GTG is composed of a gold moiety attached covalently to glucose (Debons et al., 1977). During an initial toxicological study when rodents were injected interperitoneally (i.p.) with GTG, the rodents subsequently became hyperphagic and morbidly obese (Brecher and Waxler, 1949). Sectioning of the mouse brain treated with GTG found distinct and reproducible damage primarily in the VMH (Marshall et al., 1955). It was hypothesized that the glucose molecule was essential for the lesions caused by GTG. Chemicals similar to gold thiolglucose such as gold thiolgalactose and gold thiosorbitol failed to induce any lesions in the VMH (Mayer and Marshall, 1956). The effects of GTG could also be inhibited by prior treatment with sodium thioglucose or 2-deoxy-D-glucose, neither of which damage the VMH but are glucose analogues (Likuski et al., 1967). Furthermore inhibitors of glucose transport such as phlorizin have been shown to block the effects of GTG (Debons et al., 1974). Finally, diabetic mice are protected from the effects of GTG until they are treated with insulin, which appears to restore the sensitivity of neurons to both glucose and GTG (Debons et al., 1969; Debons et al., 1968). As the VMH has been found to be rich in glucose-receptive neurons, it was hypothesized that GTG caused lesions primarily in these

glucose-responsive neurons of the VMH.

The VMH plays a key role in energy homeostasis. According to the “dual center” hypothesis mentioned briefly above, the VMH serves as a “satiety center” while the lateral hypothalamus serves as a “feeding center.” This hypothesis arose from lesion studies such as those done with GTG. Electrolytic lesions of the VMH and the nearby arcuate nucleus caused a profound hyperphagia and obesity. Therefore, these hypothalamic nuclei were thought to control feeding impulses in a negative/catabolic manner. Additionally, glucose is known to activate VMH neurons, while it inhibits LH neurons (Oomura, 1983). Following the glucostatic theory proposed by Mayer, VMH has been classified as having glucose-receptive neurons that are activated when blood glucose levels are high leading to suppression of food intake. However, the role of the VMH and the hypothalamus has proven to be much more complex. While other hypothalamic nuclei involved in the energy homeostatic pathway have begun to be well characterized at a molecular level, the VMH has remained strangely devoid of any new findings. Strikingly, there have been no neuropeptides or neurotransmitters localized in the VMH that have shown strong and conclusive evidence for a role in energy homeostasis. The VMH does contain several receptors and thus may serve as a “receptive” center.

A former post-doctoral fellow in the laboratory, Hong Fei, conducted a search for hypothalamic genes involved in energy homeostasis. Fei used GTG to induce obesity in mice (Fei et al., 1997). Subtraction hybridization followed by a ribonuclease protection assay (RPA) was used to identify genes that may have been differentially regulated between GTG treated and wildtype mice. She found one clone whose RNA expression was down-regulated after GTG treatment and identified it as a putative orphan G-protein-coupled receptor (GPCR) (Figure 6). The gene was orthologous to a previously published human orphan GPCR, *GPR7* (Figure 7a) (O'Dowd et al., 1995). *In situ* hybridization by Fei and from published works from others have established *GPR7* to be in key hypothalamic nuclei and in other regions of the brain (Figure 8, data not shown) (Lee et al., 1999; O'Dowd et al., 1995). Specifically, in rodent brains, the gene has high expression levels in the following regions: hippocampus, hypothalamus, and midbrain. In the hypothalamus, *GPR7* expression was found in the arcuate nucleus, ventromedial nucleus, paraventricular nucleus, and suprachiasmatic nucleus. All of the above hypothalamic nuclei are believed to be involved in regulating energy homeostasis.

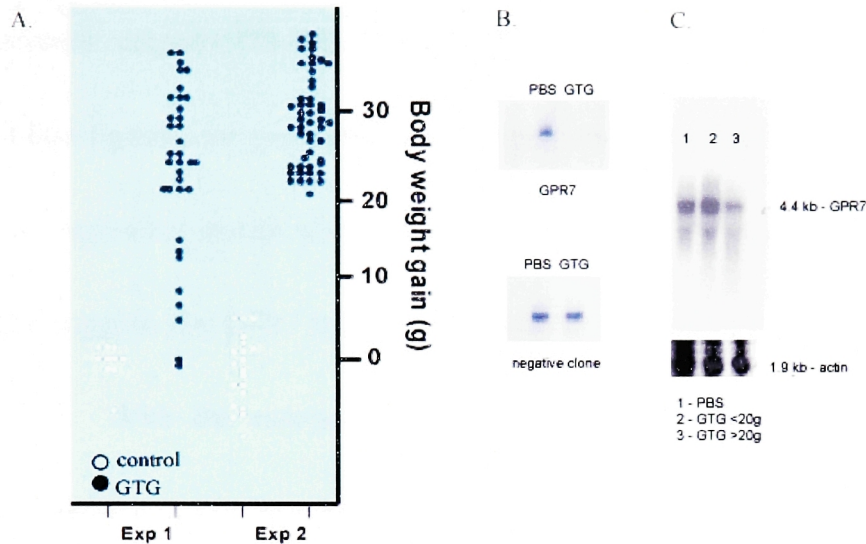


Figure 6) GTG causes obesity in mice and down-regulates hypothalamic GPR7 expression. A) Body weight gain in female CBA/J wildtype mice 4 weeks after a single i.p. injection of 2mg/g body weight GTG (control – empty circles; GTG – filled circles). B) RNase Protection Assay on hypothalamic RNA after PBS and GTG injection. C) Northern blot analysis of hypothalamic RNA after treatment with GTG. Lane 1 – PBS Control, Lane 2 – GTG injection with a body weight gain of less than 20g (failure to gain obesity), Lane 3 – GTG injection with a body weight gain greater than 20g (successful weight gain after GTG injection).

GPR7, an intronless orphan GPCR, has some sequence similarities to other GPCRs. The same group that had initially identified *GPR7* also cloned another related GPCR, *GPR8*, by degenerate PCR in humans, rabbits, and monkeys but could not be isolated in rats or mice (O'Dowd et al., 1995). Furthermore, an analysis of published mouse genome sequence has revealed that *GPR8* in mice, at least, appears to be a pseudogene (data not shown). *GPR8* has 64% identical amino acids with *GPR7* (Figure 7a, b). *GPR7* and *GPR8* have the highest sequence similarities with the opioid receptors

and somatostatin receptors (30-40% amino acid similarity). However, neither opioid and opioid-like ligands nor somatostatin have been shown to bind the receptor in a heterologous expression system with high affinity (O'Dowd et al., 1995; Tanaka et al., 2003). This suggests that GPR7 is not an opioid receptor and has a different non-opioid peptide ligand. With the endogenous ligand still unknown at this point and the receptor's expression in key hypothalamic nuclei, GPR7 knockout mice were generated in order to elucidate the role of the receptor *in vivo*.

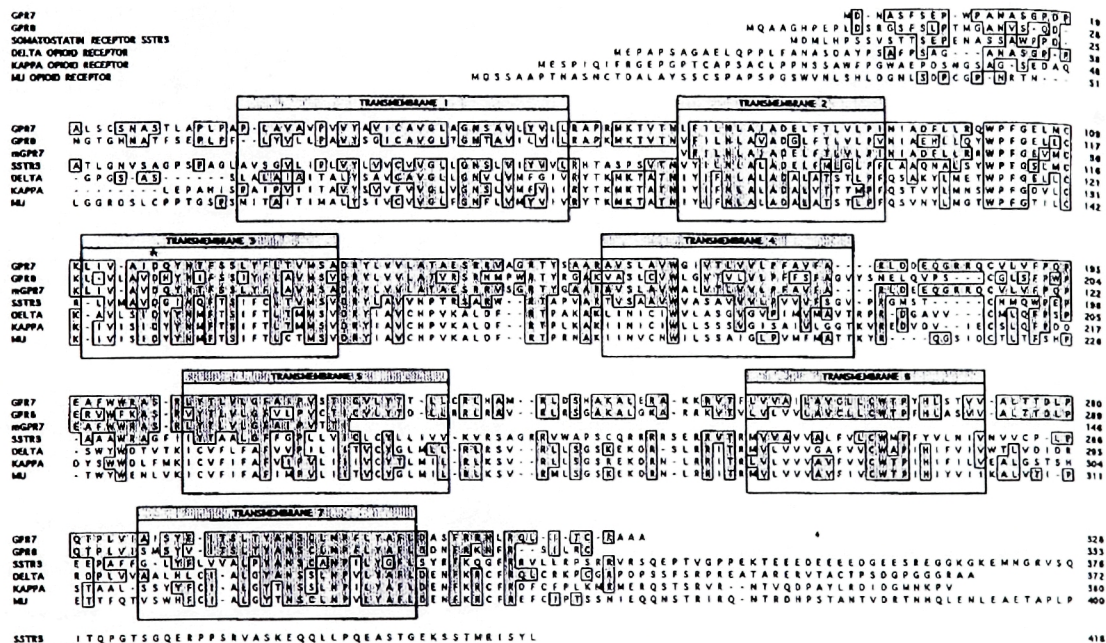


Figure 7A) Amino acid sequence alignment of GPR7 and related receptors (O'Dowd et al., 1995). All are from human sequences except for partial mouse GPR7 sequence (mGPR7). Identical amino acids are shaded. Transmembrane regions are boxed. (-) gaps were introduced to maximize alignment among the sequences.

		Transmembrane 2		Transmembrane 3			
GPR7		E L F T L V L P I N I A D F L L R Q W P F G E L M C K		L I V A I D Q Y N T F S S L Y F L T V M S A		D R Y L V V L A T A E	60
FLGPR7						Y L V V L A T A E	9
TSGPR7						Y L V V L A T A E	9
RabGPR7						Y L V V L A T A E	9
MusGPR7		E L F T L V L P I N I A D F L L R R W P F G E V M C K		L I V A V D Q Y N T F S S L Y F L A V M S A		D R Y L V V L A T A E	60
		Transmembrane 4					
GPR7		S R R V A G R T Y S A A R A V S L A V W Q I V T L V V L P F A V F A		R L D D E Q G R R Q C V L V F P Q P E A F W W R A S			120
FLGPR7		S R P V A G R T Y G A A R A V S L Q V W G S V T L V V L P F A V F A		Q L D D E Q G R R Q C V L V F P Q P E A F W W R A S			69
TSGPR7		S R P V A G R T Y G A A R A V S L A V W A L V T V V L P F A V F A		R L D D E Q G R R Q C V L V F P Q P E A F W W R A S			69
RabGPR7		S R R V A G R T Y G A A R A V S L A V W A L V T L V V L P F A V F A		R L D D E Q G R R Q C V L V F P Q P E A F W W R A S			69
MusGPR7		S R R V S G R T Y G A A R A V S L A V W A L V T L V V L P F A V F A		R L D S E Q G R R Q C V L V F P Q P E A F W W R A S			120
		Transmembrane 5		Transmembrane 6			
GPR7		R L Y T L V L G F A I P V S T I C V L Y T T L L C R L H A M R L D S H A K A L E R A K K R V T F		L V V A I L A V C L L			179
FLGPR7		R L Y T L V L A F A I P V S S I C V L Y T T L L C R L R A M R L D S Q A K A L Q R A K R V T F		L V V A I L A V C L L			128
TSGPR7		R L Y T L L L G F A I P V S T I C V L Y T T L L C R L R A M R L D S H A K A L Q R A K K R V T F		L V V A I L A V C L L			128
RabGPR7		R L Y T L V L G F A I P V S S I C V L Y T T L L C R L H S M R L D N H G K A L Q R A K K R V T F		L V V A I L A V C L L			128
MusGPR7		R L Y T L V L G F A I P V T T I					136
		Transmembrane 2		Transmembrane 3			
GPR8		G L F T L V L P V N I A E H L L Q Y W P F G E L L C K		L V L A V D H Y N I F S S I Y F L A V M S V		D R Y L V V L A T V R	60
MonGPR8		G L F T L V L P V N I A E H L L Q H W P F G E L L C K		L V L A T D H Y N I F S S I Y F L A V M S V		D R Y L V V L A T V R	60
ProGPR8		G L F T L V L P A S I A E H L L Q R W P F G E L L C K		L V L T A D H Y N I F C S V Y F L A V M S V		D R Y L V V L A T V H	60
FLGPR8						Y L V V L A T V Q	9
TSGPR8						Y L V V L A T V H	9
RabGPR8						Y L V V L A T V Q	9
		Transmembrane 4					
GPR8		S R H M P W R T Y R G A K V A S L C V W L G V T L V L P F F S F A G V Y S N E L Q V P S C G L S F P W P E R V W F K A					120
MonGPR8		S H H M P W R T Y R G A K V A S L C V W L G V T L V L P F F S F A G V Y S N E L Q V P S C G L S F P R P E R V W F K A					120
ProGPR8		S R R T P W R T Y R G A K V T S L C V W L G V T L V L P F F S F A G V Y S N E L Q V P S C G L S F P R P E R A W F Q A					120
FLGPR8		S R H V P W R T Y R G A K V A S L C V W L G V T L V L P F F S F A S V Y S N E L Q V P S C G L S F P R P E T A W F K A					69
TSGPR8		S C R V L R A T H R G A K V A C L C V W L G V T L V L P F F S F A T V Y S N E L Q V P S C G L S F P R P E T A W F K A					69
RabGPR8		S R R A P R A T H R G A K L T S L C V W L G V T L V L P F F S F A G V Y S N E L Q V P S C G L S F P R P E R A W F K A					69
		Transmembrane 5		Transmembrane 6			
GPR8		S R V Y T L V L Q F V L P V C T I C V L Y T D L L R R L R A V R L R S G A K A L G K A R R K V T V		L V L V V L A V C L L			180
MonGPR8		S R V Y T L V L Q F V L P V C T I C V L Y T D P S R R L R A V R L C S G A K A L G K A R R K V T V		L V L V V L A V C L L			180
ProGPR8		S R V Y T L V L Q F V L P V C T I C V L Y A D L L R R L R A V R L R S G A K A L S K A R R K V T V		L V L V V L A V C L L			180
FLGPR8		S R I Y T L V L Q F V L P V C T I C V L Y L D L L R R L R A V R L Q S G A K A L G K A R R K V T V		L V L A V L A V C L L			129
TSGPR8		S R I Y T S L Q F A L P V C A L C A L Y A D L L R R L R A V R L H S G A K A L G K A R R K V T V		L V L T V L A V C L L			129
RabGPR8		S R I Y T L V L Q F V L P V C T V C V L Y A D L L R R L R A V R L C S G A K A L G K A R R K V T V		L V F A V L A A C L L			129
		Transmembrane 6					
GPR8		C W T P F H L A S V V A L T T D L P Q T P L					202
MonGPR8		C W T P F H L A S V V A L T T D L P Q T P L					202
ProGPR8		C W T P F H L A S V V A L T T D L P Q T S L					202

Figure 7B) GPR7 (top) and GPR8 (bottom) sequence alignments among different animal species (Lee et al., 1999). GPR7 and GPR8 are from human. FL = flying lemur; TS = tree shrew; Rab = rabbit; Mus = mouse; Mon = monkey; Pro = lemur. Shaded and boxed regions are divergent from human sequence. Transmembrane regions are grouped together. Note that GPR8 orthologs have been cloned for many mammalian species except for rodents, mice or rats.

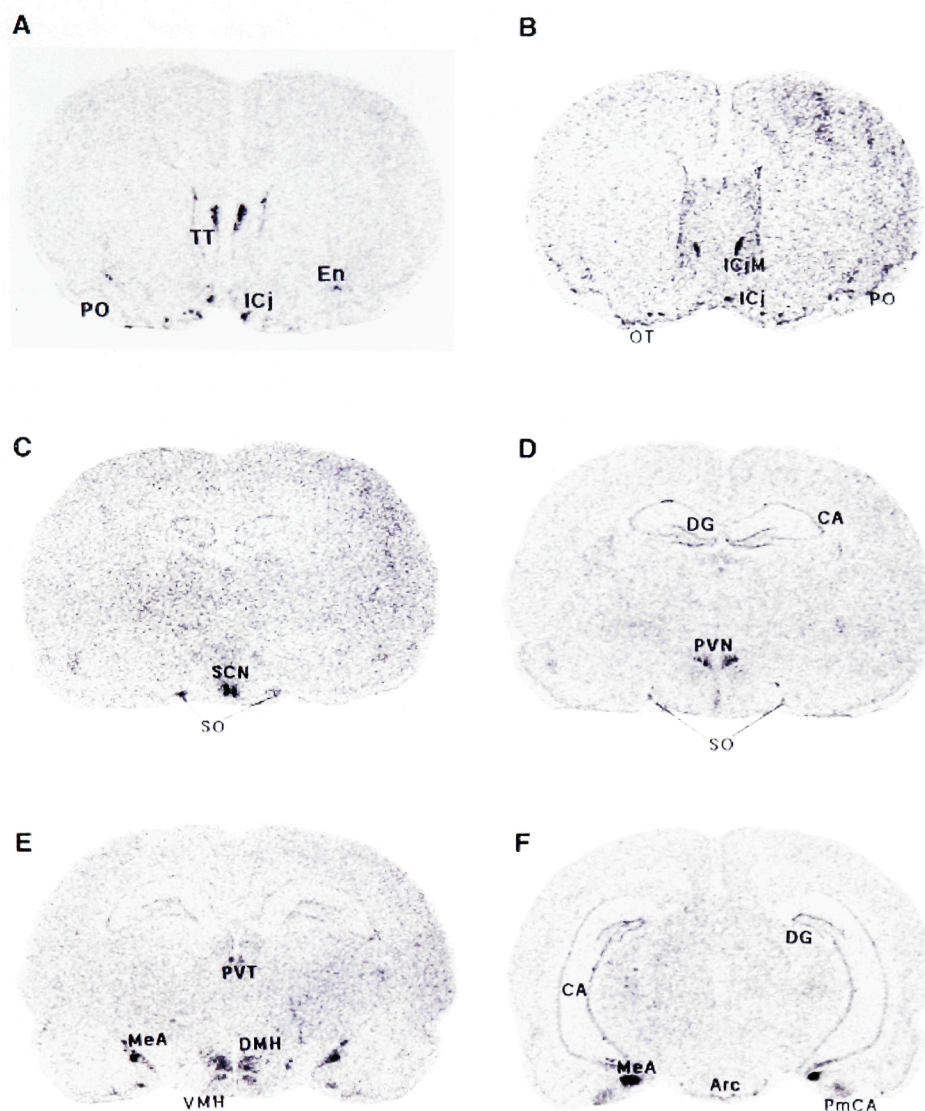


Figure 8) GPR7 mRNA distribution patterns in rat brain by *in situ* hybridization (Lee et al., 1999). Coronal rat brain sections presented rostrocaudally, showing in distance from bregma. (A) +1.7 mm, (B) +1.2 mm, (C) -1.3 mm, (D) -1.8 mm, (E) -3.3 mm, and (F) -4.3 mm. Abbreviations are as follows: TT=taenia tecta, ICj=islands of Calleja, ICjM=major island of Calleja, PO=primary olfactory cortex, En=endopyriform nucleus, OT=olfactory tubercle, SO=supraoptic nucleus, SCN=suprachiasmatic nucleus, DG=dentate gyrus, CA=fields of Ammon's horn, PVN=paraventricular nucleus, DMH=dorsomedial nucleus, VMH=ventromedial nucleus, Arc=arcuate nucleus, PVT=periventricular nucleus of thalamus, MeA=medial amygdaloid nucleus, PmCA=posteromedial amygdaloid nucleus.

GPR7 Ligands – Neuropeptide B and Neuropeptide W

While the GPR7 knockout mice were being analyzed, several groups independently identified the endogenous peptide ligands for GPR7 and its homolog GPR8 using reverse pharmacology and computational genomics techniques (Brezillon et al., 2003; Fujii et al., 2002; Shimomura et al., 2002; Tanaka et al., 2003). The ligands were named neuropeptide B (NPB) and neuropeptide W (NPW) (alternatively called by one group L7 and L8) and are formed from two distinct and novel genes that have no known homologies to other genes except for themselves. The genes encoding for NPB and NPW are similar to each other and are evolutionarily conserved from xenopus to zebrafish to mammals including rodents and primates (Figure 9). The NPB and NPW encoding genes are putatively thought to form a prepropeptide with a signal peptide cleavage site and a proteolytic processing site of a pair of dibasic arginines that can be cleaved to form NPB-23 and NPB-29 or NPW-23 and NPW-30 respectively for either a 23 amino acid peptide or a 29/30 amino acid peptide.

Both peptide ligands NPB and NPW can bind and activate GPR7 and GPR8 in nanomolar or subnanomolar concentrations (Figure 10). In order to test for the binding and activity of the ligands for GPR7 and GPR8, a xenopus melanophore assay, where human GPR7 or GPR8 cDNA was transiently transfected, was used (Tanaka et al., 2003).

A

		*
bovine NPB	WYKPTAGQGYYSVGRAGLLSGFHRSPYA	
human NPB	WYKPAAGHSSYSVGRAGLLSGLRRSPYA	
mouse NPB	WYKPAAGPHHYSVGRAGLLSSFHRRFST	
rat NPB	WYKPAAGSHHYSVGRAGLLSSFHRRFST	
xenopus NPB	WYKQSTGPSYSYSVGRAGLLSGIRRRSPDI	
zebrafish NPB	WYKQSTGPSYSYSVGRAGLLSGIRRRSPYV	
human NPW	WYKHVASPRYHTVGRAGLLMGLRRSPYLW	
mouse NPW	WYKHVASPRYHTVGRAGLLMGLRRSPYQW	
rat NPW	WYKHVASPRYHTVGRAGLLMGLRRSPYLW	

B

Prepro-NPB

bovine	1	-----?????TLVAAALALCLLLASPGLA	WYKPTAGQGYYSVGRAGLLSGFHRSPYA	48
human	1	-----M-AQSATLAAALALCLLLAPPGLA	WYKPAAGHSSYSVGRAGLLSGLRRSPYA	53
mouse	1	-----M-ARCRTLVAAALAL-LLPP--AL	WYKPAAGPHHYSVGRAGLLSSFHRRFST	50
rat	1	-----M-ARCRTLVAAALAL-LLTP--AL	WYKPAAGSHHYSVGRAGLLSSFHRRFST	50
xenopus	1	MLSPGSHSSSLFTLFCALALLSCQRTH-	WYKQSTGPSYSYSVGRAGLLSGIRRRSPDI	59
zebrafish	1	-----VAVSILISSHPTD-	WYKQSTGPSYSYSVGRAGLLSGIRRRSPYV	43
bovine	49	RRSEEP-RGGTRSLGGVGTREMRPNL-----	RSALVCVEVT	84
human	54	RRSQPYRGAEPFGAGASPELQLHPRL-----	RSALVCQDDVA	91
mouse	51	RRSESPALRVGTGPLRNLEMRPSV-----	RSALVCVKDVT	85
rat	51	RRSESPALRVGTGPLRNLEMRPSV-----	RSALVCVKDVT	85
xenopus	60	RRSESPENSMESTEIPETYNLSLGVKRGAVLKSM-----	RLCVKDVDS	102
zebrafish	44	RRSEGESALDSGETPGVNSVLAELSSNSGRQTPVRLQTFVNLLCAAFSFC	RLCVKDIS	103
bovine	85	PNLQSCPELPDGRATFCCKADVFLSLASSTC		115
human	92	PNLQRCERLPDGRGTQCKANVFLSLRAADGLAA		125
mouse	86	PNLQSCQRQLNSRGTFCCKADVFLSLHETDQST		119
rat	86	PNLQSCQRQLNSRGTFCCKADVFLSLHKAFCQSA		119
xenopus	103	PNLHSCCELLPDTSTSTFCCKAQIYLSLDTSCGLAP		136
zebrafish	104	PNLQSCCELLQDGSSSFCCKADVFLSLDSLTCFTS		137

Prepro-NPW

human	1	----LAWRPGER---CAPASRPRLAL	LLLLLLLLPLPSGAWYKHVASPRYHTVGRAGL	51
mouse	1	----LASNREVRGFGCHPRNRPL	LLLLLLLLPLPSAWYKHVASPRYHTVGRAGL	55
rat	1	MDLSALASSREVRGFGCAPVNRPL	LLLLLLLLPLPSAWYKHVASPRYHTVGRAGL	60
		# #		
human	52	LMGLRRSPYWRRALRAAGPLADTL	SPFPAAREAHLLLPSSWQELWEVRSSSAGCF	111
mouse	56	LMGLRRSPYWRRALGGAAGPL--SRL	PGPVAREAHLLLPSSQELWEVRSSSPAGCF	111
rat	61	LMGLRRSPYWRRALGGAAGPL--VGL	PGQMARSAHLLLPSSQELWEVRSSSAGCF	116
		↑		
human	112	VRAPRSFRAPFPALEPE-SLDFSGAQRLRRDVSRAVDPA	ANRLGLPLCLAPCF	165
mouse	112	VHAPRSFRDLGGVRCPECSLSLHSHWSEPAARAFGETLRAQ	PFWLFQQVIFALPVR---P	168
rat	117	VHATRSIRDLGGARCPCECSLSFSQSWTSAEPAARAFGEMLR	AQPFWLFQQIIFALPVRLLDDR	176
human	165			165
mouse	169	-KNRWRPHA		176
rat	177	LKNRWRPHA		185

Figure 9) Amino acid sequences of NPB and NPW (Tanaka et al., 2003). (A) Amino acid sequences of mature NPB and NPW peptides. An asterisk indicates the posttranslational bromination site of the native bovine NPB. Peptide sequences of other species are deduced from cDNA sequences. Amino acid identities between NPB and NPW are shown in black. Shaded residues are conserved only within the NPB or NPW. (B) Deduced amino acid sequences of prepro-NPB and NPW precursor polypeptides. Mature peptides are marked by equal signs. Question marks indicate undetermined sequence of bovine prepro-NPB. Human and mouse prepro-NPW cDNA do not have a translation initiator ATG codon; putative translation initiation sites are indicated by a pound sign. An arrow indicates a possible additional processing site for NPW. Identical amino acids within the orthologues are shown in black. Lightly shaded residues are conserved in more than four of six (NPB) or two of three (NPW) species.

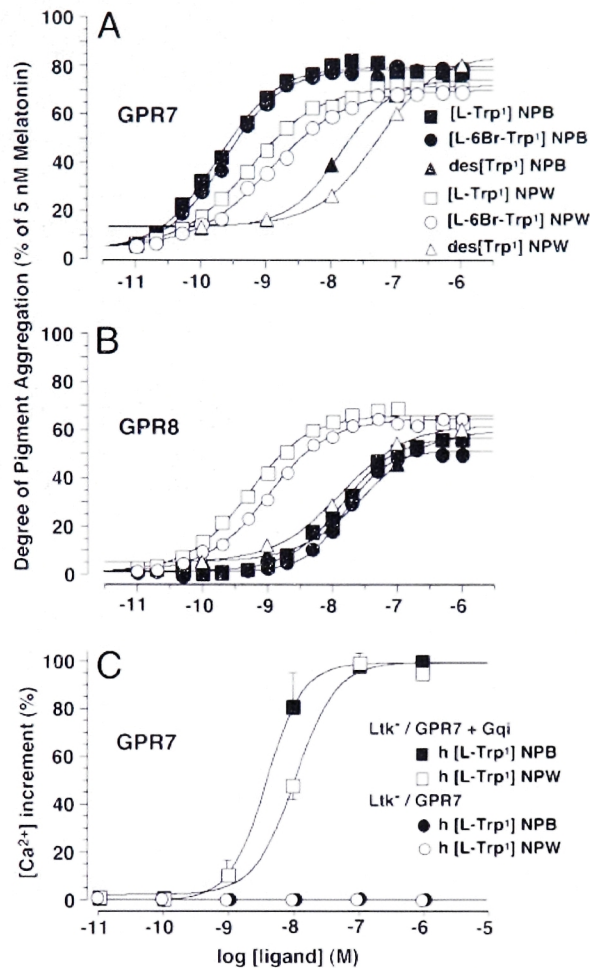


Figure 10) *In vitro* pharmacology of NPB and NPW assessed by melanophore pigment aggregation assay (A and B) and [Ca²⁺]_i transient assay (C) in mammalian cells (Tanaka et al., 2003). (A and B) *X. laevis* melanophores were transiently transfected with human GPR7 (A) or GPR8 (B) cDNA, and challenged with various forms of synthetic human NPB and NPW peptides. Brominated NPB and nonbrominated NPB have approximately equal potencies on GPR7 (A), whereas both of them have much weaker potencies on GPR8 (B). Brominated NPW and nonbrominated NPW both have similar potencies on GPR7 and GPR8. des[L-Trp-1]NPB and des[L-Trp-1]NPW are both much less potent on GPR7 and GPR8. Data are the mean of eight separate experiments. (C) Ltk⁻ cells were stably cotransfected with the human GPR7 cDNA and Gqi chimera cDNA, and challenged with nonbrominated synthetic human NPB and NPW. NPB has a modestly higher potency than NPW. When Gqi cDNA is not cotransfected, neither NPB nor NPW could induce the calcium mobilization (open and filled circles are all overlapping). Peak [Ca²⁺]_i values are represented as percentages of the maximum response. Data are presented as the mean \pm SEM of three experiments performed in duplicate.

Both synthetic NPB and NPW potently stimulated the aggregation of xenopus melanophores, a process known to involve G_i -coupled signaling pathways. In this assay, NPB appears to have a stronger affinity for GPR7 over GPR8 (EC_{50} of 0.2nM for GPR7 and EC_{50} of 14nM for GPR8). On the other hand, NPW has equal affinity for GPR7 or GPR8 (EC_{50} of 0.56nM for GPR7 and EC_{50} of 0.51nM for GPR8). In another study, Chinese hamster ovary (CHO) cells were transfected with either human GPR7 or GPR8 (Shimomura et al., 2002). Synthetic NPB and NPW both potently and dose-dependently inhibited the cAMP accumulation induced by forskolin. This effect was abolished by preincubation with pertussis toxin. Both the xenopus melanophore and cAMP assays support that upon ligand binding and activity through either NPB or NPW, GPR7 and GPR8 signal by coupling with a G_i protein.

Interestingly, NPB that was purified from brain extracts was found to have a brominated C-6 L-tryptophan in the first amino acid position (Fujii et al., 2002; Tanaka et al., 2003). This brominated tryptophan was not found in NPW. Also, non-brominated tryptophan could not be appreciably found in any peptide fractions isolated from bovine hypothalamus indicating that the brominated form of NPB is the dominant endogenous form. The role of the brominated tryptophan is unclear as non-brominated NPB had similar binding affinities and activity for the receptors. Brominated tryptophan has been

reported in conotoxin peptides derived from marine snails, but this represents the first known bromination modification of an amino acid in non-marine animals (Craig et al., 1997; Jimenez et al., 1997). It is possible that bromination of NPB helps in the stability of the neuropeptide or other function outside of ligand binding.

Also, an unusual start codon or translation initiator site was found for both human and mouse prepro-NPW gene. Instead of a standard AUG methionine start codon, prepro-NPW starts with a CUG leucine start site (Tanaka et al., 2003). The sequence surrounding the CUG start site confirms to Kozak's rule. Furthermore, *in vitro* mutational results showed that both CUG and AUG start sites produced equal amounts of the prepro-NPW peptide. Therefore, CUG appears to be the natural start site for this gene. Interestingly, both porcine and rat prepro-NPW and all known sequences of prepro-NPB have a standard AUG start site (Shimomura et al., 2002; Tanaka et al., 2003). The significance of this CUG start codon for prepro-NPW is unknown.

While both NPB and NPW were isolated from brain tissues, the ligands are expressed in both central and peripheral tissues (Tanaka et al., 2003). *In situ* hybridization of NPB and NPW in the mouse brain has localized the two ligands to different neuronal populations (Figure 11). NPB mRNA was detected in several distinct brain regions including the hippocampus, paraventricular hypothalamic nucleus,

Edinger-Westphal nucleus, motor and sensory root of the trigeminal nerve, locus coeruleus, among other areas (Tanaka et al., 2003). NPW had the highest expression in the Edinger-Westphal nucleus. NPW mRNA was less widespread in the mouse brain with highest mRNA levels detected in the periaqueductal gray matter, ventral tegmental area, Edinger-Westphal nucleus, and dorsal raphe nucleus (Tanaka et al., 2003). An

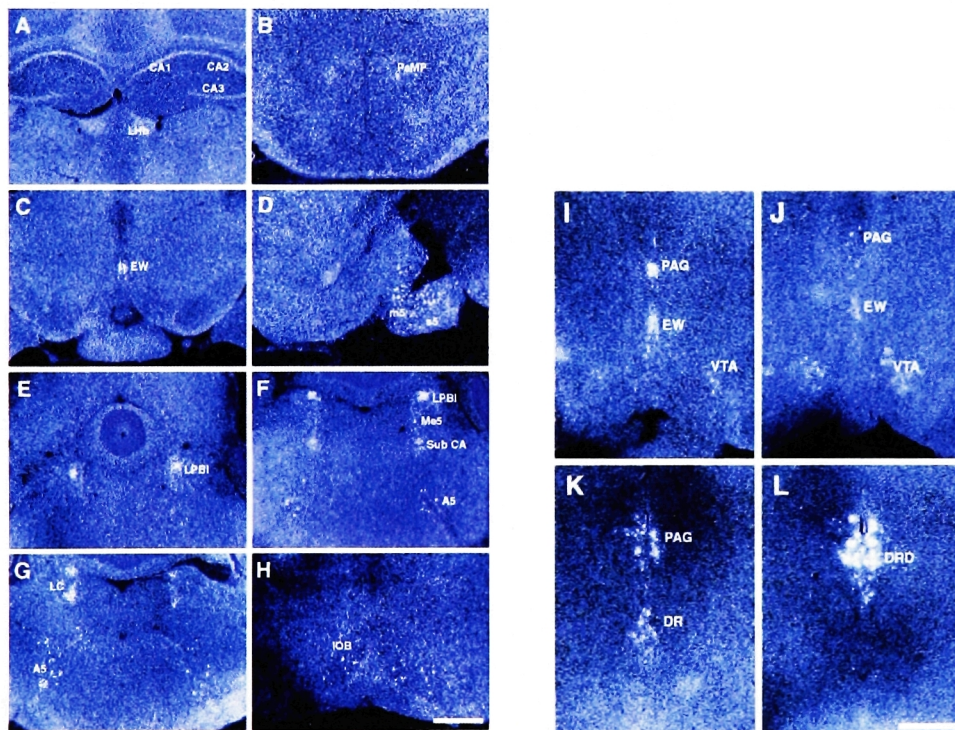


Figure 11) *In situ* hybridization of NPB (A-H) and NPW (I-L) mRNA on mouse brain sections (Tanaka et al., 2003). (Scale bars are 300 μ m.) (A-H) NPB mRNA in mouse brain. CA1-3, CA1-3 field of hippocampus; LHb, lateral habenular nucleus; PaMP, paraventricular hypothalamic nucleus medial parvicellular part; EW, EW nucleus; m5, motor root of the trigeminal nerve; s5, sensory root of the trigeminal nerve; LPBI, lateral parabrachial nucleus internal part; Me5, mesencephalic trigeminal nucleus; Sub CA, subcoeruleus nucleus α part; A5, noradrenergic cell group A5; LC, locus coeruleus; IOB, inferior olive subnucleus B. (I-L) NPW mRNA in mouse brain. PAG, periaqueductal gray matter; EW, EW nucleus; VTA, ventral tegmental area; DR, dorsal raphe nucleus; DRD, dorsal raphe nucleus dorsal part.

independent study using a polyclonal antibody raised against rat NPW-23 peptide showed immunoreactive cells in the paraventricular nucleus (mainly in the parvocellular division), supraoptic nucleus, accessory neurosecretory nuclei, dorsal and lateral hypothalamus, perifornical nucleus, arcuate nucleus, and anterior and posterior pituitary (Dun et al., 2003). The different localization of NPW between the two studies could possibly be due to different techniques used, mRNA versus protein expression pattern. In periphery, NPB was highly expressed in stomach, spinal cord, and testis, while NPW expression was strongly detected in stomach and lung (Tanaka et al., 2003). The distinct expression patterns of NPB and NPW in the brain and periphery suggest separate physiological roles for the ligands even though both act on one common receptor GPR7 in rodents or on two receptors, GPR7 and GPR8, in other mammals including humans.

Pharmacological injections of the peptide ligands have a number of disparate effects on rodents. An ICV bolus injection of NPB at the onset of the dark phase initially elicits a small transient increase in food intake followed by a much larger, sustained suppression of food intake (Figure 12) (Tanaka et al., 2003). Synergistic decrease in feeding was seen when corticotropin releasing factor (CRF) was coadministered with NPB. In addition, locomotor activity was increased when NPW was injected into rats during either light or dark cycle (Tanaka et al., 2003). These data

suggest that NPB could be acting pharmacologically as a centrally active catabolic factor.

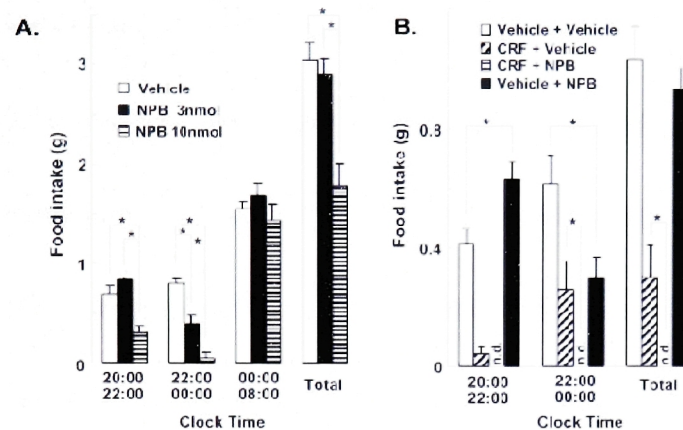


Figure 12) *In vivo* pharmacological effects of i.c.v.-injected NPB on food intake (A and B) (Tanaka et al., 2003). (A) Vehicle or 3 or 10 nmol of synthetic rat NPB was i.c.v. injected in bolus into freely fed mice, and food consumption was measured. Injections were performed at 20:00 (beginning of dark phase) and food intake was measured at 22:00, 00:00, and 08:00 the next morning (end of dark phase). The data represent food intake between the indicated times (mean \pm SEM, $n = 4-5$ per group). (B) Anorexic effect of NPB is enhanced by pretreatment with CRF. CRF (0.3 nmol) was i.c.v. injected 15 min before the injection of 3 nmol of synthetic rat NPB in mice. NPB was i.c.v. injected at 20:00 (beginning of dark phase), and food intake was measured at 22:00 and 00:00. n.d., no food intake detected (bars invisible). The data represent food intake between designated times in dark phase (mean \pm SEM, $n = 7$ per group). * indicate significant difference ($P < 0.05$, one-way ANOVA, Fisher's post hoc analysis).

NPB and NPW have various other effects when centrally administered to rodents including enhancing analgesia and stimulating the release of prolactin and corticosterone but inhibiting the release of growth hormone (Baker et al., 2003; Shimomura et al., 2002; Tanaka et al., 2003). Analgesic activity for centrally administered NPB was seen only

in the formalin test and not by the thermal induced paw flick test (Tanaka et al., 2003). As the licking response in the formalin test is mainly believed to be due to a complex supraspinal behavior including both affective and motivational processing of nociception, this could represent a role for GPR7 signaling in supraspinal analgesia as opposed to inflammatory analgesia (Donahue et al., 2001). The control of prolactin, corticosterone, and growth hormone release by NPW suggest that GPR7 signaling has important neuroendocrine functions. These effects appear to be mediated through the hypothalamus as direct exogenous administration of NPW on dispersed, anterior pituitary cells, which also express GPR7, had no effect (Baker et al., 2003). The physiological relevance of any of these pharmacological effects is currently unknown.

Specific Aims

This thesis aims to elucidate the physiological role of GPR7 signaling in mammals. GPR7 was initially identified as a candidate obesity gene from an earlier screen of GTG down-regulated hypothalamic genes. First, GPR7 knockout mice were generated by disrupting the single intronless coding region with a STOP-IRES-tau-EGFP cassette. These mice were analyzed for a variety of physiological and behavioral disturbances. The initial focus was on defining possible metabolic defects and any role it might play in common energy homeostasis signaling pathways such as leptin and melanocortin. Second, due to the observed metabolic defects in the GPR7 knockout mice, the localization and possible metabolic regulation of GPR7 and its ligands were explored. Third, further studies with the GPR7 knockout mice concentrated on defining potentially other behavioral phenotypes including anxiety, depression, sleep-wake cycles, and circadian rhythms. Feeding behavior is often associated with the same neural circuits involved in regulating other complex behaviors. Finally, a summary of the results of this current study with those in the literature elucidating the role of GPR7 and its ligands in mammalian physiology is presented along with directions for future studies.

Chapter 2: Materials and Methods

Animal Care and Maintenance. Unless otherwise indicated, all mice were maintained under the following conditions. Mice were maintained under a strict 12 hour light:dark cycle (lights ON 7AM) in a temperature and humidity controlled room and fed *ad libitum* on a standard rat diet (Diet 5001 – 12% kcal fat, 23.5% kcal protein, 64.5% kcal carbohydrate or Diet 5053 – 12% kcal fat, 23.5% kcal protein, 64.5% kcal carbohydrate, Lab Diet) and filtered water. Mice were weaned at four weeks of age and group-housed (2 to 5 animals per cage) according to sex. All tail clipping for genotyping was done at time of weaning. All animal work was conducted in accordance with the guidelines of the Rockefeller University Laboratory Animal Research Center or the appropriate institutional review board.

Targeted Disruption of GPR7. A stop codon-IRES-tau-EGFP-thymidine kinase-neomycin cassette was inserted into a unique *StuI* site in the coding sequence of a genomic clone of the *GPR7* gene. 129/Ola embryonic stem (ES) cell line was transfected with linearized vector by electroporation. Transfected ES cells were screened by neomycin resistance and by Southern analysis of *BamHI* digested genomic

DNA to identify clones that had undergone successful homologous recombination. A heterozygote cell was expanded and thymidine kinase-neomycin was excised by cre recombinase. Correctly targeted ES clones were injected into blastocytes and implanted into pseudopregnant mice. Chimaeric mice were generated and bred to C57BL/6J female mice.

Genotyping GPR7 knockout mice by Southern blotting. Successful germline transmission and all genotyping were confirmed by tail genomic DNA Southern analysis. Tail genomic DNAs were extracted in a lysis buffer [50mM Tris, pH 8; 100mM EDTA; 0.5% SDS] with freshly added proteinase K [350µg per tail] at 55°C with shaking overnight followed by a phenol:chloroform extraction, isopropanol precipitation, ethanol wash, and dissolved in an appropriate volume of ddH₂O and stored at 4°C until use. The purified tail genomic DNAs were then digested overnight at 37°C with BamHI and were separated on a 0.8% agarose gel in TAE buffer (60-90V for 4 to 6 hours). The gel was washed for 30 minutes in denaturing solution (1.5M NaCl, 0.5M NaOH) at room temperature (RT) with mild shaking followed by 30 minutes in neutralizing solution (1.5M NaCl, 0.5M Tris-Cl, pH 8) at RT with mild shaking and then transferred to Hybond membrane (positive charged nylon membrane, Amersham) using 10XSSC (1.5M

NaCl, 0.15M sodium acetate) transfer buffer overnight. The blot was dismantled, and the membranes briefly rinsed in 10XSSC to remove excess agarose and dried at RT. The membranes were then UV auto-crosslinked with a Stratalinker (Stratagene). For hybridization studies, all membranes were prehybridized for at least two hours using RapidHyb buffer (Amersham) at 65°C. Hot ^{32}P DNA probes were synthesized using PCR under the following conditions. The DNA probe template was a 220bp fragment approximately 440bp upstream of the ATG start site and was cloned from genomic DNA obtained from a wildtype C57BL/6J mouse. Forward primer: 5' CAC CTC TGC TGA ATT CGC 3'; Reverse primer: 5' TCC AAG GCT GGA GAC AGA 3'. PCR conditions used for both synthesis of cold DNA template and subsequent hot PCR amplification: 95°C x 30 seconds, 55°C x 30 seconds, 72°C x 30 seconds for 35 cycles using a standard Perkin Elmer thermocycler. For the hot probe synthesis, dCTP was replaced with fresh $\alpha^{32}\text{P}$ dCTP. 1,000,000 CPM/ml buffer was added to each membrane and hybridized at 65°C for several hours (4-8 hours) or overnight (14-20 hours). Membranes were washed twice with 2XSSC, 0.1%SDS at 65°C for 15 minutes each followed by a more stringent wash at 0.1XSSC, 0.1%SDS at 65°C for 15 to 30 minutes. The membranes were then exposed to film (Kodak Biomax MS film) at -80°C overnight or to a Storage Phosphor screen (Amersham) at RT overnight. All Storage Phosphor screens were analyzed using

a Typhoon 9200 scanner (Amersham) and ImageQuant software version 5.2 (Molecular Devices). The recombinant band is 5kb in length, and the wildtype is approximately 6.5kb.

Generating and genotyping ob/ob and Ay/a GPR7 double mutant mice

All GPR7 mutant mice used for breeding were backcrossed at least six generations to C57BL/6J mice (N6) unless otherwise noted. C57BL/6J ob/+ and Ay/a mice were purchased from Jackson Laboratories and mated to GPR7^{+/-} mice to generate C57BL/6J double heterozygote mice (ob/+ GPR7^{+/-} and Ay/a GPR7^{+/-}). All ob/ob GPR7 double mutants were offspring of double heterozygote crosses, while Ay/a GPR7 double mutants were generated with a double heterozygote male crossed to a GPR7^{+/-} female mouse (i.e., ob/+ GPR7^{+/-} x ob/+ GPR7^{+/-} and Ay/a GPR7^{+/-} x a/a GPR7^{+/-}). The *ob* gene was genotyped by PCR as previously described (Erickson et al., 1996b). Briefly, the following PCR primers were used to amplify a 247bp fragment of the *ob* gene. Forward primer: 5' GAC TTC ATT CCT GGG CTT CA 3'; Reverse primer: 5' TCT GTG GAG TAG AGT GAG GC 3'. 95°C x 45 seconds, 55°C x 45 seconds, 68°C x 1 minute and 30 seconds for 40 cycles. The resulting PCR amplified DNA fragment of the *ob* gene was digested with DdeI at 37°C for 4 hours to overnight and analyzed on a 2% agarose gel.

The ob/ob mutation inserts an extra DdeI site into the *ob* gene yielding a 105bp, 47bp, and 32bp fragment from the amplified PCR DNA compared to only two fragments of 152bp and 32bp in the wildtype mouse. Agouti mutation was selected by visual inspection for agouti fur coat color, which was transmitted as a dominant trait as expected.

Body Weight, Food Intake, Metabolic Rate and Locomotor Activity Measurements.

Body weights were measured once a week for group-housed mice except for mice fed a high fat diet (D12451 45% kcal fat, Research Diets), which were all single-caged and weighed weekly. Food intake was carefully measured in single caged animals with an acclimation period of at least one week before measurement. Energy expenditure and locomotor activity was measured using the Oxymax and OptoM3 system (Columbus Instruments). Air flow into the calorimeter sensors was set at 0.5L/min of room air with water in the air removed by passing the air through dehumidifier columns filled with magnesium perchlorate (Fisher). The O₂ and CO₂ sensors were calibrated with a known span gas (20.5% O₂, 0.5% CO₂, 79% N₂; TW Smith) before each test run. Mice were individually placed in the calorimeter chambers and stabilized for one day before measurements were recorded for two full days. Mice in the chambers had free access to

both standard rat diet and water. Locomotor activity was monitored every minute for each infrared beam break in the three planes (x, y, and z) for the 12 hour light and dark phases. Metabolic rate was considered as a “resting” value when the mice showed no movement in all three planes as recorded by infrared beam breaks lining the cage.

Plasma and Body Composition Measurements and Liver Histology. Mice were sacrificed by CO₂ asphyxiation following a four hour fast during the light cycle (food removed 11:00AM, sacrificed 3:00PM). Blood was immediately collected by cardiac puncture using an EDTA-treated syringe needle. Plasma was obtained by centrifuging the blood and stored at -20°C or lower until further analysis. Glucose was analyzed by the glucose oxidase method using a commercial glucometer (Bayer). Insulin and leptin were measured by ELISA (Alpco, R&D respectively). Hypothalamus, whole brain, and a small piece of liver (~150mg) were removed and snap frozen in liquid N₂ before body composition analysis of the same mouse. Body composition was analyzed as previously described by a chloroform:methanol biochemical extraction using a Soxhelt system (Cohen et al., 2001). The animal carcasses were dried in a 90°C oven until their weight remained constant (>2 weeks), and all the body water had evaporated. The difference in weight before and after drying was taken as total body water weight. The dried

carcasses were homogenized in a blender, and a 1g extract was removed for lipid extraction. Lipids were extracted with boiling 3:1 chloroform:methanol solution for greater than 3 hours until no trace of lipids could be seen. The ratio of difference in the weight before and after lipid extraction was used to calculate lean and fat mass for each individual animal. All lipid extractions were carried out in duplicates. Liver histology was performed following standard hematoxylin and eosin staining techniques in paraffin embedded formaldehyde-fixed tissues.

Fasting and refeeding response in GPR7^{-/-} mice. Weight-matched adult male N10-C57BL/6J GPR7^{-/-} mice and wildtype littermate controls (GPR7^{+/+}, n=7; GPR7^{-/-} n=6; age 30-38 weeks of age) were acclimated to single cage housing for several months (>4 months) prior to start of experiment. The initial body weight and baseline food intake was recorded 24 hours prior to start of fast. Food was removed for 24 hours (starting at 12PM – light cycle), while water was freely available throughout the whole study period. Standard rat chow was reintroduced after the 24 hour fast period. Body weight was recorded immediately following the fast (time 0) and 6, 24, and 48 hours after food was reintroduced. Food intake was monitored 1, 3, 6, 24 and 48 hours after food was reintroduced.

Glucoprivic Feeding Response in GPR7^{-/-} Mice. N6 or N10-C57BL/6J male GPR7^{+/+} and GPR7^{-/-} mice between 33 and 44 weeks of age were acclimated to single cage housing for greater than 1 week. Mice were handled daily for a minimum of five consecutive days to minimize stress prior to i.p. injection of either sterile PBS or 2-deoxy-D-glucose (500mg/kg body weight or 250mg/kg body weight, Sigma). 2-deoxy-D-glucose was dissolved in sterile filtered PBS to make a 100mg/ml or 200mg/ml solution. Each mouse received no more than 100µl of solution by i.p. Food intake was monitored immediately following each injection at 2, 4, and 5 hours post-injection. ICV injections of 2-deoxy-D-glucose followed procedures as given below.

Cannulation of animals. N10-C57BL6J male mice between 20 to 24 weeks old were anesthetized with sodium pentobarbital (Nembutal, 50-60mg/kg body weight i.p.) and placed in a stereotaxic apparatus (Kopf Instruments). Guide cannulas with a threaded cylindrical plastic pedestal molded around a stainless steel tubing extending 1.5mm below the pedestal (Plastics One) were implanted 0.5mm posterior to bregma and 1.0mm lateral to the midline (Paxinos and Franklin, 2001). All guide cannulas were adhered to

the skull with cyanoacrylate gel (Loctite 454) and dental cement applied to the base of the pedestal. The mice were sutured to cover their surgical wounds and allowed to recover for a minimum of 10 days. Each surgery lasted less than one hour per mouse from induction of anesthesia to the end of suturing. During the recovery time, all mice were monitored daily for any signs of infection or loss of body weight and were extensively handled to minimize stress.

ICV injections in GPR7^{-/-} mice. On the day of injection, the mice were moved to a procedure room in their home cages and allowed to acclimate to the room for two hours. During the acclimation period, all food was removed from the cages. All doses were delivered through an injector cannula projecting 1mm past the implanted guide cannula (Plastics One). The injector cannula was attached with PE50 tubing to a 25µl gas-tight syringe (Hamilton). 2-deoxy-D-glucose (500µg/µl) or sterile PBS was injected in a volume of 2µl over a period of one minute followed by the needle remaining in position for an additional minute to ensure complete dispersal of the injected volume. Mice were returned to their home cage, where fresh pre-weighed standard rodent chow was immediately reintroduced. Food intake was monitored 2 and 4 hours after administration. Four to seven days passed between injections.

Ligand Binding and Activity in a Xenopus melanophore system. To test for ligand activity to mouse GPR7, a xenopus melanophore assay was used as previously reported (DeCamp et al., 2000; Tanaka et al., 2003). Mouse GPR7 cDNA was subcloned in pcDNA3.1 (+) expression vector (Invitrogen) and transfected into β_2 -7 cell line of Xenopus melanophores. After 48 hours, absorbance at 650nm was measured before (A_i) and after 1 hour incubation with synthetic ligands (A_f) with a 96 plate well reader (Molecular Devices). The equation $1-A_f/A_i$ was used to quantify melanosome aggregation, which is an index of G_i signaling (Lerner, 1994).

RNA isolation and cDNA synthesis. Frozen tissues were homogenized with a polytron, and RNA was extracted using Trizol reagent (Invitrogen) following the manufacturer's protocol. Some RNA samples were enriched for polyA RNA by using Oligotex beads (Qiagen). After RNA was isolated from individual tissue, contaminating DNA was removed with DNase I (DNAfree, Ambion) followed by cDNA synthesis by reverse transcription using random hexamer priming (Applied Biosystems).

Measurement of Gene Expression by Real-Time PCR. Quantitative real-time PCR from

hypothalamic cDNA was performed using the TaqMan® system analyzed with the ABI Prism 7700 Sequence Detection System using the Sequence Detection System software version 1.9.1 following the manufacturer's recommendations (Applied Biosystems). All expression data was normalized to cyclophilin expression levels from the same individual sample and carried out in duplicates. The reported results are relative values normalized to cyclophilin levels and are relative values compared to a standard curve based on wildtype brain or stomach expression levels unless otherwise noted. All primer and probe sequences were constructed using the Primer Express software (Applied Biosystems) using the specifications listed for the Taqman® assay system. Primer and probe sequences, labeled with 5'-FAM (except for cyclophilin labeled with 5'-VIC) and 3'-TAMRA are listed below*:

Gene	TAMRA Probe (5'-3')	Forward Primer (5'-3')	Reverse Primer (5'-3')
NPY	CAGAAAACGCCCCAGAACAAGGC	CACCAGACAGAGATATGGCAAGA	TTTCATTTCCCATCACACATG
POMC	CAGTGCCAGGACCTCACCACGGA	TGCTTCAGACCTCCATAGATGTGT	GGATGCAAGCCAGCAGGTT
MCH	GGTGTATGCTGGGAAGAGTCTACCGACC	GGAAGGAGAGATTTTGACATGCT	GCAGGTATCAGACTTGCCAACA
GPR7	TGTAGCCGTCGACCAGTACAACACTTTCTCTAGCC	GGAGGTCATGTGCAAGCTCA	CTCATGACGGCGAGGAAGTAG
NPB	ATCCACGCGACGCTCCGAGTCTCCA	CTGTCGAGTTTCCACAGTTCC	TTGCGCAGAGGTCCGGTTCC
NPW	CGCTTCGTGCCCAGCCATGG	GAGGAGCCCGCTGCTAGAG	GATCGGCAAGATGACTTGCT
Cyclophilin	ACACGCCATAATGGCACTGGTGG	TGTGCCAGGGTGGTGACTT	TCAAATTTCTCTCCGTAGATGGACTT

*All sequences are based on mouse sequences except MCH, which is from rat.

Northern blot analysis of gene expression. 1% formaldehyde agarose gels were used to separate RNA for Northern blotting using standard techniques. 20µg of total RNA or 4µg of polyA enriched RNA were loaded into each lane. Ethidium bromide stained 28S rRNA bands from the gel before transfer was visualized by UV and quantitated using Multi-Analyst Software version 1.0.2 (Biorad). Each gel was washed in DEPC treated ddH₂O for 15 minutes at RT with mild shaking followed by two washes in 10xSSC for 15 minutes at RT with mild shaking. The RNA was then transferred by 10xSSC overnight to a positively charged nitrocellulose membrane (Hybond, Amersham). After dismantling the blot, it was quickly rinsed in 10xSSC to remove excess agarose and allowed to dry at RT before it was UV crosslinked (Stratalinker, Stratagene) and stored at -80°C until use. For hybridization of the blots, the blots were initially prehybridized in Ultrahyb (Ambion) at 42 to 45°C for 1 to 2 hours. Probe template cDNAs were synthesized by RT-PCR with primers listed below. Hot probe was synthesized by PCR as previously described, and 1,000,000CPM/ml buffer was added. The probe was allowed to hybridize for 14 to 20 hours at 42 to 45°C. The blots were washed twice at 42°C with a low stringency (2xSSC, 0.1%SDS) wash for 5 minutes each and twice at 42°C with a higher stringency (0.1xSSC, 0.1%SDS) wash for 15 minutes each. After

the washes, the blot was exposed to film or a Storage Phosphor (Amersham) for analysis. Exposed Storage Phosphor cassettes were analyzed using a Typhoon 9200 scanner (Amersham) and Image Quant software version 5.2 (Molecular Devices). Median background was subtracted from each image before equal sized boxes of each band was quantitated. Each sample RNA was normalized to its 28S rRNA to control for loading variations.

Gene	Tissue RNA Origin	Forward Primer (5'-3')	Reverse Primer (5'-3')
NPW	Lung	GCCCCTGCTGCTGCTTCTGCTC	GGGGGCGCCATCGGTTCTT
NPB	Brain (Cerebellum)	GCCCGGTGTAGGACGCTGGTG	GCATATGGGGGTTGGGAGAGTCA
GPR7	Brain (Hypothalamus)	GTAGCAGTGCCTGTCGTCTA	GTGAAGAGCTCATCGGCG
Cyclophilin	Liver	AGTTCCATCGTGTCATCAAGG	GTTTCTCCACTTCGATCTTGC

Differential gene regulation in altered feeding states. Two separate age-matched groups (younger group 14 weeks old, older group 64 weeks old) of male C57BL/6J wildtype mice (Jackson Laboratories) were group-housed (five per cage) and had free access to standard rodent chow and water as described above. The fasted group had their food pellets removed for 48 hours, while the thirst group had the water bottles removed for 48 hours. The refeeding group had food removed for 44 hours followed by a 4 hour

feeding period (during light cycle 11:00 and 15:00). After 4 hours, all mice in the refeeding group had stopped eating and were quietly sleeping with noticeably distended stomachs. Mice from each group were individually weighed at the start of experiment, 24 hours later, and immediately before sacrifice. All mice were immediately sacrificed by CO₂ asphyxiation, blood drawn by cardiac perfusion, and tissues removed and frozen immediately in liquid nitrogen for future analysis. Plasma was separated from blood as previously described and stored at -80°C with the tissue samples.

Chronic Leptin Treatment. Female C57BL/6J ob/ob and control mice 8 weeks of age were purchased from Jackson Laboratories. Subcutaneous osmotic leptin pumps were implanted into mice as previously described (Soukas et al., 2000). Alzet 2002 mini-osmotic pumps (Alza, Palo Alto, CA) were filled with PBS or 400ng/μl leptin (Amgen, Thousand Oaks, CA) and incubated in sterile 0.9% NaCl overnight at 37°C. Mice were anesthetized with halothane, and the osmotic pumps were implanted subcutaneously. Pair-fed animals received the same amount of food eaten by the leptin treated group. Individual body weight and food intake were measured daily in each treatment group (PBS, leptin and pair-fed). Animals were sacrificed 2, 4, and 12 days after treatment. Plasma and tissues were collected as before and stored at -80°C until

use.

Behavior Tests for GPR7 Knockout Mice. All behavior tests were conducted either at Rockefeller University or University of Texas Southwestern Medical Center in Dallas. All procedures were approved by the appropriate institutional review board. For studies conducted at UT Southwestern, adult mice were shipped to the local animal facility from mice derived from the colonies maintained at Rockefeller University. All mice were acclimated to their new surroundings for a minimum of 6 weeks prior to any behavior tests. Studies at Rockefeller University were conducted in a behavior room separate from the animal colony rooms. All animals were exposed to the test conditions once unless specified below. Each test at Rockefeller University was videotaped by a camera positioned directly above the test field and scored offline blind to the genotype of the test animal.

Sleep Recordings in GPR7 Knockout Mice. Adult N10-C57BL/6J GPR7 male mice (n=5 per genotype, 20-24 weeks of age, 28-30g at time of surgery) were implanted with custom lightweight EEG/EMG implants and cabling for chronic sleep activity monitoring. Custom EEG/EMG electrodes were made as detailed previously (Chemelli et al., 1999).

Briefly, the electrode was based on a six-pin double inline microcomputer connector (board mount socket 929 series from 3M, part number 929975-01-36) that was modified into a four-pin EEG electrode with each pin 1.3mm x 0.3mm (h x w) positioned 4.6mm x 2.9mm (l x w) apart with two EMG electrodes soldered to the center pins. The completed EEG/EMG electrodes were gold-plated by heating in a gold cyanide solution (Oromerse N Gold Solution; Technic Inc., Cranston, RI) at 70°C for two hours. Finally, the electrodes were sterilized in alcohol before implantation.

All surgeries were conducted under standard sterile procedures. Mice were anesthetized with sodium pentobarbital (Nembutal, 50-60mg/kg i.p.) and placed in a stereotaxic apparatus (Kopf Instruments). The cranium was exposed and four small holes were drilled, anterior and posterior to bregma, bilaterally (AP 1.2mm, ML \pm 1.47mm and AP -3.5mm, ML \pm 1.47mm) according to the atlas of Franklin and Paxinos (Paxinos and Franklin, 2001). The EEG/EMG electrode was then inserted into these four holes, cemented with dental acrylic (3m ESPE Ketac Cem Aplicap, 3M), and the EMG electrode was secured into the nuchal musculature. The EEG/EMG implantation technique described above allows for the precise and reproducible insertion of the electrodes that target bilaterally the frontal and occipital cortices at a defined and consistent depth, where the electrode is touching the dura with minimal trauma to

surrounding tissues.

Following the implantation of the EEG/EMG electrodes, the mice were housed individually and the head-mounted connector was using a 15cm light weight cable to a slip ring commutator, which was suspended from a counter-balanced arm mounted to a standard rodent cage. This allows free movement of the tethered mice in the cage. Food and water was provided ad libitum. All mice were allowed to recover from surgery and habituated to these conditions for greater than ten days before recordings. For sleep monitoring, each mouse was recorded for three consecutive 24 hour periods, beginning at lights off at 19:00. Mice were not disturbed during this period except for daily checks of food and water at 19:00. All EEG/EMG signals were amplified using a Grass Model 78 (Grass Instruments, West Warwick, RI) and filtered (EEG: 0.3-100Hz, EMG:30-300Hz) before being digitized at a sampling rate of 250Hz, displayed on a custom paperless polygraph system, and archived to CD-R for offline sleep staging and analysis. Each EEG/EMG record was divided into 20 second epochs and visually scored as “Awake,” “REM sleep,” and “non-REM sleep” according to standard criteria for rodent sleep states (Rafulovacki 1984). Mice that had difficult or ambiguous EEG/EMG signals were ignored for final analysis (one mouse in each genotype). Differences between knockout mice and wildtype mice were analyzed using repeated

measurements ANOVA and student t-test as necessary (Graphpad Prism v4.00).

Running Wheel Behavior. These studies were conducted at UT Southwestern. Adult N10-C57BL/6J female GPR7 mice (age 14-17 weeks) that were previously used for the open field tests (see details below) were placed in a running wheel system (Mimitter's Vital view system) and had free access to food and water. Eight total cages (4 per genotype) were run simultaneously. The mice were acclimated for a week on a 12 hour LD (light:dark) cycle. After the initial week of LD cycle running, another week of LD cycle was recorded before the light cycle was switched to a DD (dark:dark) cycle. All measurements were automatically recorded in 10 minute interval or bin sizes by the given software. Analysis was made offline. Tau (periods) were calculated using a freely available software program (<http://www.circadian.org/software.html>) based on the chi-square periodogram analysis procedure developed by Sokolove and Bushell (Refinetti, 1993; Sokolove and Bushell, 1978). For the data collected for analysis, bin size was set at 10 minutes with a step set at 0.2. For each LD or DD cycle, 7 days of measurements were analyzed.

Open Field Test. N10-C57BL/6J Male and female GPR7 mice naïve to the open field

apparatus were used. Two different apparatus were used for the studies. The initial studies were conducted on adult mice (13 to 19 weeks of age) at UT Southwestern. All mice were acclimated to the test room for at least two hours prior to the experiment. An Accuscan (Versamax) system was employed with an open field test apparatus of 36 X 36cm in dimensions with 15 X 15 infrared beam arrays with 2.4cm interval. Each individual mouse was placed in the center of the test apparatus and allowed to freely move for 15 minutes. All tests were conducted during the light cycle (13:00 to 17:00). Two animals of each genotype were simultaneously tested. After each test, the animals were returned to their home cages, and the apparatus was thoroughly cleaned with 30% ethanol and dried completely before the next test run. Scoring was conducted automatically by the Accuscan system and analyzed offline.

The second set of studies was conducted at Rockefeller University with adult mice 16 to 20 weeks of age essentially as described before (Romeo et al., 2003). On the day of testing the mice were transferred to the testing room and allowed to acclimate for at least two hours prior to the experiment. All tests were conducted during the animal's light cycle (13:00 to 17:00) and lasted for 15 minutes per animal. The open field test apparatus consisted of a 70 X 70 X 30cm field with a grid floor composing of 25 squares (16 outer and 9 inner) that were 14 X 14cm each. A single 150-W light bulb provided

illumination for the test. Each animal was singly placed in the same corner of the open field apparatus at the beginning of the test and allowed to freely move within the apparatus. The experimenter was not in the room during the duration of the test. At the end of the test, the animal was returned to its home cage, and the open field apparatus was thoroughly cleaned with 30% ethanol and dried to remove any trace of ethanol. Scoring for the test was conducted offline. All four paws had to cross the line of a center square to be considered an entry into the center of the open field. The overall testing environment between the two studies, Rockefeller University and UT Southwestern, were unfortunately not uniform with separate and different testing apparatuses and conditions.

Elevated Plus Maze. The elevated plus maze tests were conducted in the same Rockefeller University behavior test room as with the open field tests during the light cycle (13:00 to 16:00) as described before (Romeo et al., 2003). The same animal from the open field tests were used two days after the open field tests and were naïve to the elevated plus maze. The maze apparatus was 40.6cm above the floor and each arm of the plus maze was 64.77cm long and 5.08cm wide. The two closed arms have 22.86cm high black plastic walls. At the beginning of the test, each animal was placed in the

center of the elevated plus maze facing an open arm. All tests were conducted with the same illumination conditions as with the open field and were recorded for five minutes with the same videotaping setup with the experimenter outside the test room. At the end of each test, the animal was returned to its home cage, and the elevated plus maze was cleaned with 30% ethanol. Scoring was conducted offline blind to the genotype. All four paws had to cross the entry of the open or closed arm to be considered an entry.

Porsolt Forced Swim Test. The Porsolt forced swim test was conducted essentially as previously described based on a modification of the original forced swim test (Lucki, 1997; Lucki et al., 2001; Porsolt et al., 1977a). Adult N10-C57BL/6J male GPR7 mice (n=5-8 per genotype) 18 to 22 weeks of age were acclimated to the behavior test room for at least two hours prior to testing. A 4 liter cylinder (17cm diameter, Nalgene) was filled to a depth of 17cm with tap water that was acclimated to room temperature overnight. Videotaping was conducted in a similar fashion as previous behavior experiments. The observer was in the same room behind an opaque screen monitoring the mouse in the order to observe for any sign of overt distress while in the water cylinder. The first swim test was performed with the male mice group housed with their littermates. The second test was performed with the identical set of mice after four weeks of single

cage isolation. For each test, the mouse was individually placed into the swim cylinder. The videotape was set to record for fifteen minutes. After each swim, the mouse was placed into a clean cage and allowed to dry itself. The water in the swim cylinder was replaced and cleaned as needed. Analysis of the tapes was made offline. The first two minutes for each swim test was ignored and the next four minutes were observed for time of immobility. Immobility of the mouse was defined as when a mouse makes only the minimal movements needed to keep the head afloat.

Statistics. All values are reported as means \pm s.e.m. Results were analyzed by unpaired Student's t-test for comparison of two means or ANOVA followed by analysis using Tukey's or Dunnet's post-test for comparisons of three or more means (Prism version 4.00 for Windows, GraphPad Software, San Diego, CA). *P* values less than 0.05 were considered as significant.

Fried Ginger Chicken Recipe. All recipes have been approved by the Taste Buds of Higher Eating. Cut skinless, boneless chicken thighs (free range chicken, not Purdue) to bite-size pieces. Marinate overnight (or greater than 30 minutes) in special sauce at 4°C. Special sauce was made with 1 part soy sauce (Kikkoman or equivalent); 0.5-1 part *mirin*

(alternatively *sake* with sugar added) and ginger juice to taste. Ginger juice was extracted from freshly grated gingers (peel skin from ginger before grating). Pat dry marinated chicken thighs with paper towel and cover with corn starch (pat down lightly but remove any excess starch). Heat vegetable oil (Crisco or equivalent) in frying pan to medium temperature (170-180°C). Deep fry for 2-3 minutes until chicken turns golden brown. Sprinkle with sea salt while still hot and serve. Garnish with lemon slice if desired.

Miso flavored Eggplant and Peppers. Prepare *miso* sauce by bringing 150ml *mirin* and 0.5 to 1.5 part *sake* to boil for 20 seconds to evaporate alcohol. Turn heat down to low and add 450g miso paste (use white for a lighter taste, red for stronger) and mix with wooden spoon until paste dissolves. Constantly mix with spoon to prevent *miso* from burning. Add granulated sugar (225g) to *miso* paste while mixing. Turn heat off when sugar has completely dissolved and allow to cool to RT. Wash and cut vegetables (Japanese eggplant, yellow onions, green and red bell peppers) to appropriate size (I prefer lengthwise slices of about 2 to 4cm each). After making sure vegetables are dry marinate in the *miso* sauce for 20 minutes or longer at 4°C or RT. Heat cooking oil (use vegetable or sesame oil) in wok and stir-fry vegetables to taste.

Chapter 3: Results

Gene Targeting Strategy. The following gene targeting strategy was adopted (Figure 13a). An Internal Ribosomal Entry Site (IRES) followed by a tau-Enhanced Green Fluorescent Protein (EGFP) cassette was introduced into the mouse genomic sequence of GPR7 to disrupt the sequence. Specifically, the insertion was in the putative third transmembrane region (amino acid 112) of the orphan GPCR. Directly upstream of the insertion of the cassette a STOP codon was also placed. The IRES-tau-EGFP knock-in GPR7 knockout strategy should result in disruption of the gene as well as EGFP labeling of neurons that would normally express GPR7. A similar strategy was adopted in the knockout of the neuropeptide Y Y2 receptor by Naveilhan et al. (Naveilhan et al., 1999). Instead of EGFP labeling, their cassette for disruption was IRES-tau-LacZ. This group was able to successfully knockout gene expression of NPY Y2 receptor and to identify neurons normally expressing Y2 receptor by immunohistochemistry. With the targeting construct finished, we proceeded to inject the construct into 129/Ola ES cells using standard homologous recombination techniques to generate a chimeric mouse. Four chimeric mice were generated, and one founder line was generated with successful germ line transmission.

Generation of GPR7^{-/-} Mice. Genotype was determined by Southern blotting of tail genomic DNA (Figure 13b). An intercross between heterozygote littermates produced wildtype (+/+), heterozygote (+/-), and knockout (-/-) mice in Mendelian ratios. Northern analysis and quantitative RT-PCR of hypothalamus from GPR7^{-/-} mice confirmed a lack of full length intact GPR7 RNA (Figure 13c-d). Mice were initially analyzed on a mixed 129Ola/BL6 strain; however, in order to minimize strain effects for

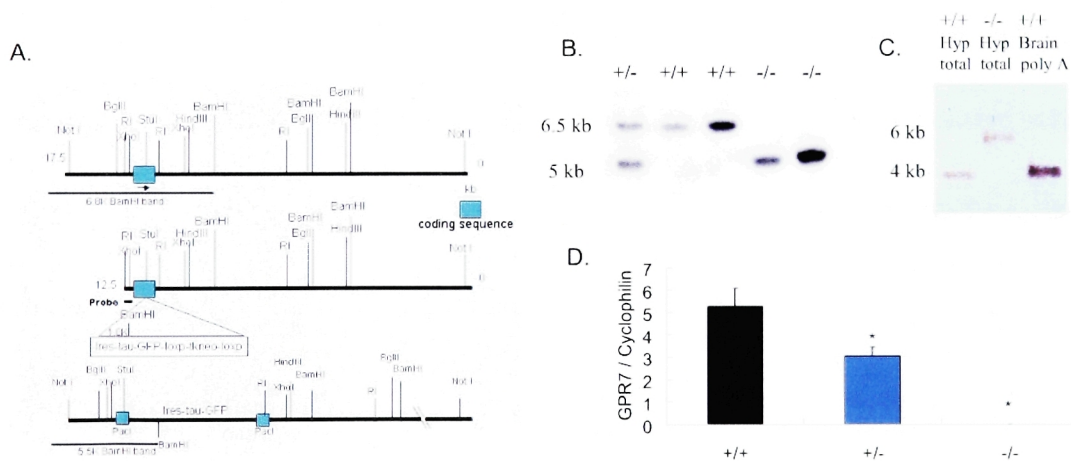


Figure 13) Gene targeting strategy and confirmation of *GPR7* deletion. A) Map of gene targeting strategy for insertion of IRES-tau-GFP cassette into mouse *GPR7*. B) Tail genomic DNA Southern blot of heterozygous brother-sister mating (6.5kb is wildtype band; 5kb is recombinant band). C) Northern blot of hypothalamic and brain RNA for *GPR7* (4kb is wildtype transcript; 6kb is transcript with insertion). *GPR7* Northern probe targeted upstream of insertion site. D) *GPR7* Taqman® real-time RT-PCR analysis of hypothalami from adult male *GPR7*^{+/+}, *GPR7*^{+/-}, and *GPR7*^{-/-} mice (n=6/group). Taqman® *GPR7* probe spanned insertion site. * denotes p<0.05 compared to *GPR7*^{+/+} levels.

phenotypic analysis, mice were backcrossed to C57BL/6J mice for six or more generations unless otherwise noted. The phenotypic differences seen in the GPR7^{-/-} mice between the mixed 129Ola/BL6 strain and the C57BL/6J strain are minimal, and both strains showed essentially the same metabolic phenotype when studied until one year of age.

Effect of GPR7 Disruption on Body Weight and Composition. GPR7^{-/-} mice were viable, fertile, and showed no gross abnormalities from birth to weaning. By 10 weeks of age, a significant increase in body weight ($25.4 \pm 0.4\text{g}$ $+/+$ versus $26.9 \pm 0.4\text{g}$ $-/-$, $p < 0.05$) was evident in the N6-C57BL/6J male GPR7^{-/-} mice (Figure 14). This increase in body weight was evident throughout adulthood and was even more pronounced by 52 weeks of age ($37.1 \pm 1.2\text{g}$ $+/+$ versus $42.5 \pm 1.9\text{g}$ $-/-$, $p < 0.05$) (Figure 14b and Figure 15). Furthermore, when the mice were fed a high fat diet (45% kcal fat), the difference was markedly increased and also evident at an earlier age ($29.4 \pm 0.5\text{g}$ $+/+$ versus $35.8 \pm 1.4\text{g}$ $-/-$ at 24 weeks of age, $p < 0.05$; Figure 14c).

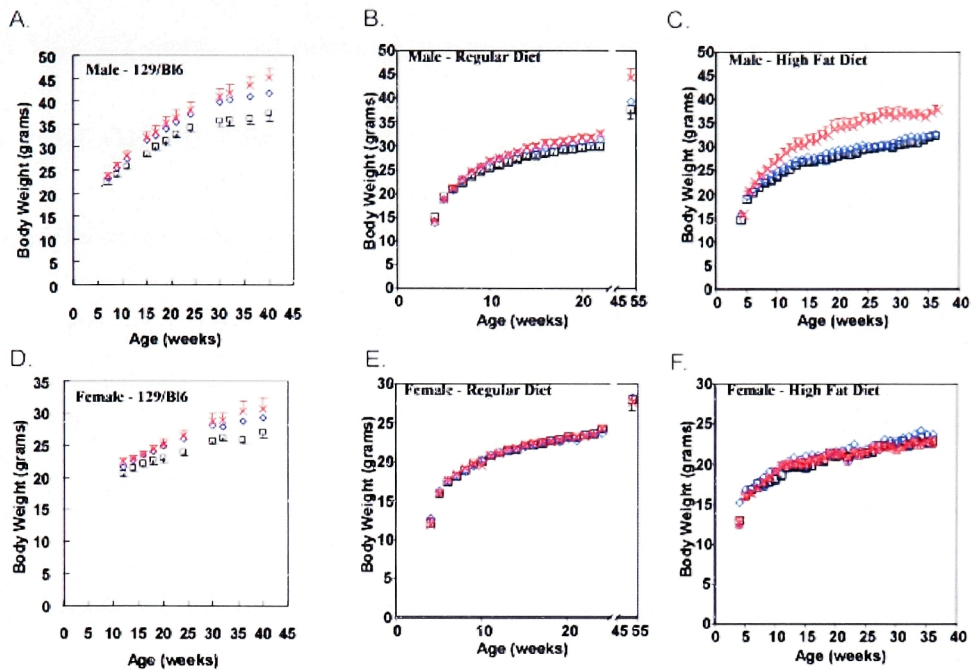


Figure 14) Body weight curves of male GPR7 mice (a-c) and female GPR7 mice (d-f). Mice are either N3 (52 week old mice only) or N6-C57BL/6J (b-c, e-f) or mixed 129Ola/BL6 (a, d) fed a standard low-fat diet (a-b, d-e) or a high fat diet (c, f). $n > 6$ for all genotypes in all groups. $p < 0.05$ from 10 to 52 weeks all male on low fat diet, 6-12, 17-32 weeks for high fat diet. $p > 0.05$ for all female mice.

Body composition was evaluated by carcass analysis of mice at 24 and 52 weeks of age fed a low fat diet. At 24 weeks of age, there was a trend towards higher total body lipid mass in male GPR7^{-/-} mice (Figure 16c, Table 2). At 52 weeks of age, the total body lipid mass in male GPR7^{-/-} mice was double that of GPR7^{+/+} mice with GPR7^{+/-} mice having an intermediate phenotype (5.83 ± 0.74 g ^{+/+} versus 11.25 ± 1.26 g ^{-/-}, $p < 0.05$; Figure 16d, Table 2). Full gross and histological necropsy studies were conducted on a set of older adult male GPR7^{-/-} mice on the original 129/BL6 strain and

the N3-C57BL/6J strain. At necropsy, a pale enlarged liver was evident in the 129/BL6 and the N3-C57BL/6J GPR7^{-/-} male mice. Liver histology showed large vacuoles throughout the entire liver section consistent with severe hepatic steatosis (Figure 17c, d). Hepatic steatosis or fatty liver is a clinicopathologic syndrome that is commonly associated with obesity and the metabolic syndrome (Angulo, 2002). While there was a dramatic fat accumulation throughout many tissues including the grossly fatty livers and increased amounts of subcutaneous fat, there were no other gross histological abnormalities in all the major organs investigated (Figure 17).

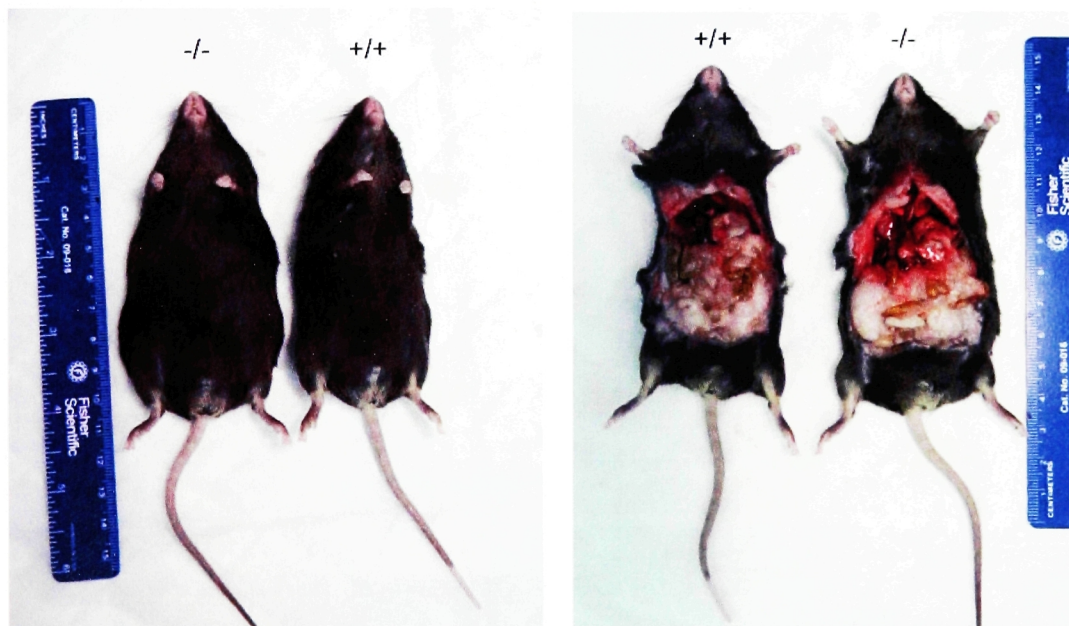


Figure 15) Gross necropsy of representative 52 week old male N3-B16 GPR7^{+/+} and GPR7^{-/-} littermates. No obvious abnormalities or lesions were detected except for an increase in general adiposity and an enlarged grossly fatty liver in GPR7^{-/-} mice.

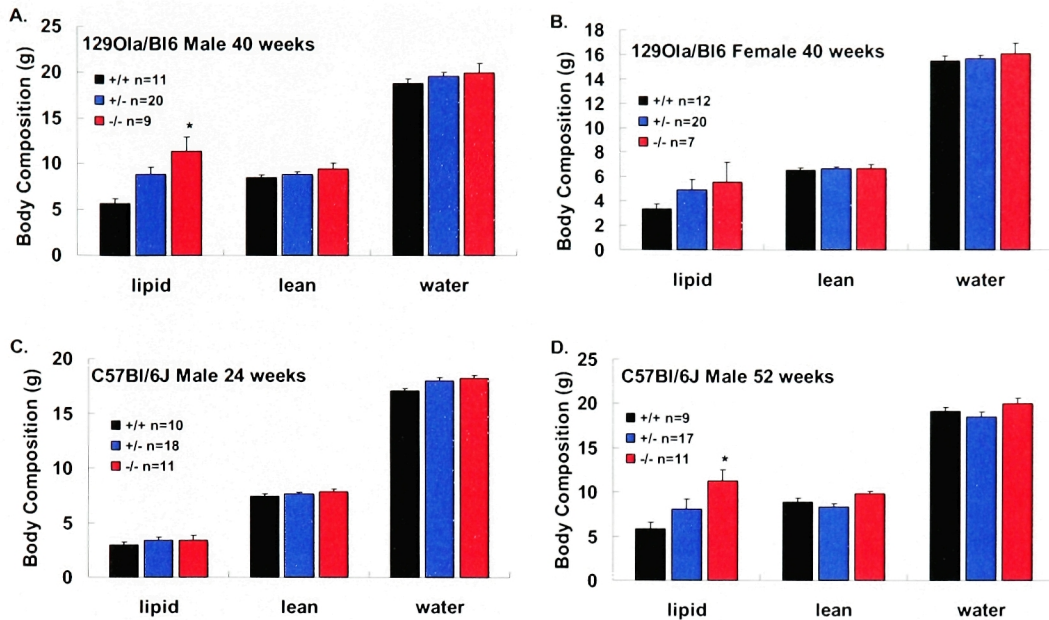


Fig 16) Body composition analysis of GPR7 mice. A-B) 40 week old adult male (A) and female (B) GPR7 mice from the original 129Ola/BL6 strain. Male GPR7^{-/-} mice had a significant increase in total lipid mass compared to GPR7^{+/+} littermates ($p < 0.05$). Female GPR7^{-/-} mice had a statistically insignificant trend towards increased adiposity. C) 24 week old male GPR7^{-/-} mice (N6-C57BL/6J) had a slight trend towards increased adiposity compared to GPR7^{+/+} littermates. D) 52 week old male GPR7^{-/-} mice (N3-C57BL/6J) had a significantly increased total lipid mass compared to GPR7^{+/+} littermates. This was similar in magnitude to the adiposity seen in the mixed 129Ola/BL6 strain.

Table 2: Percent body composition of male GPR7 mice (young and old)

% Body Composition	24 week old Male GPR7 Mice			52 week old Male GPR7 Mice		
	+/+ (10)	+/- (18)	-/- (11)	+/+ (9)	+/- (17)	-/- (11)
% Lipid	10.57 ± 0.96	11.58 ± 0.92	11.45 ± 1.24	16.92 ± 1.77	21.89 ± 2.19	26.75 ± 2.15*
% Lean	27.11 ± 0.42	26.28 ± 0.38	26.69 ± 0.41	26.12 ± 0.78	24.22 ± 0.88	24.17 ± 1.07
% Water	62.32 ± 0.77	62.14 ± 0.90	61.86 ± 1.11	56.96 ± 1.64	53.89 ± 1.58	49.07 ± 1.32*

* denotes a significant difference compared to same age GPR7^{+/+} littermate controls. Number of animals in each genotype group is designated in parentheses. 24 week old mice are N6-C57BL/6J, while 52 week old mice are N3-C57BL/6J mice.

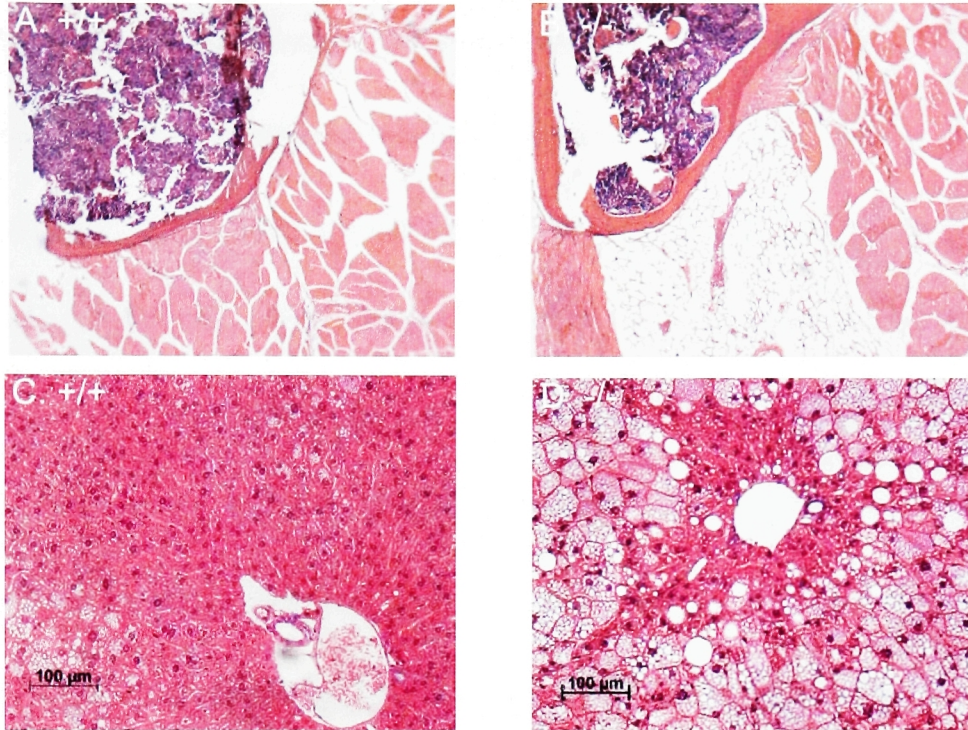


Figure 17) Increased fat acclimation in tissues and hepatic steatosis in older male GPR7^{-/-} mice. All sections were from formaldehyde treated samples that were stained with H&E. A-B) Tissue surrounding sternum with increased fat acclimation in GPR7^{-/-} mice (B). Magnification 100x (A-B). C-D) Liver sections showing hepatic steatosis in GPR7^{-/-} mice (D). Magnification 200x (C-D).

While these metabolic abnormalities were readily evident in the male GPR7^{-/-} mice, the female GPR7^{-/-} mice had at best a mixed phenotype. Initially, 129/BL6 mixed female GPR7^{-/-} mice did show a trend towards an increase in body weight and fat mass similar to male GPR7^{-/-} mice (Figure 14d, Figure 16b). However, female GPR7^{-/-} mice did not show any significant differences in body weight or fat mass when fed a low or high fat diet once on a pure C57BL6/J background (Figure 14e-f).

Metabolic Defects: Food Intake, Metabolic Rate and Locomotor Activity. We next investigated the energy intake and output in adult male GPR7 mice. Food intake in 24 week old male GPR7^{-/-} mice was consistently increased by 10% compared to GPR7^{+/+} littermates (Figure 18). Male GPR7^{-/-} mice on a regular diet had decreased resting oxygen consumption ($3,260 \pm 116 \text{ ml/kg/hr}$ ^{+/+} versus $2,860 \pm 80 \text{ ml/kg/hr}$ ^{-/-}, $p < 0.05$; Figure 19a), decreased carbon dioxide production ($2,800 \pm 133 \text{ ml/kg/hr}$ ^{+/+} versus $2,350 \pm 83 \text{ ml/kg/hr}$ ^{-/-}, $p < 0.05$; Figure 19b), and decreased spontaneous locomotor activity during the dark cycle (12 hour dark cycle: $29,100 \pm 2,390$ beam breaks ^{+/+} versus $20,900 \pm 2,310$ beam breaks ^{-/-}, $p < 0.05$; Figure 20a, b). The combination of hyperphagia and decreased energy expenditure, possibly in part due to decreased spontaneous locomotor activity, is a likely cause of the adult-onset obesity seen in the GPR7^{-/-} male mice. Female GPR7^{-/-} mice showed a slight statistically insignificant trend towards an increase in metabolic rate when compared to GPR7^{+/+} littermates (resting VO_2 : $3,650 \pm 200 \text{ ml/kg/hr}$ ^{+/+} versus $4,100 \pm 140 \text{ ml/kg/hr}$ ^{-/-}; $p > 0.05$; resting VCO_2 : $3,200 \pm 710 \text{ ml/kg/hr}$ ^{+/+} versus $3,700 \pm 390 \text{ ml/kg/hr}$ ^{-/-}; $p > 0.05$; Figure 19c, d). Female GPR7^{-/-} mice did show a similar trend of decreased spontaneous locomotor activity (12 hour dark cycle: $61,500 \pm 18,500$ beam breaks ^{+/+} versus $46,800 \pm 12,000$ beam breaks ^{-/-}, $p > 0.05$; Figure 20c, d) as seen with male GPR7^{-/-} mice.

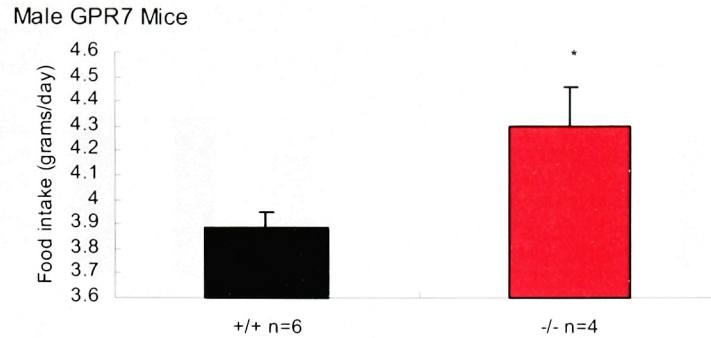


Figure 18) Food intake of adult male GPR7 mice. 24 week old mice were individually caged for greater than four weeks before weekly food intake of regular rodent chow was measured. Food intake was measured at least on four different occasions with two different sets of male mice. Representative data is shown here. * denotes $p < 0.05$ compared to GPR7 $^{+/+}$ littermates.

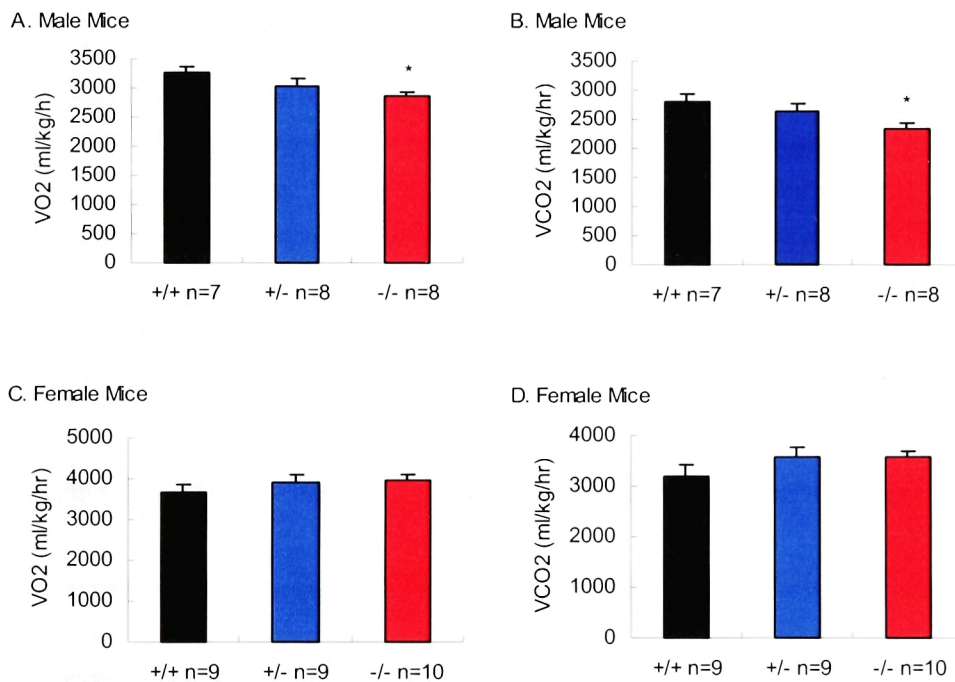


Figure 19) Resting metabolic rate for adult N6-C57BL/6J GPR7 mice on a standard low-fat rodent chow. Data is an average of a 24 hour cycle. A-B) Adult male mice 24 weeks old. C-D) Adult female mice 24 weeks old. * denotes a significant difference compared to GPR7 $^{+/+}$ mice ($p < 0.05$). Male GPR7 $^{-/-}$ mice had significantly decreased resting VO₂ and VCO₂ even when normalized for lean body mass only (data not shown).

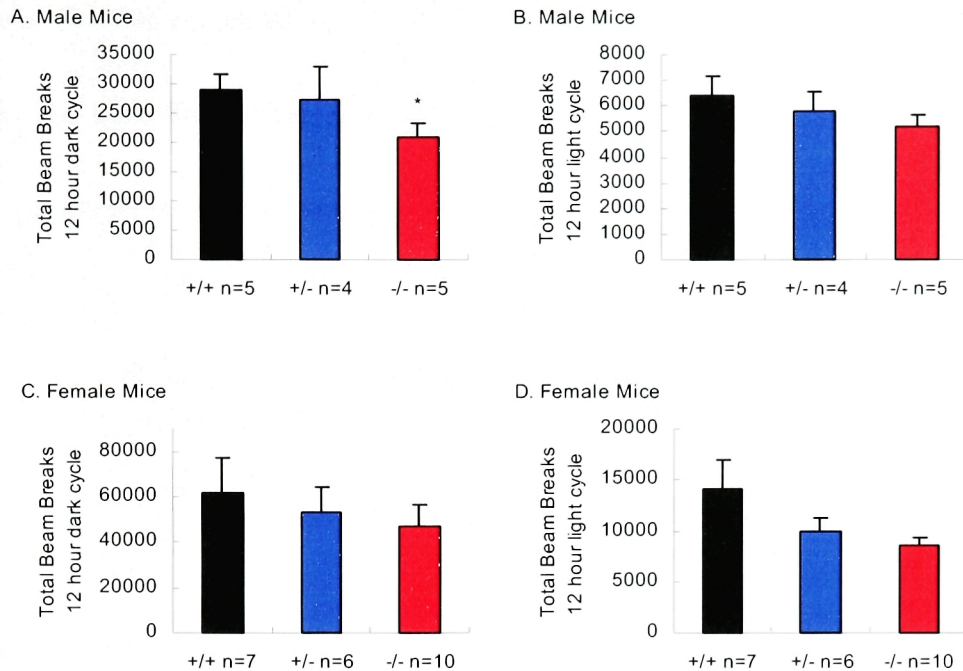


Figure 20) Locomotor activity for N6-C57BL/6J GPR7 Mice. A-B) Spontaneous locomotor activity for 24 week old male GPR7 mice during a 12 hour dark cycle (A) and 12 hour light cycle (B). * denotes significant difference when compared to GPR7+/+ mice. C-D) Spontaneous locomotor activity for 24 week old female GPR7 mice during a 12 hour dark cycle (C) and 12 hour light cycle (D). A trend towards decreased locomotor activity was seen for female GPR7-/- mice, but no significant differences were seen between the female groups at either dark or light cycle.

Plasma Values in GPR7-/- Mice. Analysis of plasma from 24 week old male mice on a regular diet showed normal glucose levels but a slight increase in insulin and a trend towards higher leptin levels in GPR7-/- mice (Table 3). By 52 weeks of age, GPR7-/- mice were hyperglycemic and remained hyperinsulinemic (Table 3). The older male GPR7-/- mice were also significantly hyperleptinemic. Leptin levels are highly correlated with percent body fat in mammals (Maffei et al., 1995). When the plasma

leptin levels were compared to percent body fat in male GPR7^{-/-} mice, they were found to have the same linear relationship as the GPR7^{+/+} mice (Figure 21). No significant differences were seen in the plasma levels of 52 week old female mice (Table 3).

Table 3: Plasma values for 24 week and 52 week old adult GPR7 male and female mice.

Sex, Age Genotype	Male 24 weeks old			Male 52 weeks old			Female 52 weeks old		
	+/+	+/-	-/-	+/+	+/-	-/-	+/+	+/-	-/-
Glucose (mg/dl)	208.6 ± 11.8	204.4 ± 13.6	202.2 ± 9.8	173.8 ± 8.86	200.1 ± 15.2	228.9 ± 12.6 [#]	185.6 ± 17.6	157.9 ± 7.97	149.8 ± 7.74
Leptin (ng/dl)	2.73 ± 0.61	3.40 ± 0.60	3.89 ± 0.56	11.53 ± 2.34	25.77 ± 8.33	50.10 ± 9.5 [#]	9.04 ± 3.03	6.58 ± 1.2	5.04 ± 0.32
Insulin (ng/dl)	0.76 ± 0.11	0.97 ± 0.16	1.28 ± 0.23 [*]	3.01 ± 0.62	4.12 ± 1.15 [!]	7.75 ± 3.02 [!]	1.16 ± 0.35	1.40 ± 0.50	0.73 ± 0.11

Student's unpaired t-test: ^{*} p<0.05 versus +/+; [#] p<0.005 versus +/+; [!] p<0.10 versus +/+; Differences not statistically significant unless noted. n=5-11 for each group. 52 week old mice are N3-C57BL/6J.

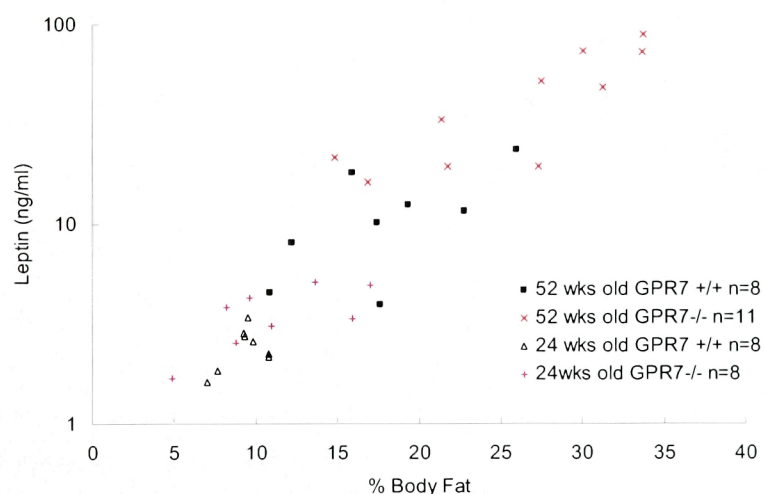


Figure 21) Linear relationship between plasma leptin levels and body fat percentage in male GPR7 mice. Adult male mice of 24 and 52 weeks of age had similar linear relationship between leptin and body fat regardless of genotype. Data was analyzed by bivariate linear regressions assuming two-sided normal distribution of all data using the software program Stata.

Fasting-induced Feeding Response in GPR7^{-/-} mice. As GPR7 signaling appears to be a “satiety” signal with mice lacking functional *GPR7* becoming hyperphagic and obese, the response to fasting-induced refeeding was measured in GPR7^{-/-} mice. 30 to 38 week old male GPR7^{+/+} and GPR7^{-/-} mice were fasted for 24 hours (beginning at 12:00) before reintroduction of food. GPR7^{-/-} mice significantly ate more food after the 24 hour fast than GPR7^{+/+} mice in the short and long term (Figure 22). This overcompensation was seen even though the two groups were matched for their body weights (GPR7^{+/+} male 35.0±1.1g versus GPR7^{-/-} male 35.6±1.1g; p=0.71; NS).

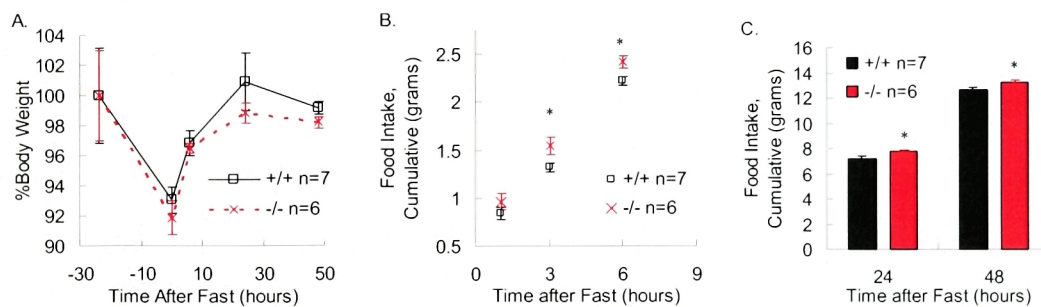


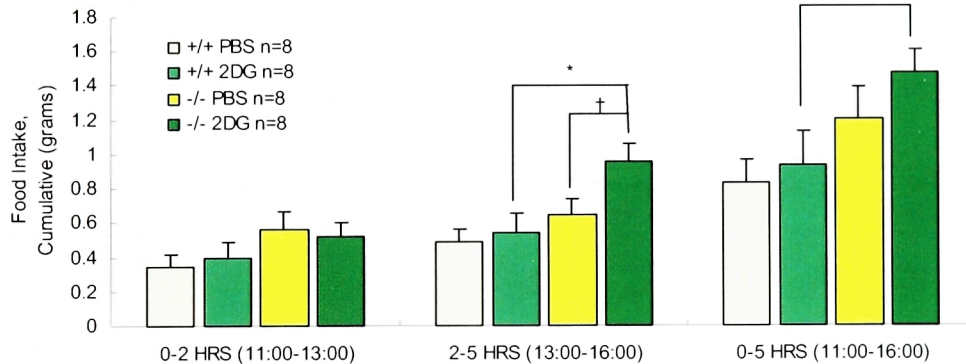
Figure 22) Feeding response of adult male GPR7 mice after a 24 hour fast (n=7 for GPR7^{+/+}; n=6 for GPR7^{-/-}). A) Percent body weight change after 24 hour fast. All mice were matched for their weights before the experiment. No significant difference between the groups was seen at all time points measured. B) Food intake during first few hours after the 24 hour fast. GPR7^{-/-} mice ate significantly more food than GPR7^{+/+} shortly after food was reintroduced. C) Food intake after 24 and 48 hours after the fast. GPR7^{-/-} mice continued to slightly eat significantly more than GPR7^{+/+} mice.

Glucoprivic Feeding in GPR7^{-/-} Mice – 2-deoxy-D-glucose. With the abnormal response to fasting-induced feeding, adult male GPR7^{-/-} mice's feeding response to decreased glucose utilization or glucoprivation was investigated by administering 2-deoxy-D-glucose (2DG). 2DG is a glucose analog that acts as a specific inhibitor of intracellular glucose utilization by directly inhibiting phosphohexose isomerase, which leads to a reduction in glycolysis, in brain, muscle, liver, and other tissues (Brown, 1962; Horton et al., 1973). Administration of 2DG to mammals leads to an increase in blood glucose levels and a robust feeding response (Smith and Epstein, 1969). This feeding response to 2DG persists even after the centrally mediated sympathoadrenal hyperglycemia subsides (Ritter et al., 1978). Furthermore, the effects of glucoprivation are centrally mediated as doses too low to have an effect peripherally will have an effect when injected into the lateral ventricles (Miselis and Epstein, 1975).

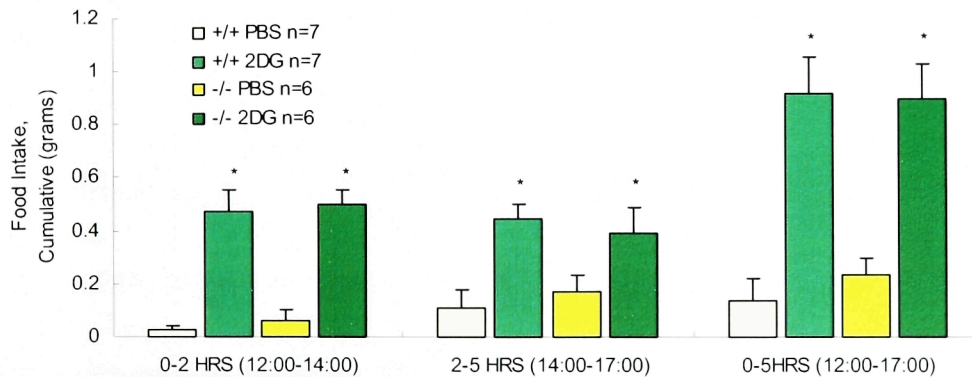
Adult male GPR7 mice were initially peripherally injected with a dose (500mg/kg body weight) known to elicit a robust glucoprivic feeding response in rodents. All mice at this dose regardless of genotype became obtunded and fell into a stupor. They remained in this stupor for up to 90 minutes after which they recovered without any long lasting ill effects. Glucoprivic induced feeding at this dose of 2DG was confounded by this stupor as GPR7^{+/+} failed to show an increase in feeding after 2DG

administration (Figure 23a). Another group of animals were tested using a lower but still effective dose of 2DG (250mg/kg body weight). At this lower dose of 2DG, no mice became obtunded, and both GPR7^{+/+} and GPR7^{-/-} mice displayed a normal response to glucoprivation (Figure 23b). Furthermore, central administration of 2DG also resulted in a normal glucoprivic feeding response in both GPR7^{+/+} and GPR7^{-/-} mice. Therefore, GPR7 signaling is not critical for feeding after a decrease in central glucose utilization.

A. Male GPR7 Mice - 500mg/kg BW 2DG



B. Male GPR7 Mice - 250mg/kg BW 2DG



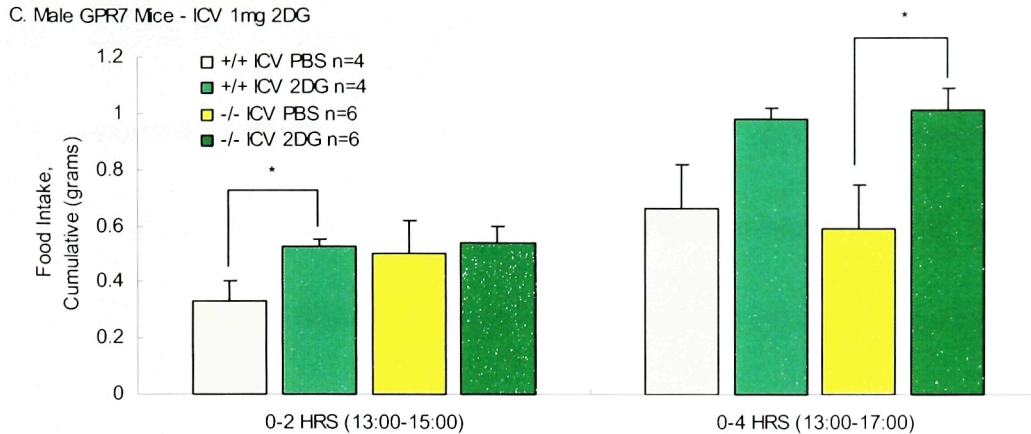


Figure 23) Response to glucoprivation by 2-deoxy-D-glucose in male GPR7 mice. A) Feeding response after a peripheral injection of 500mg 2DG/kg body weight. All mice became obtunded. B) Both GPR7^{+/+} and GPR7^{-/-} mice showed a similar robust increase in feeding after peripheral injection of a lower dose of 2DG (250mg/kg body weight) C) Feeding response to a single bolus ICV injection of 2DG (1mg/animal). Both GPR7^{+/+} and GPR7^{-/-} mice had an increase in food intake. * denotes $p < 0.05$ and † denotes $p < 0.1$.

Hypothalamic Neuropeptide Levels in GPR7^{-/-} Mice. To explore the possible role of the adipocyte hormone leptin in the pathogenesis of the obesity in male GPR7^{-/-} mice, we measured whole hypothalamic RNA levels of NPY and POMC using real time quantitative RT-PCR. Leptin is secreted from adipocytes into the blood stream and acts directly on the hypothalamus, where it reduces neuropeptide Y (NPY) expression and activates proopiomelanocortin (POMC) expression (Elmqvist et al., 1999; Friedman and Halaas, 1998; Zhang et al., 1994). In contrast to leptin deficient ob/ob mice, which have increased NPY levels and decreased POMC levels, NPY levels were decreased and POMC levels were increased in GPR7^{-/-} male mice (Figure 24a, b). Levels of MCH, an

orexigenic signal that is thought to be downstream of NPY and POMC, but still part of the leptin-regulated pathway, were identical in the GPR7^{+/+} and GPR7^{-/-} mice (Figure 24c) (Qu et al., 1996). These data suggest that the mechanism underlying obesity in GPR7^{-/-} mice is different from that evident in leptin deficient mice and that the NPY and POMC levels of these mice are more characteristic of a lean state.

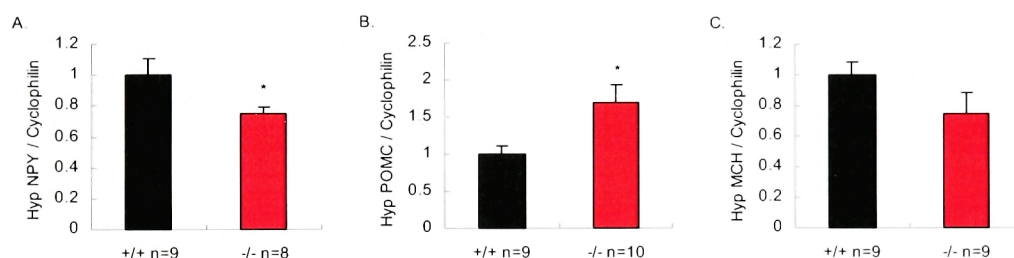


Figure 24) Hypothalamic neuropeptide expression levels in 24 week old N6-C57Bl/6J male GPR7 mice. Taqman® real-time RT-PCR was used to determine levels of NPY (A), POMC (B), and MCH (C) in hypothalami of adult male GPR7 mice. All data have been normalized to the cyclophilin levels and are shown as relative values compared to GPR7^{+/+} levels. * denotes a significant difference between GPR7^{-/-} and GPR7^{+/+} mice.

When expression levels for hypothalamic neuropeptides were investigated in older 52 week old adult male or female GPR7 mice, there was no change for either NPY or POMC levels (Figure 25). This lack of a coordinated compensatory response of decreasing NPY and increasing POMC levels seen in the younger male GPR7^{-/-} mice could also account for the obesity seen in the older male GPR7^{-/-} mice.

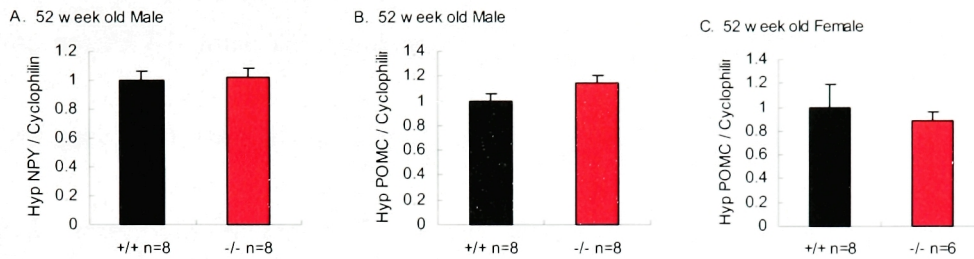


Figure 25) Hypothalamic levels of NPY and POMC in 52 week old N3-C57BL/6J GPR7 Mice. Taqman® real time RT-PCR was used to measure levels of NPY (A) and POMC (B-C) in 52 week old male (A-B) and female mice. By 52 weeks, all male GPR7^{-/-} mice were significantly heavier with increased adiposity and hyperleptinemia. No significant difference seen in any group compared to GPR7^{+/+} littermate control levels.

Body Weights and Metabolic Activity of ob/ob GPR7^{-/-} and Ay/a GPR7^{-/-} Mice. In order to establish whether the effect of a GPR7 mutation was independent of the orexigenic pathways activated by leptin deficiency, double mutant ob/ob GPR7^{-/-} mice were generated. The male double mutants (ob/ob GPR7^{-/-}) were more obese than standard ob/ob mice (16 weeks of age: 55.3±1.1g ob/ob ^{+/+} versus 60.0±1.1g ob/ob ^{-/-}, p<0.05; Figure 26a), while female double mutant mice weighed the same as normal ob/ob female mice at all ages (Figure 26b). Lethal yellow Agouti (Ay/a) mice, which have deficient melanocortin signaling, were also mated to generate Ay/a GPR7^{-/-} mice (Cone, 1999). Similar to the ob/ob GPR7^{-/-} animals, the male Ay/a GPR7^{-/-} mice were more obese than standard Ay/a male mice (16 weeks of age: 38.6±1.1g Ay/a GPR7^{+/+} versus 42.3±0.6g Ay/a GPR7^{-/-}, p<0.05; Figure 26c), while female Ay/a GPR7^{-/-} mice again had similar body weights to female Ay/a GPR7^{+/+} mice (data not shown). Furthermore,

male Ay/a GPR7^{-/-} mice ate significantly more food compared to male Ay/a GPR7^{+/+} mice (Figure 26d) but showed only a modest non-significant decrease in resting metabolic activity (VO₂: 2860±130ml/kg/hr Ay/a GPR7^{+/+} versus 2590±120ml/kg/hr Ay GPR7^{-/-}; Figure 27a, b) and locomotor activity (12hr dark cycle: 17900±3440 beam breaks Ay/a GPR7^{+/+} versus 15900±1500 beam breaks Ay/a GPR7^{-/-}; Figure 27c, d). The resting metabolic rate and locomotor activity was significantly decreased when Ay/a GPR7^{+/+} mice were compared to wildtype (a/a GPR7^{+/+}) mice (Figure 27c). These data strongly suggest that GPR7 affects energy homeostasis by a novel mechanism independent of the orexigenic pathways activated by defective leptin or melanocortin signaling.

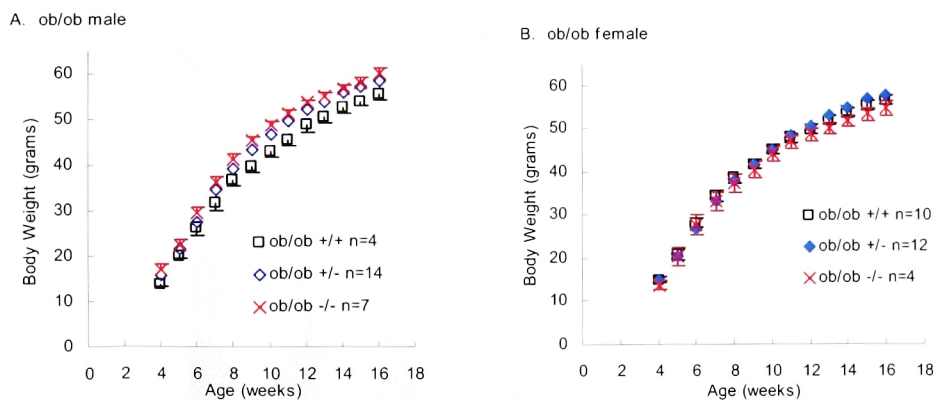


Figure 26 A-B) Body weight curve for ob/ob GPR7 mice. A) Body weight curve of male ob/ob GPR7 mice. Male ob/ob GPR7^{-/-} weighed significantly more than ob/ob GPR7^{+/+} mice ($p < 0.05$). B) Body weight curve of female ob/ob GPR7 mice. Female ob/ob GPR7^{-/-} had similar body weights when compared to littermate ob/ob mice. $p < 0.05$ for all male ob/ob GPR7^{-/-} from 8 to 16 weeks of age when compared to ob/ob GPR7^{+/+} mice.

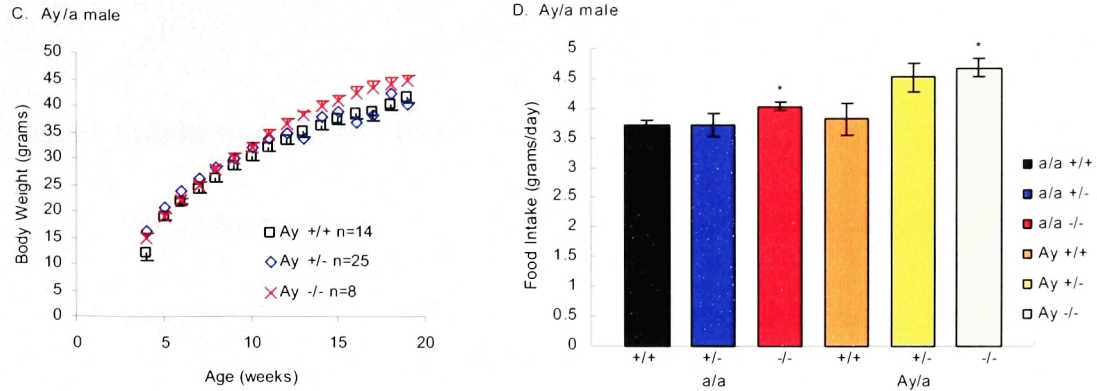


Figure 26 C-D) Body weight and food intake of double Ay/a GPR7 mice. C) Body weight curve of adult Ay/a GPR7 mice. Male Ay/a GPR7^{-/-} mice weighed significantly more than Ay/a GPR7^{+/+} mice ($p < 0.05$). D) Food intake in male Ay/a GPR7 mice. Male Ay/a GPR7^{-/-} mice ate significantly more than Ay/a GPR7^{+/+} mice ($p < 0.05$, $n = 4-6$ in all groups). $p < 0.05$ for all body weights of male Ay/a GPR7^{-/-} mice from 8 to 16 weeks of age.

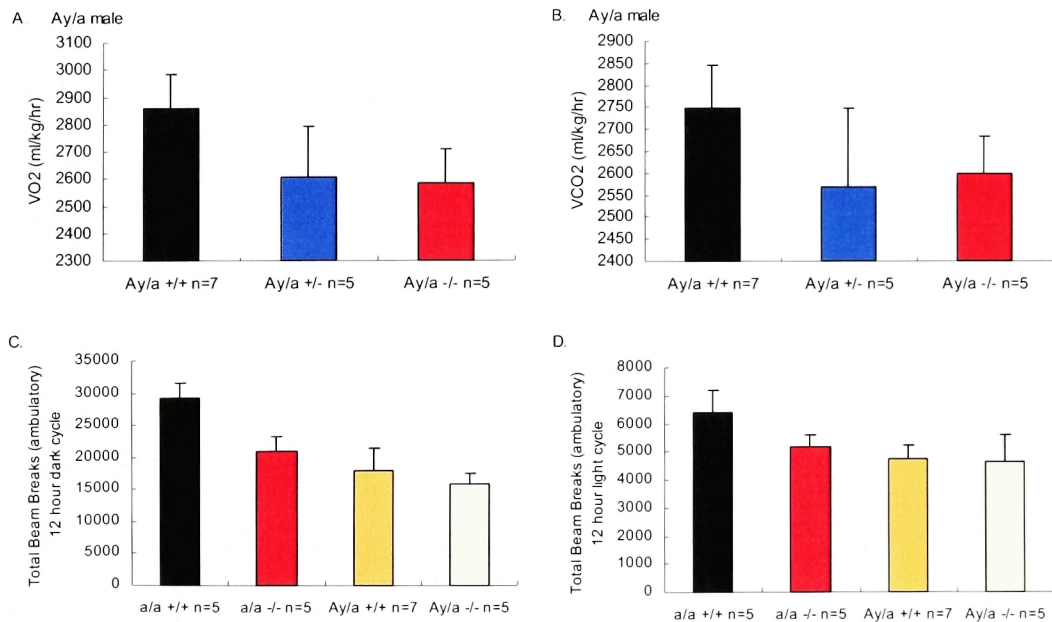


Figure 27) Metabolic and locomotor activity of 24 week old male Ay/a GPR7 mice. A) Resting oxygen consumption (VO₂) of Ay/a GPR7 mice. B) Resting carbon dioxide production (VCO₂) of Ay/a GPR7 mice. C-D) Locomotor activity comparison of a/a GPR7 and Ay/a GPR7 mice during the 12 hour dark cycle (C) and 12 hour light cycle (D). No significant difference for all data.

Ligand Activity and Binding Data to Mouse GPR7

The endogenous ligands for GPR7 have been recently identified by reverse pharmacology (Fujii et al., 2002; Shimomura et al., 2002; Tanaka et al., 2003). In these previous reports, the pharmacological studies used non-rodent samples to isolate and test the ligand binding and activity to GPR7 and GPR8. To determine whether the ligands for GPR7, NPB and NPW, possess the same activity and binding characteristics on mouse GPR7, a xenopus melanophore assay identical to one conducted for human GPR7 and GPR8 was conducted using cells transfected with the full coding sequence from the cloned mouse *GPR7* gene (Tanaka et al., 2003). The cells transfected with mouse *GPR7* had identical dose response curves to NPB and NPW when compared to cells transfected with human *GPR7* (Figure 28). Therefore, as expected, the cloned mouse sequence is the definitive mouse GPR7 sequence and is the endogenous receptor for the ligands NPB and NPW in mice.

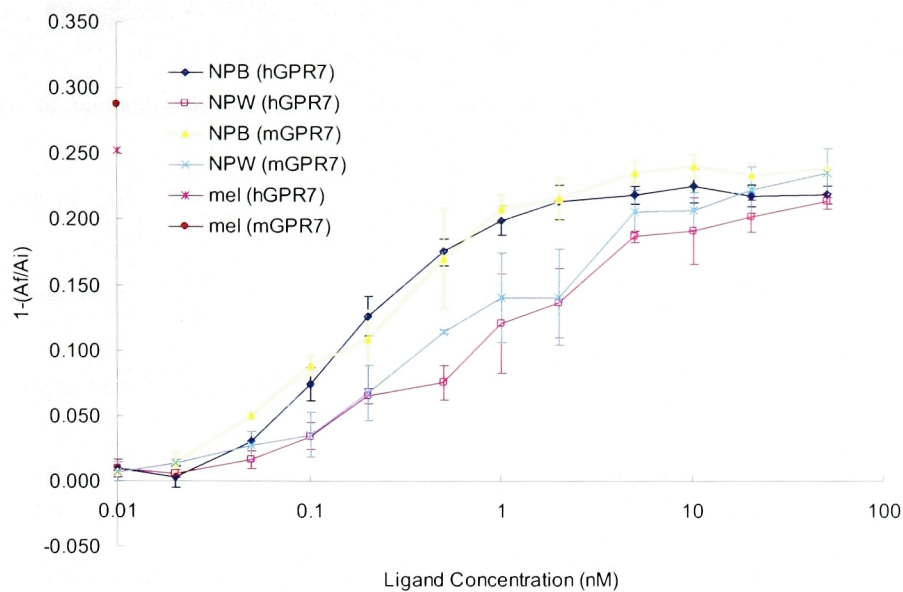


Figure 28) *Xenopus* melanophore assay for ligand binding to mouse GPR7. The assay was performed essentially as described before (Tanaka et al., 2003). NPB had a higher affinity for GPR7 (both human and mouse) compared to NPW. hGPR7 = human GPR7; mGPR7 = mouse GPR7; mel = melanosome positive control reaction.

Tissue Distribution of GPR7 and its ligands, NPB and NPW

GPR7 was initially cloned and found to have high RNA levels in various discrete areas of the rodent brain and the pituitary gland (O'Dowd et al., 1995). The ligands for GPR7 were also isolated from the brain of various species (Fujii et al., 2002; Shimomura et al., 2002; Tanaka et al., 2003). The gene expression profile of GPR7 and its ligands in other tissues outside the central nervous system in mice was explored. Select tissue RNA was isolated from adult male wildtype C57BL6/J mice, and gene expression of

GPR7 and its ligands NPB and NPW were analyzed by real time RT-PCR. GPR7 was expressed at appreciable levels only in neuronal tissues including hypothalamus and the spinal cord (Figure 29a). Very low levels were also seen in the stomach, lungs, and testis but not in the other peripheral tissues examined. These levels were only slightly above background levels, and their physiological relevance is unknown. For the GPR7 ligands NPB and NPW, high levels of gene expression were seen in the CNS as well as in peripheral tissues (Figure 29b, c). NPB had the highest levels in the spinal cord followed by testis, stomach and spleen. NPW had the highest levels in the lung, whereas neither GPR7 nor NPB showed any appreciable levels, followed by stomach, spinal cord, spleen, and hypothalamus. The high levels of gene expression of the peptides in tissues where GPR7 is not highly expressed suggests that these ligands could act as secreted endocrine hormones that are synthesized in these tissues and travel to the CNS or other areas that have high levels of GPR7. Furthermore, the disparate expression of the ligands could potentially account for any different physiological roles between them.

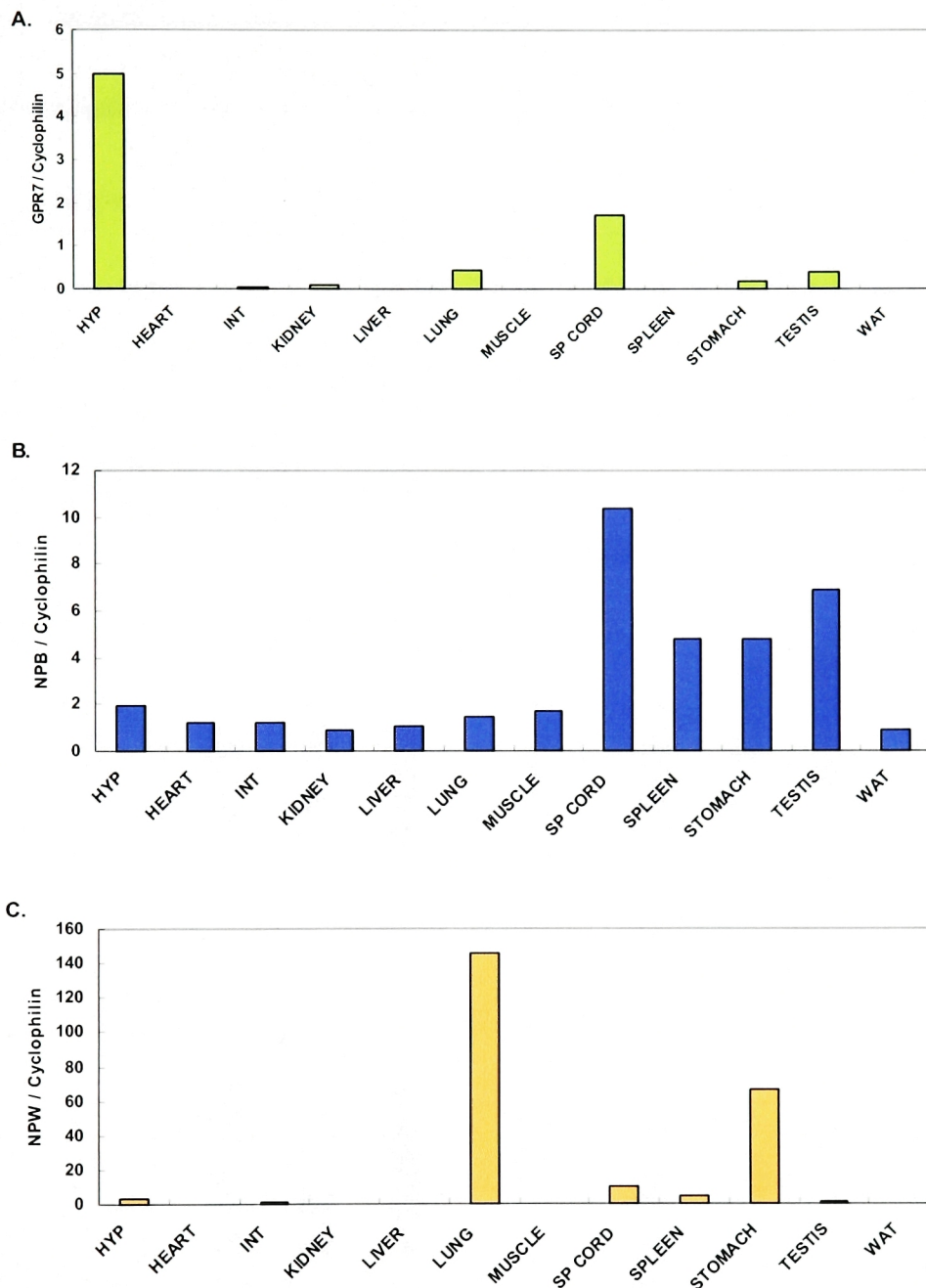


Figure 29) Tissue distribution of GPR7, NPB and NPW in mice. Taqman® real time RT-PCR was used to analyze differential tissue expression in an adult male C57BL/6J wildtype mouse for GPR7 (A), NPB (B) and NPW (C). All samples were normalized to cyclophilin expression levels and are expressed as a relative value compared to whole brain expression (i.e., a value of 1 is equivalent to the expression levels found in whole brain/cyclophilin). Hyp = hypothalamus; Int = small intestine; Sp cord = spinal cord; WAT = white adipose tissue.

The gene expression levels of the ligands, NPB and NPW, were investigated in the hypothalami of male *GPR7*^{-/-} mice. Neither NPB nor NPW changed expression levels to compensate for the loss of *GPR7* in either 24 or 52 week old male mice (Figure 30). This could be due to lack of transcriptional regulation of the peptide ligands in the hypothalamus or as a loss of compensatory changes in aging *GPR7*^{-/-} mice. The levels in peripheral tissue such as stomach were not measured.

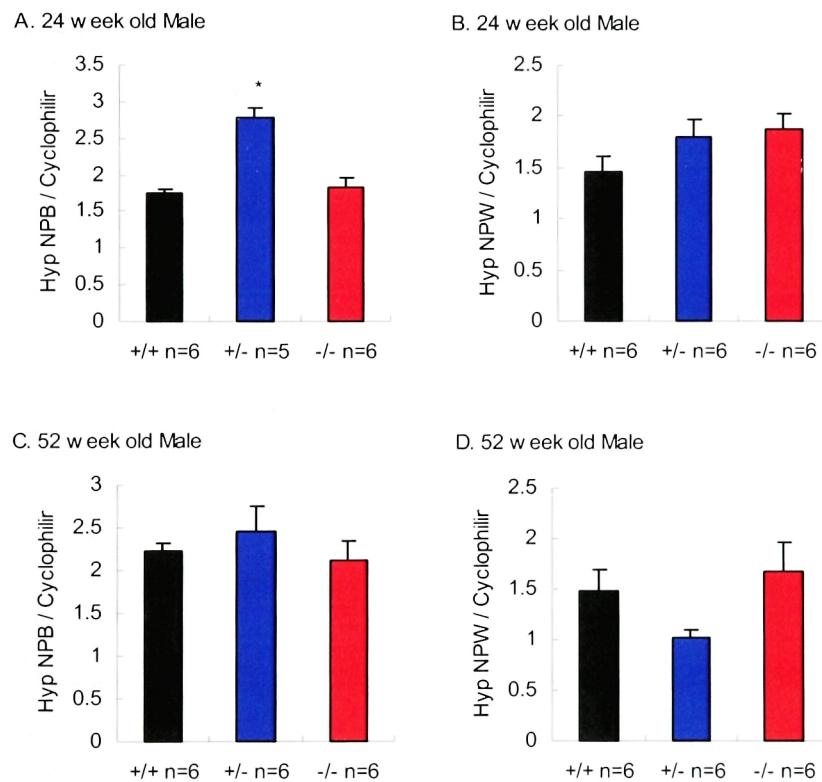


Figure 30) Hypothalamic NPB and NPW levels in adult *GPR7* mice. Taqman® real-time RT-PCR analysis was conducted on hypothalami from 24 week old (A-B) and 52 week old (C-D) adult male mice for NPB (A, C) and NPW (B, D). * denotes a significant difference compared to *GPR7*^{+/+} littermates from the same age group. Note that there is no significant difference between *GPR7*^{+/+} and *GPR7*^{-/-} mice for any of the gene expression levels at either age groups.

Effects of Feeding and Metabolic States on the Regulation of NPB, NPW, and GPR7

The data from the GPR7 knockout mice strongly suggested that NPB and NPW could serve as an anorectic signaling peptide ligand. Two separate age groups of male C57BL/6J wildtype mice were investigated for the effects of various feeding states on gene expression of GPR7 and its ligands in different tissues. The first younger set of 14 week old wildtype mice was separated into three different cages with five animals each. One group was fasted for 48 hours, another had the water bottle removed (thirsting group) for 48 hours, and the last group was a control group that had free access to both food and water. Both the fasted and thirsted group lost significant body weight compared to the control group (Figure 31a). The hypothalamic levels of NPB, NPW and GPR7 in each group under the three conditions (fed, fasted 48 hours, and thirsted 48 hours) were investigated. There was no significant difference in the hypothalamic levels of NPB or GPR7, but there was a modest trend towards decreased NPW levels after fasting (Figure 31b-d).

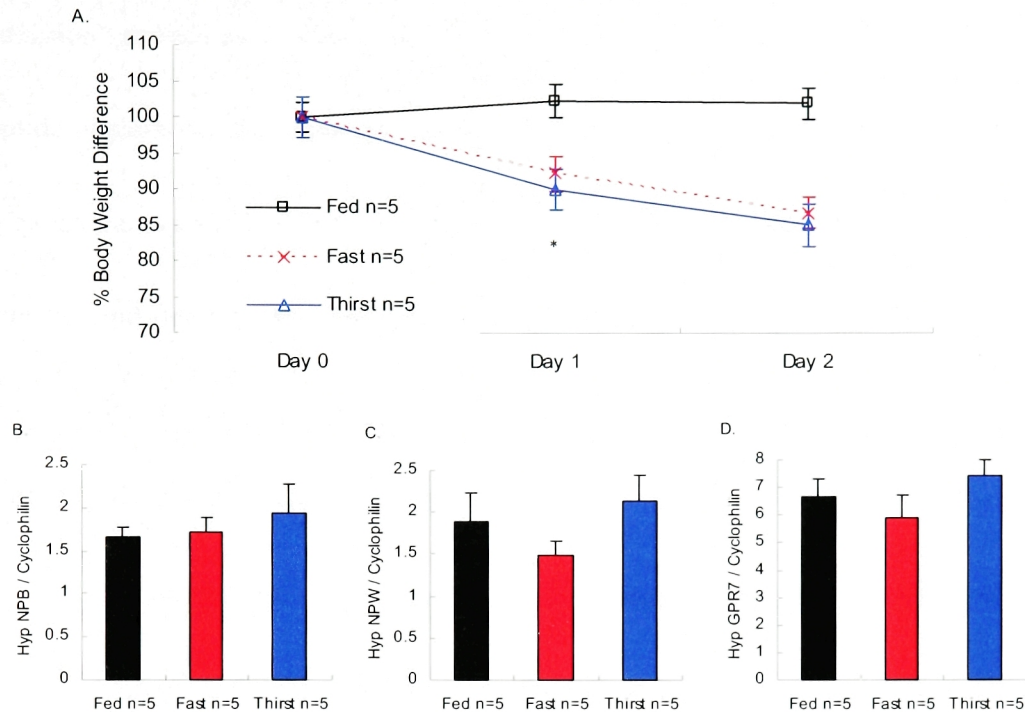


Figure 31) Effects of 48 hours of fasting and thirsting (dehydration anorexia) on hypothalamic NPB, NPW, and GPR7 gene expression levels. A) Percent body weight change under 48 hour fast or 48 hour dehydration anorexia conditions for young adult (14 week old) C57BL/6J male mice. Both fasting and thirsting mice weighed significantly less than fed control groups after 24 hours (day 1) and 48 hours (day 2). B-D) Hypothalamic levels of NPB (B), NPW (C), or GPR7 (D) under these conditions. No significant differences were seen in any of the different groups.

The older set of wildtype mice was separated into three different cages with five animals each. One group was fasted for 48 hours as before, the second group was fasted for 44 hours and food was reintroduced to the cages for 4 hours of refeeding, and the third group had free access to both food and water. The fasting group lost a significant amount of body weight compared to the fed control (Figure 32). The 4 hour refeeding group had noticeably distended stomachs and could represent a state of “gastric

distension” as well as a satiated state. Due to the high levels of gene expression of the peptide ligands in the stomach, it was hypothesized that NPB and/or NPW could potentially act as an anorectic gut peptide in a similar but opposite fashion as the recently identified gut peptide ghrelin (Kojima et al., 1999; Nakazato et al., 2001; Tschop et al., 2000). Therefore, levels of gene expression for the ligands were examined in the stomach as well as the hypothalamus.

As with the earlier experimental group, hypothalamic levels of NPB, NPW and GPR7 did not significantly change upon fasting or refeeding (Figure 33). However, stomach levels of NPW significantly decreased upon fasting (Figure 34b, d), while stomach levels of NPB paradoxically and in an opposite fashion increased with fasting and decreased significantly with refeeding (Figure 34a, c). NPW appears to follow a pattern typical of a catabolic signal, while NPB appears to be more similar to an anabolic signal. These opposing effects of fasting on stomach NPW and NPB could perhaps explain the biphasic feeding response seen after bolus ICV administration of the ligand (Tanaka et al., 2003).

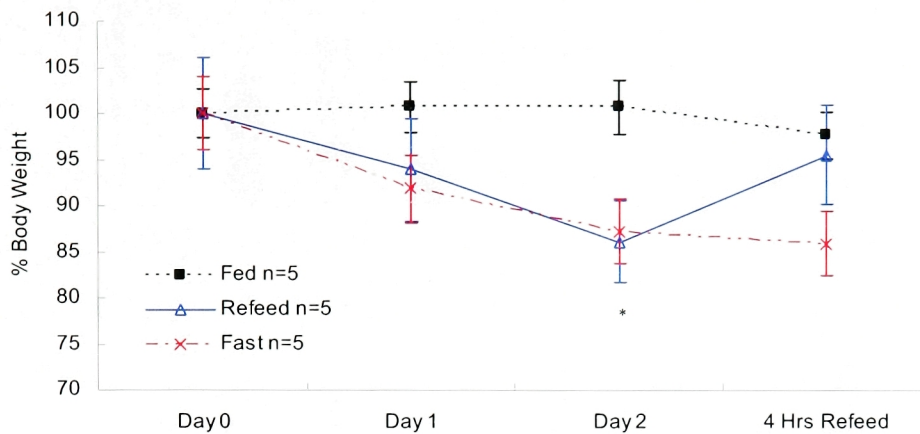


Figure 32) Change in body weight in adult male C57Bl/6J mice after a 48 hour fast. Mice were separated into three different groups: fed control group (black squares), 48 hour fasted group (red crosses), and a 44 hour fasted with 4 hour of refeeding group (blue triangle). After 44 hours of fasting, the fasted and refeeding groups had significantly lower changes in body weight compared to the fed control group ($p < 0.05$, $n = 5$ all groups)

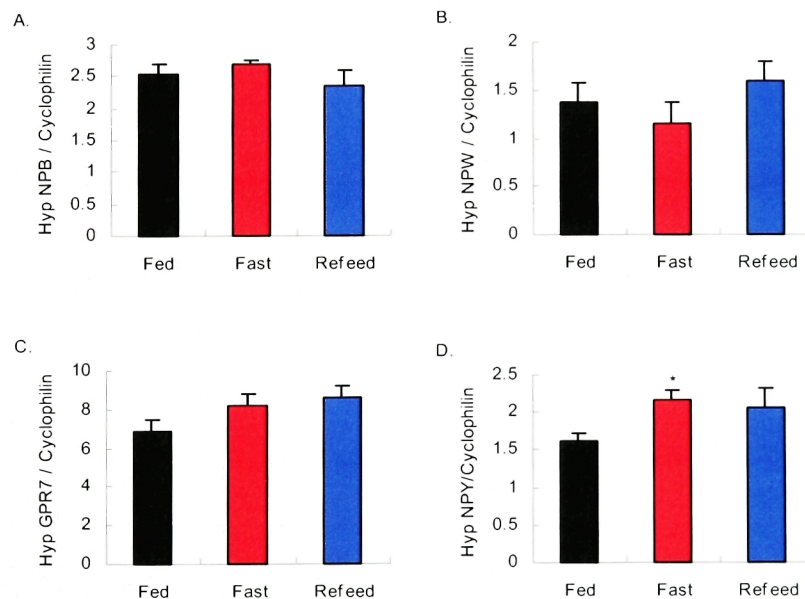


Figure 33) Hypothalamic expression levels after a 48 hour fast. Taqman® real-time RT-PCR analysis of hypothalamic levels of NPB (A), NPW (B), GPR7 (C), and NPY (D). Hyp = hypothalamic. * denotes a significant difference compared to fed states ($n = 5$ in all groups). All samples were normalized to cyclophilin levels as before.

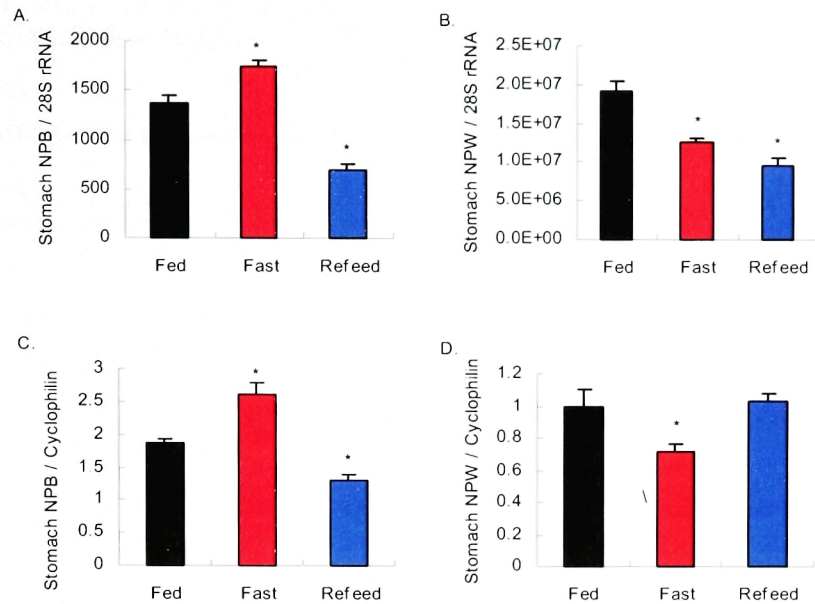


Figure 34) Stomach NPB and NPW expression levels after a 48 hour fast. A-B) Northern blot analysis of stomach NPB (A) and NPW RNA (B). All samples were normalized to UV intensity of 28S rRNA band. C-D) Taqman® real time RT-PCR analysis of the same samples. All samples were normalized to cyclophilin expression as before. * denotes a significant difference compared to fed states (n=5 in all groups).

Finally, possible regulation of stomach NPB and NPW by leptin was examined in female ob/ob mice that were chronically treated with a subcutaneous pump containing leptin (400ng/hour). Subcutaneous chronic leptin infusion at this high dose led to a dramatic decrease in body weight and food intake compared to PBS control ob/ob animals (Figure 35a, b). The effects were comparable to previously published results (Halaas et al., 1997; Soukas et al., 2000).

Previously, it was shown that disrupting GPR7 on an ob/ob background resulted in an additive body weight gain (Figure 26a). Hypothalamic neuropeptide profile of the

GPR7^{-/-} mice was also suggestive more of a lean state. Therefore, it appears that GPR7 signaling affects energy homeostasis independent of leptin signaling. This result was further confirmed when we analyzed the RNA or cDNA levels of stomach NPB or NPW in leptin treated ob/ob mice. While different metabolic states such as fasting can alter stomach levels of NPB and NPW, chronic leptin treatment for twelve days had no effect on NPB and NPW RNA levels compared to twelve day PBS treated or pair-fed animals (Figure 35c, d).

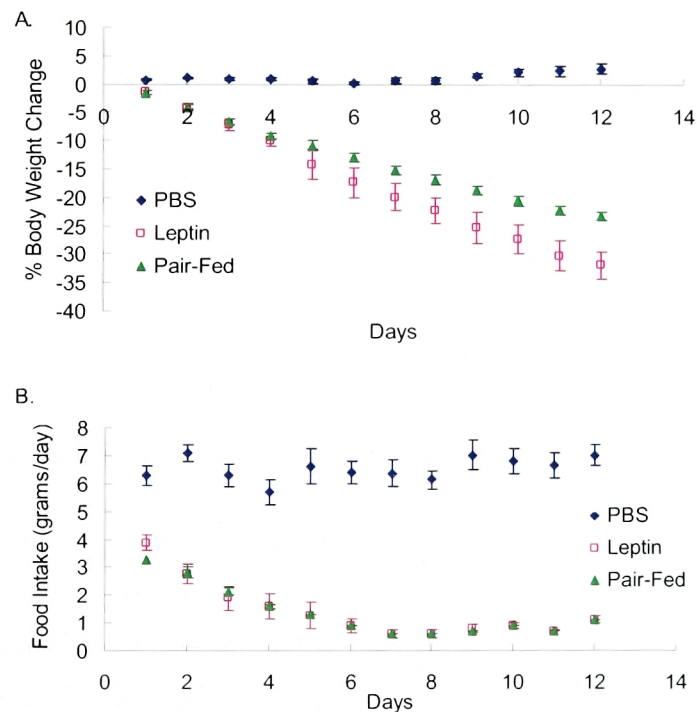


Figure 35 A-B) Chronic subcutaneous leptin administration's effect on stomach NPB and NPW expression levels. A) Percent body weight change of adult female ob/ob mice treated with leptin, PBS control, or pair-fed (n=4-6 in each group). B) Food intake of adult female ob/ob mice treated with leptin, PBS control, or pair-fed.

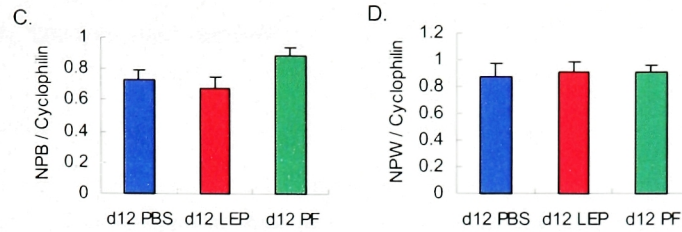


Figure 35 C-D) Chronic subcutaneous leptin administration's effect on stomach NPB and NPW expression levels. Taqman® real time RT-PCR analysis of stomach expression levels of NPB (C) and NPW (D) in 12 day treated ob/ob mice (d12 LEP) compared to PBS control (d12 PBS) and pair-fed animals (d12 PF). There were 4 to 6 animals in each group. No significant differences were seen in all groups for either stomach NPB or NPW levels. Similar results were obtained by Northern blot analysis (data not shown).

Behavioral Analysis of GPR7^{-/-} mice

The initial study of the GPR7^{-/-} mice focused on analyzing the effects on energy homeostasis due to *GPR7* being initially identified as a gene down-regulated after GTG treatment. However, the localization of the GPR7 and its ligands to various discrete locations in the brain suggests the possibility that GPR7 signaling has other physiological roles. In particular, strong GPR7 mRNA levels have been found in the hypothalamus, hippocampus, amygdala, and ventral tegmental area (Lee et al., 1999; O'Dowd et al., 1995). These areas are known to be involved in regulating a wide range of behavioral functions including anxiety, stress, fear, depression, and arousal (Nestler et al., 2002; Nestler et al., 2001; Walker et al., 2003). Therefore, we investigated the role of GPR7 for possible disturbances in a few key behavioral modalities including sleep regulation,

circadian rhythm, anxiety, and depression.

Sleep Recordings – Investigating the potential role of GPR7 in sleep homeostasis

Sleep is critically protected under a tightly regulated homeostatic system. In mammals, the sleep-wake cycle is divided into three distinct states each with defined behavioral and neurophysiological characteristics (Jones, 1998). Sleep activity is monitored in mammals by using an electroencephalography (EEG), which measures electrical activity from the brain, and electromyography (EMG), which measures electrical activity from muscles. During wakefulness, the first stage in the sleep-wake cycle, the animal is fully conscious, which is associated with low-voltage, mixed frequency, fast activity on EEG, purposeful eye movements, and high muscular tone and activity on EMG. Non-REM sleep or slow-wave sleep is characterized as when an animal is behaviorally quiet and progressively becoming unresponsive to environmental stimuli. It is associated with high-voltage slow activity on EEG, absent eye movement, and reduced muscular tone and activity on EMG. REM sleep is characterized as when an animal is behaviorally quiet and further unresponsive to environmental stimuli. The EEG reading during REM sleep is similar to that during wakefulness with low voltage fast activity. Tonic muscle tone is completely absent; however, there can be frequent

twitches and small movements in the extremities. Sleep normally progresses from wakefulness to non-REM sleep to REM sleep.

A recent study reported that a single bolus ICV injection of 400pmoles (1 μ g) of NPW into the lateral ventricles of rat increased the amount of REM sleep to 14.34% compared to 6.7% when only vehicle was injected (Winsky-Sommerer et al., 2003). This suggested that GPR7 signaling could modulate REM sleep in mammals. In order to investigate the possible role of GPR7 in maintaining the sleep-wake cycle, custom EEG/EMG electrodes were implanted into adult male GPR7 mice for recording of normal baseline sleep-wake cycle. EEG/EMG recordings were taken for three consecutive days. No mice showed any signs of spontaneous epileptic seizures in the EEG/EMG recordings. Typical hypnograms for the mice are shown (Figure 36). There were no significant differences between the GPR7^{+/+} and GPR7^{-/-} groups in any of the sleep state parameters measured included time spent in REM sleep, and the measured results were similar to previously published data for wildtype mice (Figure 37, Table 4) (Chemelli et al., 1999; Hara et al., 2001; Willie et al., 2003). Furthermore, there was no fragmentation of the sleep or wake cycles as seen in narcoleptic orexin knockout mice nor evidence of spontaneous seizures (Chemelli et al., 1999). This data strongly suggests that GPR7 does not play a significant role in regulating basal sleep homeostasis.

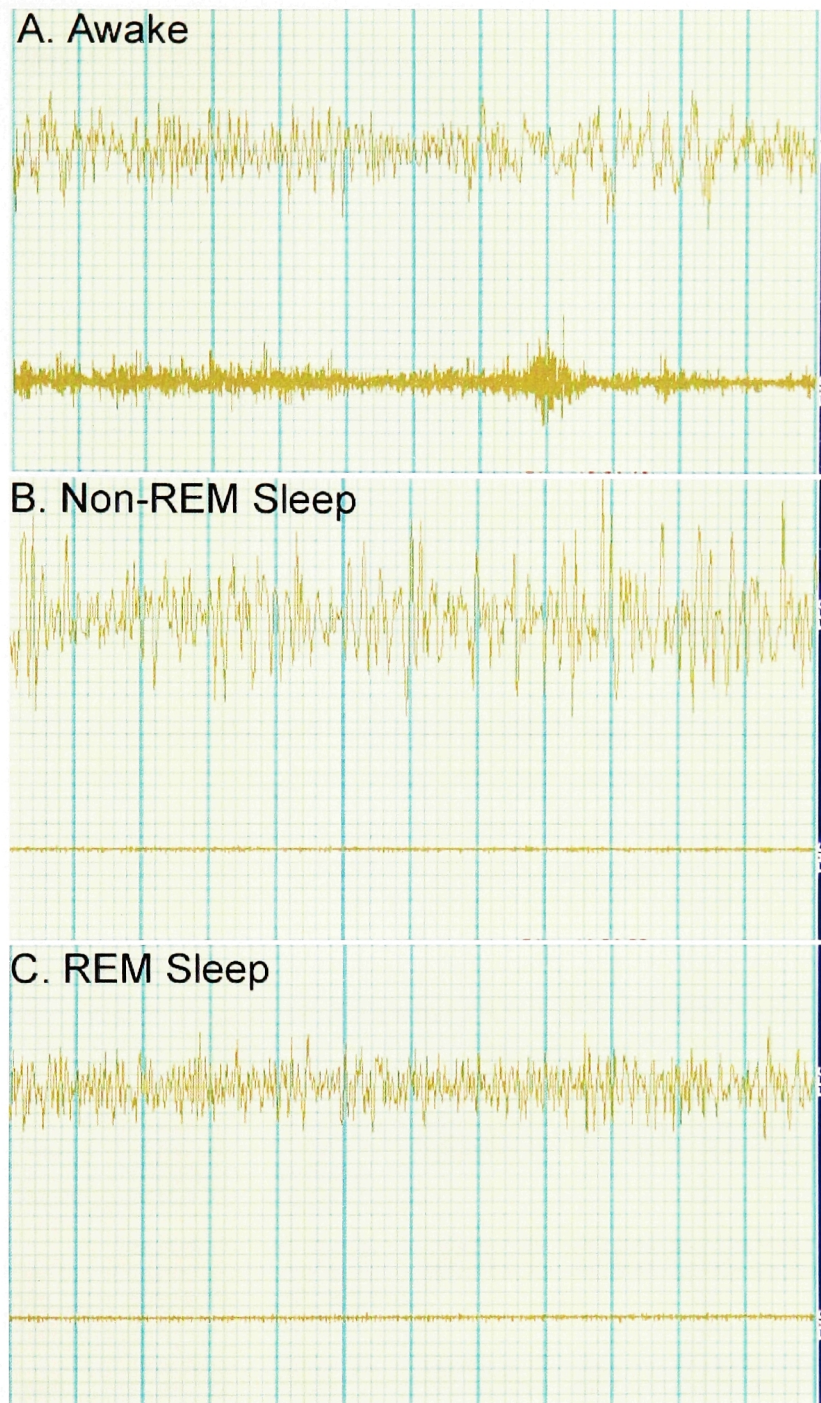


Figure 36) Example of EEG and EMG Recordings of different sleep-wake states in adult mice. A) Awake B) Non-REM sleep or slow wave sleep C) REM sleep or paradoxical sleep. EEG recordings are depicted at the top of each chart with the corresponding simultaneously measured EMG recordings on the bottom half. Each 20 second epoch (one full screen) was manually scored offline based on previous criteria.

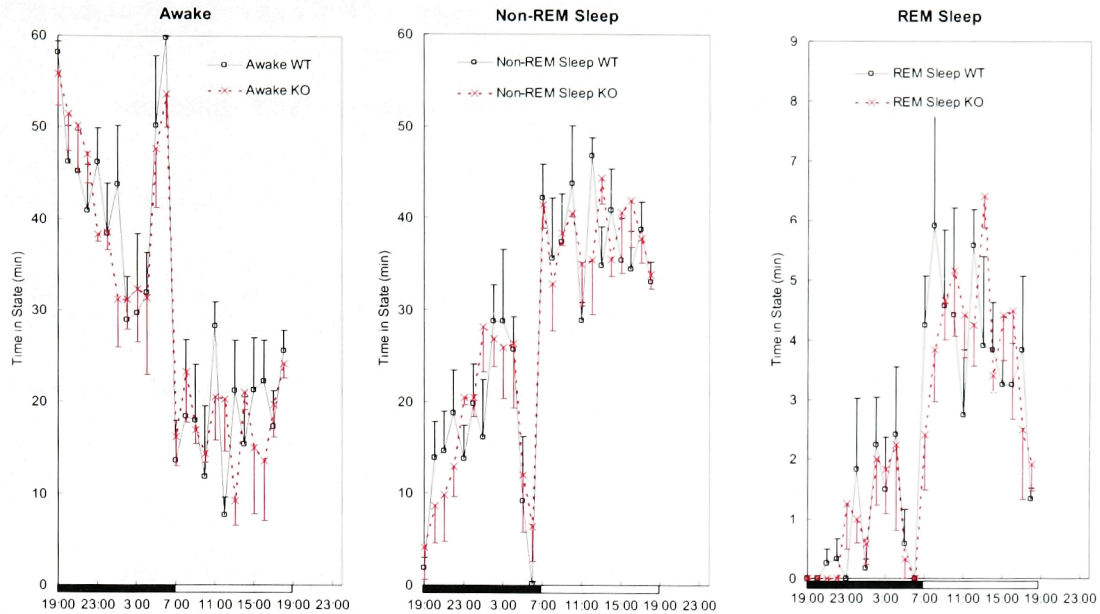


Figure 37) Time spent in each sleep state for adult male GPR7 mice by EEG recordings. Data was recorded for three consecutive 24 hour periods, scored offline with custom software, and averaged for a 24 hour day. (black squares = GPR7+/+ (WT) males; red crosses = GPR7-/- (KO) males; n=4/genotype). No significant difference between GPR7+/+ and GPR7-/- mice at any time point for any of the sleep states.

Table 4: Summary of baseline sleep recordings for male GPR7+/+ (WT) and GPR7-/- (KO) mice

	REM sleep		Non-REM sleep		Awake	
	WT	KO	WT	KO	WT	KO
24 hours						
Total time (min)	53.39±1.94	56.168±2.53	621.11±12.42	644.53±19.72	765.36±12.8	739.22±21.6
Episode duration (sec)	73.88±1.66	74.10±2.75	296.57±20.12	313.49±9.91	510.13±45.17	513.52±24.02
REM latency (min)	10.16±0.61	9.99±0.36				
Inter-REM interval (min)	25.98±1.29	25.53±2.21				
Light period						
Total time (min)	43.86±2.37	47.97±1.89	435.25±7.59	450.22±8.84	240.75±8.74	221.72±9.80
Episode duration (sec)	73.73±2.11	75.49±2.84	346.49±20.57	343.91±14.23	305.48±29.73	273.24±10.26
REM latency (min)	10.63±0.69	9.95±0.43				
Inter-REM interval (min)	18.88±0.78	17.20±0.99				
Dark period						
Total time (min)	9.53±2.27	8.20±1.26	185.86±15.17	194.31±13.97	524.61±17.22	517.50±14.72
Episode duration (sec)	67.38±7.77	66.19±3.13	225.68±25.10	260.84±10.83	738.99±77.62	825.05±66.55
REM latency (min)	7.91±0.97	9.77±0.50				
Inter-REM interval (min)	182.19±57.30	111.15±17.85				

Four animals of each genotype were used (one animal in each genotype was discarded due to poor EEG/EMG signal output). Data was collected for three consecutive 24 hour days, scored offline with custom software, and averaged for 24 hours. No significant difference in any of the categories between GPR7+/+ and GPR7-/- mice.

Circadian Rhythm in GPR7^{-/-} Mice

Mounting experimental evidence from rodents has shown the suprachiasmatic nucleus to be the site of the master circadian pacemaker in mammals (van Esseveldt et al., 2000). With strong localization of GPR7 signal in the suprachiasmatic nucleus, it was postulated that mice lacking GPR7 signaling might have disruptions in their circadian rhythm. Several behaviors are governed by circadian rhythm including hormonal control, feeding, body temperature, cardiac function, and sleeping (Rutter et al., 2002). Disruption of circadian rhythm could affect any of these behaviors.

Running wheel cages are frequently used to reproducibly monitor circadian rhythms in mice (King and Takahashi, 2000). To analyze the circadian behavior of GPR7^{-/-} mice, commercial automated home cage running wheels were used. Adult female mice were removed from their group-housed home cages and individually placed into the running wheel equipped cages. After an acclimation period of a week, running wheel behavior was recorded over a week under a 12:12 LD (light, dark) cycle. There was no significant difference in the periods between the genotypes in the circadian rhythm of a normal 12:12 LD cycle (Figure 38, Table 5). Light entrainment was removed, and free running wheel behavior of the mice placed on a strict 12:12 DD (dark, dark) cycle was monitored. Again, no significant differences were seen between the

genotypes (Figure 38, Table 5). Furthermore, all mice were able to maintain a strict circadian rhythm without light entrainment for the duration of the study. While GPR7 does not appear to grossly regulate circadian rhythms, longer study durations or different entrainment techniques, such as with feeding, may yield subtle effects of GPR7 signaling.

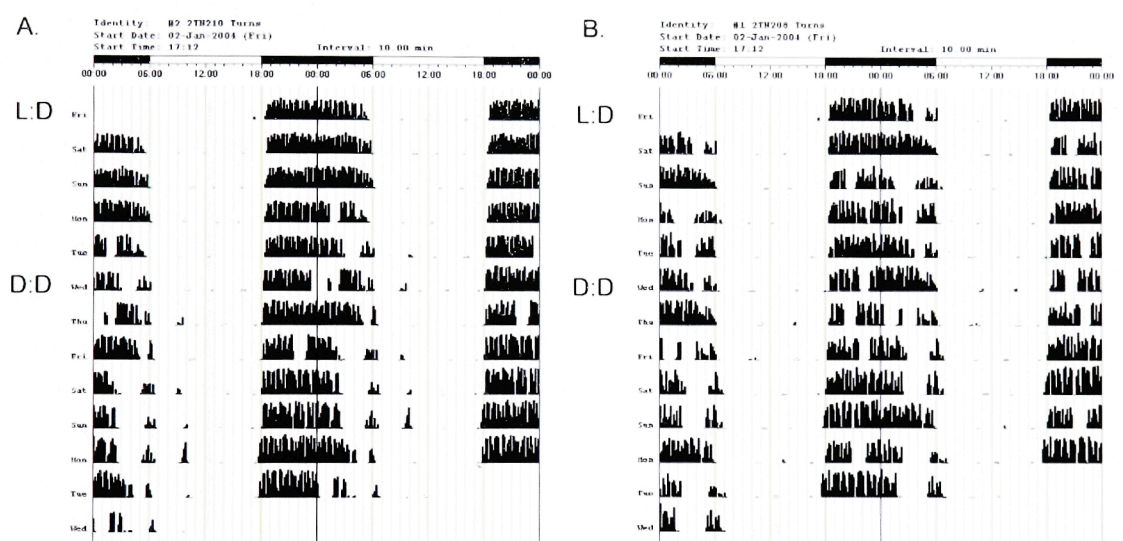


Figure 38) Representative running wheel behavior actogram double plots for adult female GPR7 mice. Both female GPR7^{+/+} (A) and GPR7^{-/-} (B) mice maintained a circadian rhythm after light entrainment was removed. L:D = 12 hour light:dark cycle; D:D = 12 hour dark:dark cycle.

tau (period)	GPR7 ^{+/+}	GPR7 ^{-/-}
LD cycle	24.15±0.10	24.05±0.05
DD cycle	23.95±0.05	23.95±0.05
N (#animals)	4	4

Table 5) tau (Period) calculations for adult female GPR7 mice. Mice were placed in individual cages equipped with a running wheel. The activity was recorded automatically by a computer for a total time period of 7 full days. Period calculations were performed using software based on chi-square periodogram algorithm. No significant differences were seen between the genotypes or the different light cycles (LD = 12 hour light:dark cycle; DD = 12 hour dark:dark cycle).

Anxiety of GPR7^{-/-} Mice – Open Field and Elevated Plus Maze

Stress and anxiety are strong mediators of energy homeostasis. Abnormally high levels of the stress hormone cortisol in humans lead to a condition called Cushing's syndrome, which is associated with altered fat distribution and increased visceral obesity (Peeke and Chrousos, 1995). Glucocorticoids such as cortisol are essential in maintaining obesity. Adrenalectomy reverses the obesity seen in ob/ob mice, while treatment with glucocorticoids can restore the obese state (Naeser, 1973; Shimomura et al., 1987; Solomon and Mayer, 1973). Also, central factors that regulate energy homeostasis often overlap with those involved in regulating anxiety-like behaviors, including corticotropin releasing factor (CRF) and related peptide pathways and the serotonin signaling pathways (Heisler et al., 2002; Steckler and Holsboer, 1999). Both the CRF and serotonin pathways have some of their respective receptors in the same neuronal regions that express GPR7. Therefore, GPR7^{-/-} mice were investigated for anxiety-like behaviors that potentially could explain the abnormal regulation of energy homeostasis.

Anxiety-like behavior was measured by two commonly used methods: the open field test and the elevated plus maze. Both the open field test and the elevated plus

maze are based on the principle that there is a conflict between the tendency of a mouse or rat to explore a novel area and its innate aversive behavior towards brightly lit, open areas (Crawley, 2000). In the open field test, a mouse is placed in a large lit open area with no dark corners. The initial reaction is for the mouse to avoid the large open center area. However, as anxiety to the new location diminishes, the mouse will start to explore more of the open field including the open center area. The time spent in the center of the open field is used as a measure of anxiety-like behavior. Administering anxiolytic drugs to a mouse prior to exposure to the open field will increase the time the mouse spends in the center. The elevated plus maze is similar in concept. There are two open arms and two closed arms on an elevated platform. The mouse tends to stay in the closed, darker arms due to their initial anxiety to the novel environment. Again, as the anxiety diminishes, the mouse has a greater tendency to explore the environment and spend more time in the open arm. Administering anxiolytic drugs prior to exposure to the elevated plus maze can increase the amount of open arm entries and the time the mouse spends in the open arms.

The initial screening was conducted on a small sample of adult mice using an automated open field test apparatus (UT Southwestern). During this screen, adult male GPR7-/- mice showed a trend towards decrease in overall locomotive activity and a

significant increase in time spent in the center (Figure 39). When the time spent in center for the male GPR7^{-/-} mice was corrected for locomotive activity, they still showed a significant increase compared to GPR7^{+/+} mice (Figure 39). Female GPR7^{-/-} mice showed no significant differences from GPR7^{+/+} littermate controls in total distance traveled or time spent in the center (Figure 40).

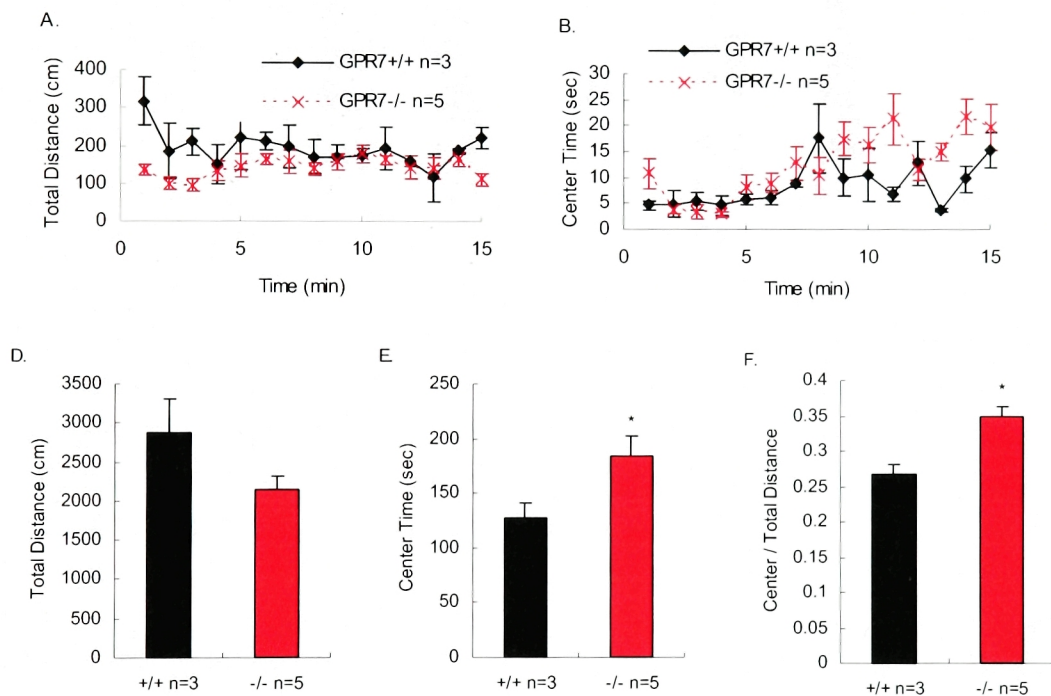


Figure 39) Open field analysis of adult male GPR7 mice using an automated system. A-B) Total distance traveled (A) and time spent in the center of the open field (B) analyzed per minute of the fifteen minute test period. C-E) Total distance traveled (C) and time spent in the center (D-E) for the sum of the fifteen minute test period. All tests were scored automatically by the provided software. *denotes a significant difference between GPR7^{+/+} and GPR7^{-/-} mice. All testing was conducted at University of Texas Southwestern Medical Center (Dallas, Texas).

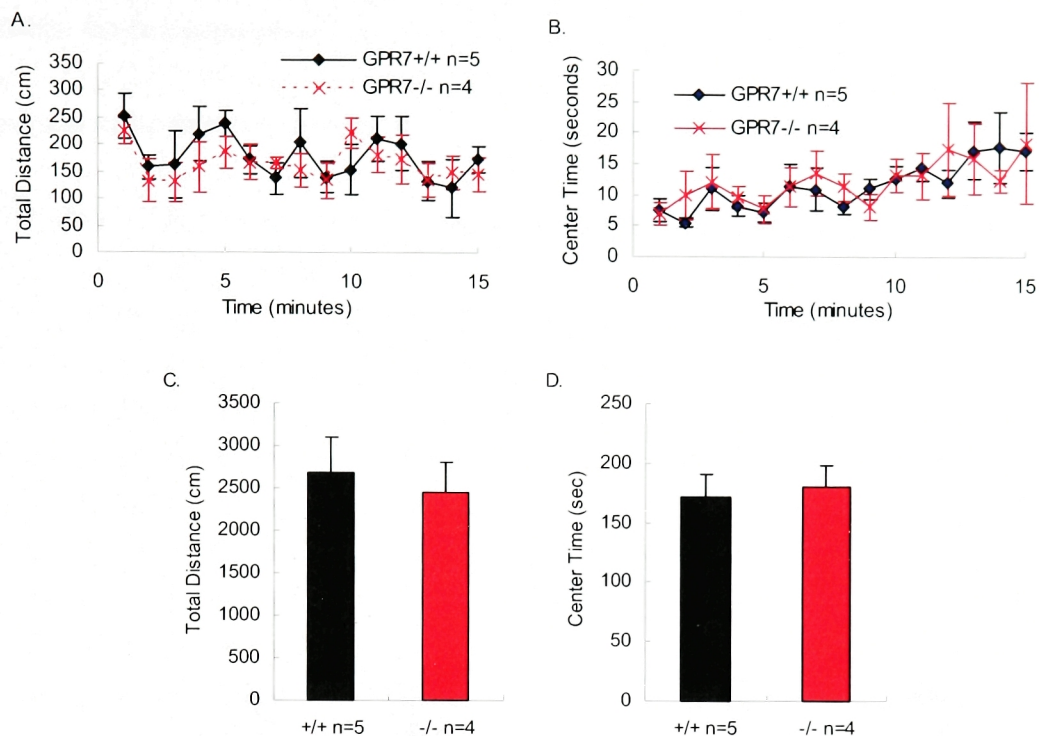


Figure 40) Open field analysis of adult female GPR7 mice using an automated system. A-B) Total distance traveled (A) and time spent in the center of the open field (B) analyzed per minute of the fifteen minute test period. C-D) Total distance traveled (C) and time spent in the center (D) for the sum of the fifteen minute test period. All tests were scored automatically by the provided software. All testing was conducted at University of Texas Southwestern Medical Center (Dallas, Texas). No significant differences were seen between female GPR7+/+ and GPR7-/- mice.

However, when a different set of adult male or female GPR7 mice was tested in another open field test apparatus in a different location (Rockefeller University), there was no significant difference in latency to center or the time spent in the center between GPR7+/+ and GPR7-/- for either sex (Figure 41). The discrepancy between the two separate test runs could be attributed to the different testing apparatuses, location and environment. Most notably the open field dimensions were of different sizes. Scoring

between the two apparatuses was also different as the first was automatically scored by a computer using infrared laser beams, while the second relied on human manual scoring of videotapes. Furthermore, behavioral measurements in mice including the open field and elevated plus maze are very sensitive to changes in the environment even if the testing conditions are nearly identical (Crabbe et al., 1999).

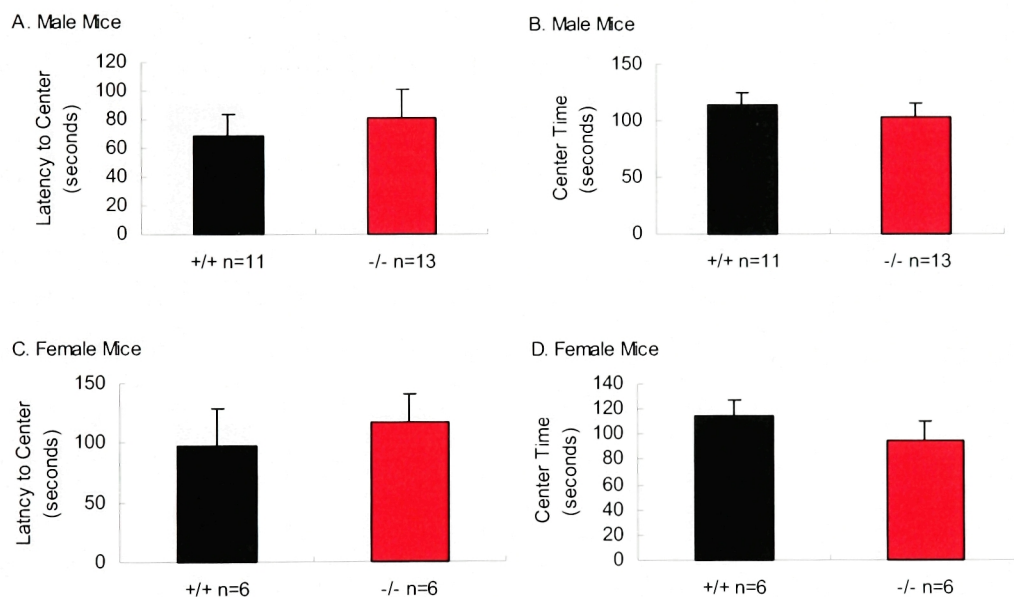


Figure 41) Open field analysis of GPR7 mice using a manual test apparatus. A fifteen minute open field analysis was conducted using a different testing apparatus in a new location (Rockefeller University, New York). All mice were manually scored for latency to center of open field (A, C) and time spent in the center field after 15 minutes (B, D). No significant differences were seen in any of the groups.

An elevated plus maze was used to further investigate potential anxiety-like behaviors in GPR7 mice. Similar to the open field test, there was no significant

difference between the genotypes in time spent in the open or closed arms or the ratio between the number of entries of the open to the closed arms (Figure 42). The larger sample size and the use of two different tests suggest that the decrease in anxiety-like behavior originally seen in the first test run of male GPR7^{-/-} mice was most likely an artifact. Therefore, GPR7 signaling does not appear to mediate anxiety-like behaviors.

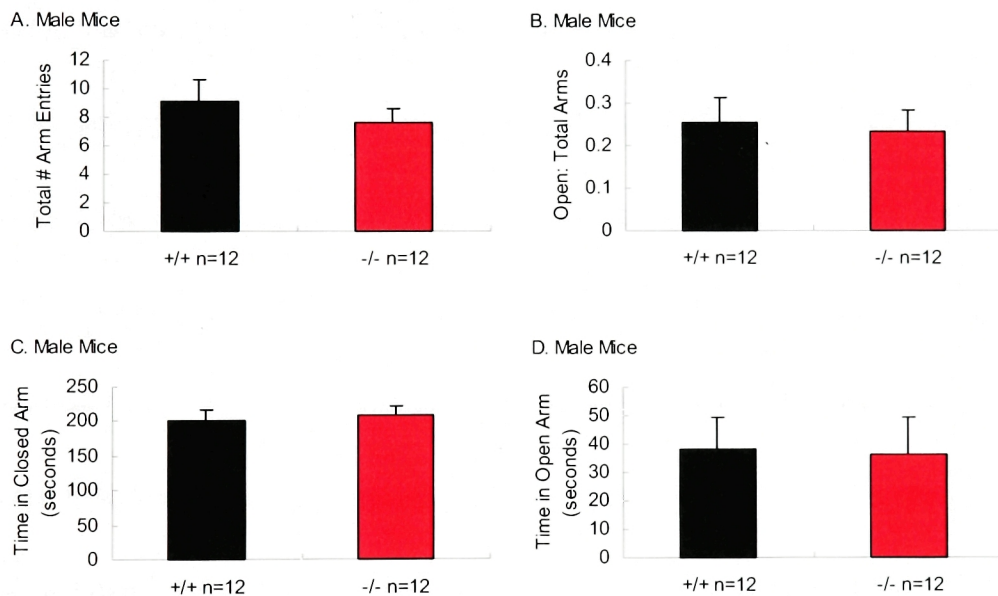


Figure 42) Elevated plus maze test on adult GPR7 mice. The same set of adult mice as used for the previous open field test was used. Only mice that stayed on the elevated plus maze throughout the testing period without falling were counted. Mice were scored manually for five minutes and analyzed for total number of arm entries (A), ratio of open to total arm entries (B), and the total time spent in the closed arm (C) and in the open arm (D). No significant differences were seen.

Depression in GPR7^{-/-} Mice – Forced Swim Test

Adult male GPR7^{+/+} and GPR7^{-/-} mice were evaluated for depression-like behaviors by a modified Porsolt forced swim test (Lucki, 1997; Lucki et al., 2001; Porsolt et al., 1977a). In this test, an animal is placed in an enclosed cylinder filled with water, where it can not reach the bottom of the cylinder floor or escape out of the cylinder in any direction. The time spent immobile is a reproducible measure of depression-like behavior that has been shown to be corrected by anti-depressant drugs (Cryan et al., 2002; Porsolt et al., 1977b). An initial group of naïve adult male GPR7^{-/-} mice were tested and showed no significant differences in the time spent immobile compared to GPR7^{+/+} mice (Figure 43). These mice were all originally group housed with their littermates. In order to stimulate depression and anxiety-like behavior, the mice were isolated from each other by single-caging the test animals. Following four weeks of social isolation, the mice were tested again in the same forced swim test. As before, there were no significant differences in the time spent immobile between GPR7^{+/+} and GPR7^{-/-} male mice (Figure 43). These data suggest that GPR7 signaling does not strongly modulate depression-like behaviors in mice.

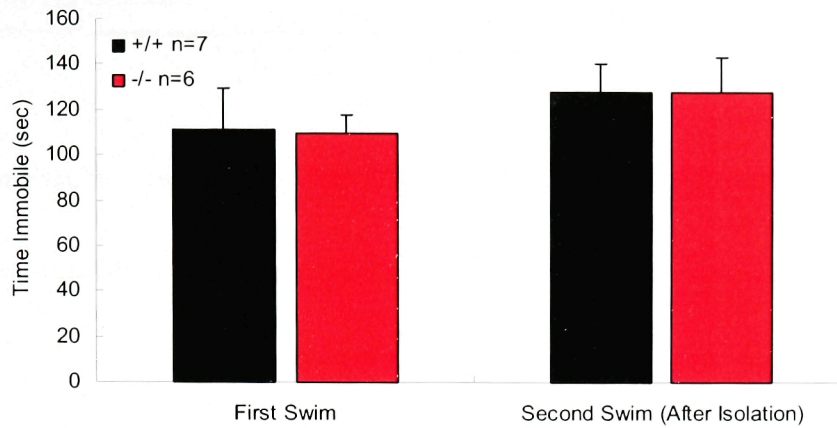


Figure 43) Forced swim test for depression analysis in adult male GPR7^{-/-} mice. Group housed male mice, naïve to the swim test, were initially tested for the time spent immobile in a swim tank (GPR7^{+/+} n=7; GPR7^{-/-} n=6). After the initial test, the same mice were individually caged and socially isolated for four weeks and retested under the same conditions as before.

Chapter 4: Discussion

The results reported here detail the role of GPR7 signaling in regulating energy homeostasis in mammals in a potentially sexually dimorphic manner. Numerous lines of evidence from the phenotype of GPR7^{-/-} mice to the differential gene regulation of the ligands to the *in vivo* pharmacological effects of the ligands in rodents have shown that GPR7 and its ligands are involved in regulating feeding and body weight. Other possible physiological roles for GPR7 signaling in mammals were also investigated including the regulation of the sleep-wake cycle, circadian rhythm, anxiety, and depression; however, none of the behavioral tests on the GPR7^{-/-} mice showed a significant role for GPR7 in controlling these behaviors.

We first identified *GPR7* as a candidate obesity gene due to a decrease in hypothalamic gene expression levels following GTG treatment in mice. This suggested that GPR7 was in the same neuronal population as those involved in the VMH mediated regulation of body weight and food intake. GPR7 mRNA expression pattern in the rodent brain is also consistent with a role in energy homeostasis. GPR7 is expressed in the arcuate and VMH of the hypothalamus, as well as in other regions known to regulate feeding, neuroendocrine pathways and the autonomic nervous system (Lee et al., 1999;

O'Dowd et al., 1995). Furthermore, GPR7 was identified as an orphan GPCR with potentially a novel peptide ligand. Orphan GPCRs are heavily investigated by both academic institutions and pharmaceutical companies. GPCRs and their target ligands currently constitute the largest drug target group with greater than 30% of the 500 clinically marketed drugs being modulators of GPCRs (Drews, 2000; Wise et al., 2004). It is also worth noting that many of the known factors involved in regulating energy homeostasis act through GPCRs. This includes the melanocortins, NPY and its related family members, MCH, CRF, orexins, ghrelin, serotonin, and many others. Therefore, the potential for finding new avenues in energy homeostasis research by unmasking the function of a novel orphan GPCR family was significant.

The physiological role of the then orphan receptor, GPR7, was investigated by generating mice with targeted disruption of the *GPR7* gene. Male GPR7^{-/-} mice display a moderate adult-onset obese syndrome that is greatly exacerbated when fed a high fat diet. The moderate adult-onset obesity seen in GPR7^{-/-} male mice is similar in magnitude to that seen in knockout mice for other anorectic hypothalamic genes. These include hormones and receptors involved in the melanocortin (MC3R) and cocaine-amphetamine-related peptide pathway (Asnicar et al., 2001; Yaswen et al., 1999); bombesin receptor subtype-3, an orphan GPCR from the bombesin peptide receptor

family (Ohki-Hamazaki et al., 1997); and other anorexigenic signals such as serotonin 5HT_{2C} receptor (Nonogaki et al., 1998) and IL-6 (Wallenius et al., 2002). Many of these signaling molecules are components of a complex network that also includes leptin. Leptin maintains energy homeostasis by at least in part changing various RNA levels of hypothalamic neuropeptides (Friedman and Halaas, 1998). In male GPR7^{-/-} mice, the hypothalamic RNA levels of NPY and POMC RNA were more characteristic of a lean rather than a leptin deficient state. In addition, both Ay/a GPR7^{-/-} and ob/ob GPR7^{-/-} male mice were heavier than their respective Ay/a and ob/ob GPR7^{+/+} littermates. Thus, GPR7 signaling is not epistatic to leptin or melanocortins and rather appears to affect energy homeostasis by a novel mechanism independent or parallel to leptin and melanocortin signaling.

The peptide ligands for GPR7, NPB and NPW, have been recently identified by several groups using reverse pharmacology and computational genomics (Brezillon et al., 2003; Fujii et al., 2002; Shimomura et al., 2002; Tanaka et al., 2003). NPB and NPW are derived from two different novel genes and represent a new uncharacterized peptide-receptor family. Both peptide ligands have subnanomolar to nanomolar affinity for GPR7 and its homolog GPR8, which is absent in rodents. NPB and NPW are expressed both centrally and in the periphery (Fujii et al., 2002; Tanaka et al., 2003).

NPB and NPW are localized in different and discrete neuronal populations. NPB had a wider distribution in the rodent brain than NPW (Tanaka et al., 2003). Peripheral expression for both ligands was exceptionally strong in the stomach with NPW also having very high levels in the lungs (Tanaka et al., 2003). These results were confirmed with Taqman® real-time RT-PCR and Northern blot analysis from our lab. The distinct expression patterns of NPB and NPW in the brain and periphery suggest separate physiological roles for the ligands even though both act most likely on one common receptor GPR7 in rodents.

The pharmacological effects of NPW or NPB on feeding behaviors have been recently studied. An intracerebroventricular (ICV) bolus injection of NPB at the onset of the dark phase elicits a biphasic feeding response with an initial small and transient increase in food intake followed by a much more significant, sustained suppression of food intake during the dark cycle (Tanaka et al., 2003). Rats injected with NPB also have increased locomotor activity (Tanaka et al., 2003). The hypophagia and hyperlocomotion in rodents after an ICV injection of NPB correlate well with the phenotype of GPR7^{-/-} male mice. Chronic ICV infusion of NPW in rats lead to sustained weight loss, decreased food intake, and increased heat production and body temperature without any signs of transient hyperphagia (Mondal et al., 2003). The data

from the chronic ICV infusion of NPW and the obese phenotype of the GPR7^{-/-} mice further suggest that the transient increase in food intake is not likely to be biologically significant, at least over the long term. Toxic, aversive or nonspecific effects of NPW on feeding were also ruled out as ICV administration of NPW did not reduce saccharin consumption in a conditioned taste aversion test (Mondal et al., 2003). Therefore, in aggregate with the genetic evidence from GPR7^{-/-} mice, the current pharmacological evidence for the ligands of GPR7 strongly suggests that GPR7 signaling serves as an endogenous catabolic signal.

Furthermore, it is not known whether NPB and NPW exert its actions directly as a neuropeptide locally in the brain or if the peptides are also released as an endocrine hormone into the blood stream from peripheral tissues such as the stomach. Several brain-gut peptides play a prominent role in regulating feeding and energy homeostasis including cholecystokinin (CCK), bombesin, glucagons-like peptide 1, pancreatic polypeptide, peptide YY 3-36 (PYY3-36), and ghrelin. Many of these peptides have been shown to be synthesized in the gut and then potentially released as peptide hormones to act on central sites including the hypothalamus. Both pancreatic polypeptide and PYY3-36 are part of the NPY peptide family and have been shown to inhibit feeding when administered peripherally (Asakawa et al., 2003; Batterham et al.,

2002). PYY3-36 has been suggested to bind and activate preferentially NPY Y2 receptors in the hypothalamus leading to decreased levels and activity of the orexigenic signal NPY (Batterham et al., 2002). With the differential regulation of stomach NPW levels following a 48 hour fast, there is some evidence to support a peripheral role for NPB and NPW in regulating feeding and energy homeostasis. The ligands for GPR7 could potentially act in a similar fashion as pancreatic polypeptide or PYY3-36 as a gut endocrine peptide that exerts an anorectic effect through receptors, found appreciably only in nervous tissues, located in the hypothalamus (Figure 44).

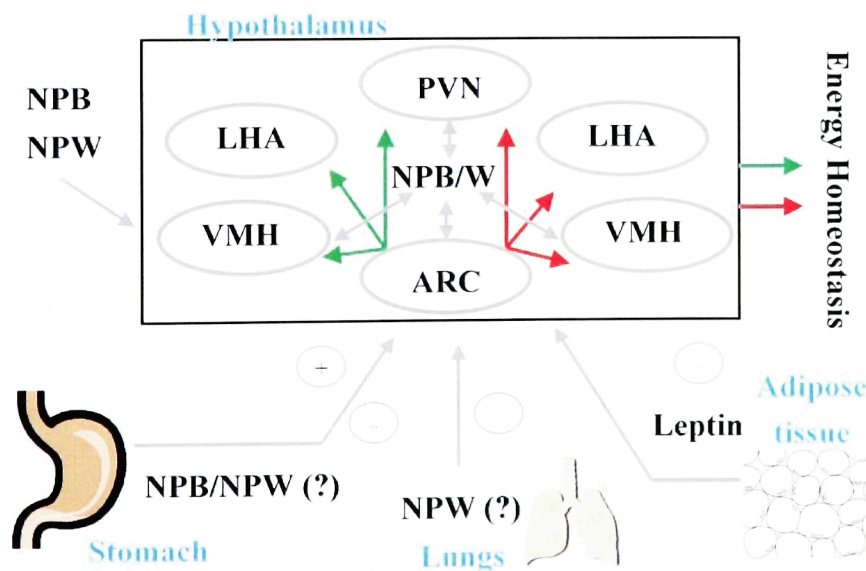


Figure 44) Regulation of energy homeostasis by Neuropeptide B and Neuropeptide W signaling pathways from peripheral tissues to the central nervous system. In this model, NPB and NPW could be synthesized and secreted from peripheral tissues that have very high RNA levels of the ligands such as the stomach and lung. Alternatively, the ligands could be working locally in the hypothalamus or could be secreted from extra-hypothalamic neurons. The exact nature of the signaling pathway is currently unknown.

Many catabolic signals are physiologically regulated under different metabolic conditions especially under starvation. Starvation leads to a wide change in metabolic and neuroendocrine function (Schwartz and Seeley, 1997). Hypothalamic orexigenic/anabolic signals are strongly induced, while hypothalamic anorectic/catabolic signals are decreased (Ahima et al., 1999; Schwartz et al., 1995). This constellation of changes in the hypothalamic regulation of energy homeostasis serves to coordinate an appropriate response to depletion of fuel stores until they are replenished. Fasting mice for 48 hours increased expression levels of hypothalamic NPY, a potent orexigenic/anabolic signal, as expected, but it had no effect on hypothalamic levels of NPB, NPW, or GPR7. While hypothalamic levels did not change, stomach levels of NPW decreased with fasting as would be expected for a catabolic signal. Many of these neuroendocrine changes seen during starvation in rodents are mediated by a fall in leptin levels (Ahima et al., 1996). While different energy states such as a 48 hour fast can significantly decrease stomach NPW RNA levels, chronic leptin treatment had no significant effect on the transcriptional regulation of the ligands in the stomach.

Besides plasma leptin levels, several other factors that may regulate energy homeostasis such as blood glucose, ketone, free fatty acid, growth hormone levels and many others are also affected by starvation (Cahill et al., 1966; Sims and Horton, 1968).

Changes in glucose levels are known to affect firing of glucose-sensitive and glucose-responsive neurons in the LH and VMH respectively (Oomura, 1983). It is appealing to think that changes in blood glucose levels could be the physiological input signal for GPR7 and its ligands. However, while the refeeding response after a 24 hour fast was abnormally high in GPR7^{-/-} mice, GPR7^{-/-} mice had a normal feeding response to glucoprivation after peripheral or central administration of moderate doses of the glucose analog 2-deoxy-D-glucose. These data suggest that central glucose signaling in GPR7^{-/-} mice are normal, and therefore glucose is not the main factor in regulating GPR7 signaling. Some other factor that changes under starvation such as glucocorticoid, free fatty acid, amino acid, or ketone levels may serve as an important input signal to GPR7 signaling. Alternatively, stomach NPW levels may be responding to the physical distension/emptying of the stomach similar to the classical model of CCK and other gut peptides (Read et al., 1994).

While the physiological input(s) modulating GPR7 signaling is not known, the effects of defective GPR7 signaling are sexually dimorphic in mice. Body weight in mammals is known to be sexually dimorphic. In humans, females tend to be more obese than males, while in mice, males are more obese than females (Cortright and Koves, 2000). Other animal models of hypothalamic obesity including the NPY Y1R^{-/-} mice

and the NPY Y5R^{-/-} mice have also shown sexual dimorphism in body weight. In contrast to GPR7^{-/-} male mice, NPY Y1R^{-/-} females weighed more than male NPY Y1R^{+/+} mice, while similar to GPR7^{-/-} male mice, NPY Y5R^{-/-} weighed more than female NPY Y5R^{-/-} (Marsh et al., 1998; Pedrazzini et al., 1998). In mice, castrating males result in decreased adiposity, whereas ovariectomizing females result in increased adiposity indicating a strong role for sex hormones in regulating body weight (Wright and Turner, 1973). While estrogens and androgens clearly modulate long term energy homeostasis in mammals, the underlying mechanisms are unclear (Heine et al., 2000; Jones et al., 2000). Additional investigation of the sexually dimorphic effects on body weight of GPR7^{-/-} mice could lead to further elucidation of the mechanism(s) by which sex hormones regulate energy homeostasis.

Although it is reasonable to speculate that NPB and NPW modulate food intake and energy homeostasis by binding to GPR7 in hypothalamic neurons, it is possible that the effects are not directly mediated by hypothalamic feeding-related neurons. As previously mentioned, GPR7 is expressed in several discrete areas in the brain. There is strong evidence that many of these areas are involved in regulating different behavioral patterns from anxiety to depression. Feeding disorders and mood disorders have at least a strong association as evident in several human clinical trials and epidemiological

studies (McElroy et al., 2004). Disturbances of diverse physiological systems from stress, fear, and anxiety responses to disruption of affective and emotive responses to feeding could possibly account for all of the “metabolic” phenotypes observed in the GPR7^{-/-} mice. However, in our initial screen for behavioral abnormalities in the GPR7^{-/-} mice including the open field and elevated plus maze as well as the Porsolt forced swim test, we found no significant differences compared to GPR7^{+/+} littermates in anxiety or depression-like behaviors. This does not rule out the possibility for some more complex or other behavioral role for GPR7 signaling such as conditioned fear responses or learning and memory, but it suggests that gross abnormalities in a few key behavior paradigms studied do not mediate the obesity syndrome seen in GPR7^{-/-} mice.

NPB and NPW have other pharmacological effects not directly related to maintaining energy homeostasis including enhancing analgesia, stimulating the release of prolactin, and increasing REM sleep (Shimomura et al., 2002; Tanaka et al., 2003; Winsky-Sommerer et al., 2003). While the role of GPR7 in analgesia and stimulating prolactin secretion still remains to be investigated, the sleep-wake cycles in GPR7^{-/-} mice have been monitored. The baseline sleep-wake parameters are essentially identical between GPR7^{+/+} and GPR7^{-/-} mice. Therefore, the increased REM sleep seen after central administration of NPW is either non-specific or largely insignificant for normal

sleep homeostasis. The availability of GPR7^{-/-} mice now provides an opportunity to further distinguish non-specific drug effects of NPB and NPW from physiological effects by comparing the ligands' effects on wildtype versus GPR7^{-/-} mice. Thus, future studies of the effects of these peptides on body weight and other systems in normal and GPR7^{-/-} mice should establish the full range of functions of the peptides *in vivo*. Due to widespread NPB and NPW mRNA expression and sequence similarity of GPR7 to opioid and somatostatin receptors, which are known to have numerous disparate physiological roles, a pleiotropic role for GPR7 signaling would not be surprising.

Further studies of GPR7 and its ligands will lead to a better understanding of its role in regulating energy homeostasis and possibly other behaviors. While some of the possible physiological inputs regulating GPR7's actions have been investigated, the exact nature of these inputs is still currently unknown. It appears that leptin and possibly glucose are not strong modulators. In order to further elucidate the nature of these inputs, the exact characteristics of the GPR7, NPB, and NPW-expressing neuronal population needs to be known. What are the other genes expressed in these neurons? Are they glucose-responsive neurons? Do these neurons respond to other metabolites such as free fatty acids? What are the inputs and outputs of the GPR7 expressing neuronal population? Some of these answers can be obtained by carrying out careful

immunohistochemical analysis of these neurons and subsequent electrophysiology. Unfortunately, the antibody against GPR7 that was generated in this lab proved to be too non-specific to be useful in answering these questions. The tau-GFP expression from the knock-in cassette was also too weak to be visualized by standard immunohistochemistry techniques. Labeling these neurons by generating BAC GPR7-GFP, NPB-GFP, and NPW-GFP transgenic mice might be useful in answering some of these questions (Liu et al., 2003; Yang et al., 1997).

Also, the sexual dimorphic nature of the obesity seen in GPR7^{-/-} mice can be followed by studying gonadectomized mice. It is reasonable to suspect that if sex hormones play a large role in the obesity syndrome of GPR7^{-/-} mice, ovariectomizing GPR7^{-/-} females (or masculinizing females) should cause them to become obese or weigh more than ovariectomized GPR7^{+/+} females. Conversely, castrating male GPR7^{-/-} mice and administering estrogen should keep the mice lean. If a role for sex hormones in GPR7 signaling can be established, it would be fruitful to know whether the neurons expressing GPR7 and the ligands also colocalize with sex hormone receptors such as estrogen receptors.

The possible separate and distinct physiological role of NPB and NPW could be demonstrated with the generation of specific individual general ligand knockout mice.

A double knockout of the ligands should be a phenocopy of the GPR7^{-/-} mice unless another currently unknown receptor or ligand exists in the same pathway. While there is no evidence to support another receptor similar to GPR7 in rodents that NPB or NPW could activate, receptor autoradiography or radioligand binding studies on GPR7^{-/-} mice could potentially prove or refute this possibility. The specific role of the ligands in the periphery could be probed with the generation of tissue specific knockout mice such as stomach specific knockouts of NPB and/or NPW. Additionally, the physiological role of the ligands in other peripheral tissues such as in lungs and immune cells is not known, but it is plausible that it is independent of its role in energy homeostasis.

Finally, the physiological nature and role for the post-translation bromination of the tryptophan in NPB is unknown. Brominated and non-brominated NPB have indistinguishable binding and pharmacological activity both *in vitro* and *in vivo* (Tanaka et al., 2003). It is reasonable to speculate that bromination is important for stability of the neuropeptide. N-terminal tryptophans tend to be more sensitive to aminopeptidase degradation by the “N-end rule” (Varshavsky, 1996), and bromination may block this degradation. It is known that loss of the N-terminal tryptophan in either NPB or NPW leads to a dramatic loss in binding and activity of the peptides (Tanaka et al., 2003). If this is true, then it is curious that brominated forms of NPW, which would presumably

face a similar stability problem without bromination, have not been found. Furthermore, the mechanism for tryptophan bromination remains a mystery. It would be exciting to speculate about the possible existence of a novel mammalian tryptophan brominating factor that has yet to be discovered. While nonspecific bromination of tyrosine residues by eosinophil peroxidase has been reported in patients with allergen-induced asthma, the identity and location of this putative brominating factor for NPB remains to be seen (Wu et al., 2000).

Since the initial cloning of GPR7 as an orphan GPCR in 1995 to the generation of the GPR7^{-/-} mice and the identification of NPB and NPW as the endogenous ligands of GPR7, many of the physiological functions of GPR7 signaling have now been elucidated (Table 6). In particular, NPB and NPW signaling via the GPR7 receptor plays a biologically important role as a catabolic signal in regulating food intake, energy expenditure and body weight. These data suggest the possibility that GPR7 agonists and other components of the GPR7 signaling pathway might have therapeutic benefits for treating obesity and related metabolic conditions.

Table 6: Summary of the known functional roles for GPR7 and its ligands (NPB and NPW)

Physiological Role	Genetics: GPR7^{-/-} Mice	Pharmacology: NPB or NPW injections
Body Weight ¹	↑	↓
Food Intake ^{1, 2, 4}	↑	↑, ↓↓
Energy Expenditure ¹	↓	↑
Locomotor Activity ²	↓	↑
Sleep ³	↔	↑
Circadian Rhythm	↔	?
Anxiety	↔	?
Depression	↔	?
Analgesia ²	?	↑
Endocrinology: Prolactin ^{4,5}	?	↑
Endocrinology: Growth Hormone ⁵	?	↓

Genetics refers to the phenotypes observed in GPR7^{-/-} mice. Pharmacology data is from various bolus or continuous ICV administration of either NPB or NPW in rodents. References: ¹Mondal et al., 2003; ²Tanaka et al., 2003; ³Winsky-Sommerer et al., 2003; ⁴Shimomura et al., 2002; ⁵Baker et al., 2003

References

Ahima, R. S., Dushay, J., Flier, S. N., Prabakaran, D., and Flier, J. S. (1997). Leptin accelerates the onset of puberty in normal female mice. *J Clin Invest* 99, 391-395.

Ahima, R. S., and Flier, J. S. (2000). Leptin. *Annu Rev Physiol* 62, 413-437.

Ahima, R. S., Kelly, J., Elmquist, J. K., and Flier, J. S. (1999). Distinct physiologic and neuronal responses to decreased leptin and mild hyperleptinemia. *Endocrinology* 140, 4923-4931.

Ahima, R. S., Prabakaran, D., Mantzoros, C., Qu, D., Lowell, B., Maratos-Flier, E., and Flier, J. S. (1996). Role of leptin in the neuroendocrine response to fasting. *Nature* 382, 250-252.

Allison, D. B., Kaprio, J., Korkeila, M., Koskenvuo, M., Neale, M. C., and Hayakawa, K. (1996). The heritability of body mass index among an international sample of monozygotic twins reared apart. *Int J Obes Relat Metab Disord* 20, 501-506.

Anand, B. K., and Brobeck, J. R. (1951). Localization of a "feeding center" in the hypothalamus of the rat. *Proc Soc Exp Biol Med* 77, 323-324.

Angulo, P. (2002). Nonalcoholic fatty liver disease. *N Engl J Med* 346, 1221-1231.

Asakawa, A., Inui, A., Yuzuriha, H., Ueno, N., Katsuura, G., Fujimiya, M., Fujino, M. A., Nijijima, A., Meguid, M. M., and Kasuga, M. (2003). Characterization of the effects of pancreatic polypeptide in the regulation of energy balance. *Gastroenterology* 124, 1325-1336.

Asnicar, M. A., Smith, D. P., Yang, D. D., Heiman, M. L., Fox, N., Chen, Y. F., Hsiung, H. M., and Koster, A. (2001). Absence of cocaine- and amphetamine-regulated transcript results in obesity in mice fed a high caloric diet. *Endocrinology* 142, 4394-4400.

Bado, A., Levasseur, S., Attoub, S., Kermorgant, S., Laigneau, J. P., Bortoluzzi, M. N., Moizo, L., Lehy, T., Guerre-Millo, M., Le Marchand-Brustel, Y., and Lewin, M. J. (1998). The stomach is a source of leptin. *Nature* 394, 790-793.

Baker, J. R., Cardinal, K., Bober, C., Taylor, M. M., and Samson, W. K. (2003).

Neuropeptide w acts in brain to control prolactin, corticosterone, and growth hormone release. *Endocrinology* 144, 2816-2821.

Bale, T. L., Contarino, A., Smith, G. W., Chan, R., Gold, L. H., Sawchenko, P. E., Koob, G. F., Vale, W. W., and Lee, K. F. (2000). Mice deficient for corticotropin-releasing hormone receptor-2 display anxiety-like behaviour and are hypersensitive to stress. *Nat Genet* 24, 410-414.

Batterham, R. L., Cowley, M. A., Small, C. J., Herzog, H., Cohen, M. A., Dakin, C. L., Wren, A. M., Brynes, A. E., Low, M. J., Ghatei, M. A., *et al.* (2002). Gut hormone PYY(3-36) physiologically inhibits food intake. *Nature* 418, 650-654.

Bjorbaek, C., Elmquist, J. K., Frantz, J. D., Shoelson, S. E., and Flier, J. S. (1998). Identification of SOCS-3 as a potential mediator of central leptin resistance. *Molecular Cell* 1, 619-625.

Bjorbaek, C., Uotani, S., da Silva, B., and Flier, J. S. (1997). Divergent signaling capacities of the long and short isoforms of the leptin receptor. *J Biol Chem* 272, 32686-32695.

Brecher, G., and Waxler, S. M. (1949). Obesity in Albino Mice Due to Single Injections of Goldthioglucose. *Proc Soc Exp Biol Med* 70, 498-501.

Brezillon, S., Lannoy, V., Franssen, J. D., Le Poul, E., Dupriez, V., Lucchetti, J., Detheux, M., and Parmentier, M. (2003). Identification of natural ligands for the orphan G protein-coupled receptors GPR7 and GPR8. *J Biol Chem* 278, 776-783.

Brobeck, J. R. (1947). Food intake as a mechanism of temperature regulation. *Yale J Biol Med* 20, 545.

Brown, J. (1962). Effects of 2-deoxyglucose on carbohydrate metabolism: review of the literature and studies in the rat. *Metabolism* 11, 1098-1112.

Cahill, G. F., Jr., Herrera, M. G., Morgan, A. P., Soeldner, J. S., Steinke, J., Levy, P. L., Reichard, G. A., Jr., and Kipnis, D. M. (1966). Hormone-fuel interrelationships during fasting. *J Clin Invest* 45, 1751-1769.

Campfield, L. A., Smith, F. J., Guisez, Y., Devos, R., and Burn, P. (1995). Recombinant mouse OB protein: evidence for a peripheral signal linking adiposity and central neural

networks. *Science* 269, 546-549.

Carpenter, L. R., Farruggella, T. J., Symes, A., Karow, M. L., Yancopoulos, G. D., and Stahl, N. (1998). Enhancing leptin response by preventing SH2-containing phosphatase 2 interaction with Ob receptor. *Proc Natl Acad Sci U S A* 95, 6061-6066.

Chehab, F. F., Lim, M. E., and Lu, R. (1996). Correction of the sterility defect in homozygous obese female mice by treatment with the human recombinant leptin. *Nat Genet* 12, 318-320.

Chehab, F. F., Mounzih, K., Lu, R., and Lim, M. E. (1997). Early onset of reproductive function in normal female mice treated with leptin. *Science* 275, 88-90.

Chemelli, R. M., Willie, J. T., Sinton, C. M., Elmquist, J. K., Scammell, T., Lee, C., Richardson, J. A., Williams, S. C., Xiong, Y., Kisanuki, Y., *et al.* (1999). Narcolepsy in orexin knockout mice: molecular genetics of sleep regulation. *Cell* 98, 437-451.

Chen, H., Charlat, O., Tartaglia, L. A., Woolf, E. A., Weng, X., Ellis, S. J., Lakey, N. D., Culpepper, J., Moore, K. J., Breitbart, R. E., *et al.* (1996). Evidence that the diabetes gene encodes the leptin receptor: identification of a mutation in the leptin receptor gene in db/db mice. *Cell* 84, 491-495.

Cheung, C. C., Clifton, D. K., and Steiner, R. A. (1997). Proopiomelanocortin neurons are direct targets for leptin in the hypothalamus. *Endocrinology* 138, 4489-4492.

Chua, S. C., Jr., Chung, W. K., Wu-Peng, X. S., Zhang, Y., Liu, S. M., Tartaglia, L., and Leibel, R. L. (1996). Phenotypes of mouse diabetes and rat fatty due to mutations in the OB (leptin) receptor. *Science* 271, 994-996.

Clark, J. T., Kalra, P. S., Crowley, W. R., and Kalra, S. P. (1984). Neuropeptide Y and human pancreatic polypeptide stimulate feeding behavior in rats. *Endocrinology* 115, 427-429.

Cohen, P., Zhao, C., Cai, X., Montez, J. M., Rohani, S. C., Feinstein, P., Mombaerts, P., and Friedman, J. M. (2001). Selective deletion of leptin receptor in neurons leads to obesity. *J Clin Invest* 108, 1113-1121.

Coleman, D., and Hummel, K. (1969). Effects of parabiosis of normal with genetically diabetic mice. *Am J Physiol* 217, 1298-1304.

Coleman, D. L. (1973). Effects of Parabiosis of Obese with Diabetes and Normal Mice. *Diabetologia* 9, 294-298.

Coleman, D. L. (1978). Obese and Diabetes 2 Mutant-Genes Causing Diabetes-Obesity Syndromes in Mice. *Diabetologia* 14, 141-148.

Cone, R. D. (1999). The Central Melanocortin System and Energy Homeostasis. *Trends Endocrinol Metab* 10, 211-216.

Cortright, R. N., and Koves, T. R. (2000). Sex differences in substrate metabolism and energy homeostasis. *Can J Appl Physiol* 25, 288-311.

Crabbe, J. C., Wahlsten, D., and Dudek, B. C. (1999). Genetics of mouse behavior: interactions with laboratory environment. *Science* 284, 1670-1672.

Craig, A. G., Jimenez, E. C., Dykert, J., Nielsen, D. B., Gulyas, J., Abogadie, F. C., Porter, J., Rivier, J. E., Cruz, L. J., Olivera, B. M., and McIntosh, J. M. (1997). A novel post-translational modification involving bromination of tryptophan. Identification of the residue, L-6-bromotryptophan, in peptides from *Conus imperialis* and *Conus radiatus* venom. *J Biol Chem* 272, 4689-4698.

Crawley, J. N. (2000). Emotional Behaviors: Animal Models of Psychiatric Diseases. In *What's Wrong With My Mouse? Behavioral Phenotyping of Transgenic and Knockout Mice* (New York, John Wiley & Sons, Inc.), pp. 179-206.

Cryan, J. F., Markou, A., and Lucki, I. (2002). Assessing antidepressant activity in rodents: recent developments and future needs. *Trends Pharmacol Sci* 23, 238-245.

Debons, A. F., Krimsky, I., From, A., and Cloutier, R. J. (1969). Rapid effects of insulin on the hypothalamic satiety center. *Am J Physiol* 217, 1114-1118.

Debons, A. F., Krimsky, I., From, A., and Pattinian, H. (1974). Phlorizin inhibition of hypothalamic necrosis induced by gold thioglucose. *Am J Physiol* 226, 574-578.

Debons, A. F., Krimsky, I., Likuski, H. J., From, A., and Cloutier, R. J. (1968). Gold thioglucose damage to the satiety center: inhibition in diabetes. *Am J Physiol* 214, 652-658.

Debons, A. F., Krimsky, I., Maayan, M. L., Fani, K., and Jemenez, F. A. (1977). Gold

thioglucose obesity syndrome. *Federation Proceedings* 36, 143-147.

DeCamp, D. L., Thompson, T. M., de Sauvage, F. J., and Lerner, M. R. (2000). Smoothed activates Galphai-mediated signaling in frog melanophores. *J Biol Chem* 275, 26322-26327.

Donahue, R. R., LaGraize, S. C., and Fuchs, P. N. (2001). Electrolytic lesion of the anterior cingulate cortex decreases inflammatory, but not neuropathic nociceptive behavior in rats. *Brain Res* 897, 131-138.

Drews, J. (2000). Drug discovery: a historical perspective. *Science* 287, 1960-1964.

Dun, S. L., Brailoiu, G. C., Yang, J., Chang, J. K., and Dun, N. J. (2003). Neuropeptide W-immunoreactivity in the hypothalamus and pituitary of the rat. *Neurosci Lett* 349, 71-74.

Elias, C. F., Kelly, J. F., Lee, C. E., Ahima, R. S., Drucker, D. J., Saper, C. B., and Elmquist, J. K. (2000). Chemical characterization of leptin-activated neurons in the rat brain. *J Comp Neurol* 423, 261-281.

Elmquist, J. K., Bjorbaek, C., Ahima, R. S., Flier, J. S., and Saper, C. B. (1998). Distributions of leptin receptor mRNA isoforms in the rat brain. *J Comp Neurol* 395, 535-547.

Elmquist, J. K., Elias, C. F., and Saper, C. B. (1999). From lesions to leptin: hypothalamic control of food intake and body weight. *Neuron* 22, 221-232.

Erickson, J. C., Clegg, K. E., and Palmiter, R. D. (1996a). Sensitivity to leptin and susceptibility to seizures of mice lacking neuropeptide Y. *Nature* 381, 415-421.

Erickson, J. C., Hollopeter, G., and Palmiter, R. D. (1996b). Attenuation of the obesity syndrome of ob/ob mice by the loss of neuropeptide Y. *Science* 274, 1704-1707.

Farooqi, I. S., and O'Rahilly, S. (2004). Monogenic human obesity syndromes. *Recent Prog Horm Res* 59, 409-424.

Fei, H., Okano, H. J., Li, C., Lee, G. H., Zhao, C., Darnell, R., and Friedman, J. M. (1997). Anatomic localization of alternatively spliced leptin receptors (Ob-R) in mouse brain and other tissues. *Proc Natl Acad Sci U S A* 94, 7001-7005.

- Fisher, B. L., and Schauer, P. (2002). Medical and surgical options in the treatment of severe obesity. *Am J Surg* 184, 9S-16S.
- Flegal, K. M., Carroll, M. D., Ogden, C. L., and Johnson, C. L. (2002). Prevalence and trends in obesity among US adults, 1999-2000. *JAMA* 288, 1723-1727.
- Friedman, J. M., and Halaas, J. L. (1998). Leptin and the regulation of body weight in mammals. *Nature* 395, 763-770.
- Friedman, J. M., and Leibel, R. L. (1992). Tackling a Weighty Problem. *Cell* 69, 217-220.
- Fujii, R., Yoshida, H., Fukusumi, S., Habata, Y., Hosoya, M., Kawamata, Y., Yano, T., Hinuma, S., Kitada, C., Asami, T., *et al.* (2002). Identification of a neuropeptide modified with bromine as an endogenous ligand for GPR7. *J Biol Chem* 277, 34010-34016.
- Hahn, T. M., Breininger, J. F., Baskin, D. G., and Schwartz, M. W. (1998). Coexpression of *Agrp* and *NPY* in fasting-activated hypothalamic neurons. *Nat Neurosci* 1, 271-272.
- Halaas, J. L., Boozer, C., Blair-West, J., Fidahusein, N., Denton, D. A., and Friedman, J. M. (1997). Physiological response to long-term peripheral and central leptin infusion in lean and obese mice. *Proc Natl Acad Sci U S A* 94, 8878-8883.
- Halaas, J. L., Gajiwala, K. S., Maffei, M., Cohen, S. L., Chait, B. T., Rabinowitz, D., Lallone, R. L., Burley, S. K., and Friedman, J. M. (1995). Weight-reducing effects of the plasma protein encoded by the obese gene. *Science* 269, 543-546.
- Hara, J., Beuckmann, C. T., Nambu, T., Willie, J. T., Chemelli, R. M., Sinton, C. M., Sugiyama, F., Yagami, K., Goto, K., Yanagisawa, M., and Sakurai, T. (2001). Genetic ablation of orexin neurons in mice results in narcolepsy, hypophagia, and obesity. *Neuron* 30, 345-354.
- Havel, P. J. (2004). Update on adipocyte hormones: regulation of energy balance and carbohydrate/lipid metabolism. *Diabetes* 53 Suppl 1, S143-151.
- Heine, P. A., Taylor, J. A., Iwamoto, G. A., Lubahn, D. B., and Cooke, P. S. (2000). Increased adipose tissue in male and female estrogen receptor-alpha knockout mice. *Proc Natl Acad Sci U S A* 97, 12729-12734.
- Heisler, L. K., Cowley, M. A., Tecott, L. H., Fan, W., Low, M. J., Smart, J. L., Rubinstein,

- M., Tatro, J. B., Marcus, J. N., Holstege, H., *et al.* (2002). Activation of central melanocortin pathways by fenfluramine. *Science* 297, 609-611.
- Hervey, G. R. (1959). The effects of lesions in the hypothalamus in parabiotic rats. *J Physiol* 145, 336-352.
- Hetherington, A. W., and Ranson, S. W. (1940). Hypothalamic lesions and adiposity in the rat. *Anat Rec* 78, 149-172.
- Hileman, S. M., Pierroz, D. D., Masuzaki, H., Bjorbaek, C., El-Haschimi, K., Banks, W. A., and Flier, J. S. (2002). Characterization of short isoforms of the leptin receptor in rat cerebral microvessels and of brain uptake of leptin in mouse models of obesity. *Endocrinology* 143, 775-783.
- Horton, R. W., Meldrum, B. S., and Bachelard, H. S. (1973). Enzymic and cerebral metabolic effects of 2-deoxy-D-glucose. *J Neurochem* 21, 507-520.
- Hummel, K. P., Dickie, M. M., and Coleman, D. L. (1966). Diabetes, a new mutation in the mouse. *Science* 153, 1127-1128.
- Huszar, D., Lynch, C. A., Fairchild-Huntress, V., Dunmore, J. H., Fang, Q., Berkemeier, L. R., Gu, W., Kesterson, R. A., Boston, B. A., Cone, R. D., *et al.* (1997). Targeted disruption of the melanocortin-4 receptor results in obesity in mice. *Cell* 88, 131-141.
- Ingalls, A. M., Dickie, M. M., and Snell, G. D. (1950). Obese, a new mutation in the house mouse. *J Hered* 41, 317-318.
- Jimenez, E. C., Craig, A. G., Watkins, M., Hillyard, D. R., Gray, W. R., Gulyas, J., Rivier, J. E., Cruz, L. J., and Olivera, B. M. (1997). Bromocontryphan: post-translational bromination of tryptophan. *Biochemistry* 36, 989-994.
- Jones, B. E. (1998). The neural basis of consciousness across the sleep-waking cycle. *Adv Neurol* 77, 75-94.
- Jones, M. E., Thorburn, A. W., Britt, K. L., Hewitt, K. N., Wreford, N. G., Proietto, J., Oz, O. K., Leury, B. J., Robertson, K. M., Yao, S., and Simpson, E. R. (2000). Aromatase-deficient (ArKO) mice have a phenotype of increased adiposity. *Proc Natl Acad Sci U S A* 97, 12735-12740.

Kalarchian, M. A., Marcus, M. D., Wilson, G. T., Labouvie, E. W., Brolin, R. E., and LaMarca, L. B. (2002). Binge eating among gastric bypass patients at long-term follow-up. *Obes Surg* 12, 270-275.

Kennedy, G. C. (1953). The role of the depot fat in the hypothalamic control of food intake in the rat. *Proc R Soc Lond B Biol Sci* 140, 578-592.

King, D. P., and Takahashi, J. S. (2000). Molecular genetics of circadian rhythms in mammals. *Annu Rev Neurosci* 23, 713-742.

Kishimoto, T., Radulovic, J., Radulovic, M., Lin, C. R., Schrick, C., Hooshmand, F., Hermanson, O., Rosenfeld, M. G., and Spiess, J. (2000). Deletion of *crhr2* reveals an anxiolytic role for corticotropin-releasing hormone receptor-2. *Nat Genet* 24, 415-419.

Kojima, M., Hosoda, H., Date, Y., Nakazato, M., Matsuo, H., and Kangawa, K. (1999). Ghrelin is a growth-hormone-releasing acylated peptide from stomach. *Nature* 402, 656-660.

Kopelman, P. G. (2000). Obesity as a medical problem. *Nature* 404, 635-643.

Kopin, A. S., Mathes, W. F., McBride, E. W., Nguyen, M., Al-Haider, W., Schmitz, F., Bonner-Weir, S., Kanarek, R., and Beinborn, M. (1999). The cholecystokinin-A receptor mediates inhibition of food intake yet is not essential for the maintenance of body weight. *J Clin Invest* 103, 383-391.

Kristensen, P., Judge, M. E., Thim, L., Ribel, U., Christjansen, K. N., Wulff, B. S., Clausen, J. T., Jensen, P. B., Madsen, O. D., Vrang, N., *et al.* (1998). Hypothalamic CART is a new anorectic peptide regulated by leptin. *Nature* 393, 72-76.

Lee, D. K., Nguyen, T., Porter, C. A., Cheng, R., George, S. R., and O'Dowd, B. F. (1999). Two related G protein-coupled receptors: The distribution of GPR7 in rat brain and the absence of GPR8 in rodents. *Mol Brain Res* 71, 96-103.

Lee, G. H., Proenca, R., Montez, J. M., Carroll, K. M., Darvishzadeh, J. G., Lee, J. I., and Friedman, J. M. (1996). Abnormal splicing of the leptin receptor in diabetic mice. *Nature* 379, 632-635.

Lerner, M. R. (1994). Tools for investigating functional interactions between ligands and G-protein-coupled receptors. *Trends Neurosci* 17, 142-146.

Levin, N., Nelson, C., Gurney, A., Vandlen, R., and de Sauvage, F. (1996). Decreased food intake does not completely account for adiposity reduction after ob protein infusion. *Proc Natl Acad Sci U S A* 93, 1726-1730.

Li, C., and Friedman, J. M. (1999). Leptin receptor activation of SH2 domain containing protein tyrosine phosphatase 2 modulates Ob receptor signal transduction. *Proc Natl Acad Sci U S A* 96, 9677-9682.

Likuski, H. J., Debons, A. F., and Cloutier, R. J. (1967). Inhibition of gold thioglucose-induced hypothalamic obesity by glucose analogues. *Am J Physiol* 212, 669-676.

Lin, L., Faraco, J., Li, R., Kadotani, H., Rogers, W., Lin, X., Qiu, X., de Jong, P. J., Nishino, S., and Mignot, E. (1999). The sleep disorder canine narcolepsy is caused by a mutation in the hypocretin (orexin) receptor 2 gene. *Cell* 98, 365-376.

Liu, C., Liu, X. J., Barry, G., Ling, N., Maki, R. A., and De Souza, E. B. (1997). Expression and characterization of a putative high affinity human soluble leptin receptor. *Endocrinology* 138, 3548-3554.

Liu, H., Kishi, T., Roseberry, A. G., Cai, X., Lee, C. E., Montez, J. M., Friedman, J. M., and Elmquist, J. K. (2003). Transgenic mice expressing green fluorescent protein under the control of the melanocortin-4 receptor promoter. *J Neurosci* 23, 7143-7154.

Lowell, B. B., and Bachman, E. S. (2003). Beta-Adrenergic receptors, diet-induced thermogenesis, and obesity. *J Biol Chem* 278, 29385-29388.

Lucki, I. (1997). The forced swimming test as a model for core and component behavioral effects of antidepressant drugs. *Behav Pharmacol* 8, 523-532.

Lucki, I., Dalvi, A., and Mayorga, A. J. (2001). Sensitivity to the effects of pharmacologically selective antidepressants in different strains of mice. *Psychopharmacology (Berl)* 155, 315-322.

Maffei, M., Halaas, J., Ravussin, E., Pratley, R. E., Lee, G. H., Zhang, Y., Fei, H., Kim, S., Lallone, R., Ranganathan, S., *et al.* (1995). Leptin levels in human and rodent: measurement of plasma leptin and ob RNA in obese and weight-reduced subjects. *Nat Med* 1, 1155-1161.

- Marsh, D. J., Hollopeter, G., Kafer, K. E., and Palmiter, R. D. (1998). Role of the Y5 neuropeptide Y receptor in feeding and obesity. *Nat Med* 4, 718-721.
- Marshall, N. B., Barnett, R. J., and Mayer, J. (1955). Hypothalamic Lesions in Goldthioglucose Injected Mice. *Proc Soc Exp Biol Med* 90, 240-244.
- Masuzaki, H., Ogawa, Y., Sagawa, N., Hosoda, K., Matsumoto, T., Mise, H., Nishimura, H., Yoshimasa, Y., Tanaka, I., Mori, T., and Nakao, K. (1997). Nonadipose tissue production of leptin: leptin as a novel placenta-derived hormone in humans. *Nat Med* 3, 1029-1033.
- Mayer, J. (1953). Glucostatic mechanism of regulation of food intake. *N Engl J Med* 249, 13-16.
- Mayer, J. (1955). Regulation of energy intake and the body weight: the glucostatic theory and the lipostatic hypothesis. *Ann N Y Acad Sci* 63, 15-43.
- Mayer, J., and Marshall, N. B. (1956). Specificity of Gold Thioglucose for Ventromedial Hypothalamic Lesions and Hyperphagia. *Nature* 178, 1399-1400.
- Mayer, J., and Thomas, D. W. (1967). Regulation of Food Intake and Obesity. *Science* 156, 328-337.
- McElroy, S. L., Kotwal, R., Malhotra, S., Nelson, E. B., Keck, P. E., and Nemeroff, C. B. (2004). Are mood disorders and obesity related? A review for the mental health professional. *J Clin Psychiatry* 65, 634-651, quiz 730.
- McGregor, G. P., Desaga, J. F., Ehlenz, K., Fischer, A., Heese, F., Hegele, A., Lammer, C., Peiser, C., and Lang, R. E. (1996). Radiommunological measurement of leptin in plasma of obese and diabetic human subjects. *Endocrinology* 137, 1501-1504.
- Mercer, J. G., Hoggard, N., Williams, L. M., Lawrence, C. B., Hannah, L. T., and Trayhurn, P. (1996). Localization of leptin receptor mRNA and the long form splice variant (Ob-Rb) in mouse hypothalamus and adjacent brain regions by in situ hybridization. *FEBS Letters* 387, 113-116.
- Miselis, R. R., and Epstein, A. N. (1975). Feeding induced by intracerebroventricular 2-deoxy-D-glucose in the rat. *Am J Physiol* 229, 1438-1447.

- Mokdad, A. H., Marks, J. S., Stroup, D. F., and Gerberding, J. L. (2004). Actual causes of death in the United States, 2000. *JAMA* 291, 1238-1245.
- Mondal, M. S., Yamaguchi, H., Date, Y., Shimbara, T., Toshinai, K., Shimomura, Y., Mori, M., and Nakazato, M. (2003). A role for neuropeptide W in the regulation of feeding behavior. *Endocrinology* 144, 4729-4733.
- Muglia, L., Jacobson, L., Dikkes, P., and Majzoub, J. A. (1995). Corticotropin-releasing hormone deficiency reveals major fetal but not adult glucocorticoid need. *Nature* 373, 427-432.
- Myers, M. G., Jr. (2004). Leptin receptor signaling and the regulation of mammalian physiology. *Recent Prog Horm Res* 59, 287-304.
- Naeser, P. (1973). Effects of adrenalectomy on the obese-hyperglycemic syndrome in mice (gene symbol ob). *Diabetologia* 9, 376-379.
- Nakazato, M., Murakami, N., Date, Y., Kojima, M., Matsuo, H., Kangawa, K., and Matsukura, S. (2001). A role for ghrelin in the central regulation of feeding. *Nature* 409, 194-198.
- Nandi, A., Kitamura, Y., Kahn, C. R., and Accili, D. (2004). Mouse models of insulin resistance. *Physiol Rev* 84, 623-647.
- Naveilhan, P., Hassani, H., Canals, J. M., Ekstrand, A. J., Larefalk, A., Chhajlani, V., Arenas, E., Gedda, K., Svensson, L., Thoren, P., and Ernfors, P. (1999). Normal feeding behavior, body weight and leptin response require the neuropeptide Y Y2 receptor. *Nat Med* 5, 1188-1193.
- Nestler, E. J., Barrot, M., DiLeone, R. J., Eisch, A. J., Gold, S. J., and Monteggia, L. M. (2002). Neurobiology of depression. *Neuron* 34, 13-25.
- Nestler, E. J., Hyman, S. E., and Malenka, R. C. (2001). Mood and Emotion. In *Molecular Neuropharmacology: A Foundation for Clinical Neuroscience* (New York, McGraw-Hill), pp. 327-354.
- Nonogaki, K., Strack, A. M., Dallman, M. F., and Tecott, L. H. (1998). Leptin-independent hyperphagia and type 2 diabetes in mice with a mutated serotonin 5-HT_{2C} receptor gene. *Nat Med* 4, 1152-1156.

O'Dowd, B. F., Scheideler, M. A., Nguyen, T., Cheng, R., Rasmussen, J. S., Marchese, A., Zastawny, R., Heng, H. H. Q., Tsui, L. C., Shi, X. M., *et al.* (1995). The Cloning and Chromosomal Mapping of 2 Novel Human Opioid- Somatostatin-Like Receptor Genes, *Gpr7* and *Gpr8*, Expressed in Discrete Areas of the Brain. *Genomics* 28, 84-91.

Ohki-Hamazaki, H., Watase, K., Yamamoto, K., Ogura, H., Yamano, M., Yamada, K., Maeno, H., Imaki, J., Kikuyama, S., Wada, E., and Wada, K. (1997). Mice lacking bombesin receptor subtype-3 develop metabolic defects and obesity. *Nature* 390, 165-169.

Ollmann, M. M., Wilson, B. D., Yang, Y. K., Kerns, J. A., Chen, Y., Gantz, I., and Barsh, G. S. (1997). Antagonism of central melanocortin receptors in vitro and in vivo by agouti-related protein. *Science* 278, 135-138.

Oomura, Y. (1983). Glucose as a regulator of neuronal activity. *Adv Metab Disord* 10, 31-65.

Paxinos, G., and Franklin, K. B. J. (2001). *The Mouse Brain in Stereotaxic Coordinates* (San Diego, Academic Press).

Pedrazzini, T., Seydoux, J., Kunstner, P., Aubert, J. F., Grouzmann, E., Beermann, F., and Brunner, H. R. (1998). Cardiovascular response, feeding behavior and locomotor activity in mice lacking the NPY Y1 receptor. *Nat Med* 4, 722-726.

Peeke, P. M., and Chrousos, G. P. (1995). Hypercortisolism and obesity. *Ann N Y Acad Sci* 771, 665-676.

Pelleymounter, M. A., Cullen, M. J., Baker, M. B., Hecht, R., Winters, D., Boone, T., and Collins, F. (1995). Effects of the obese gene product on body weight regulation in ob/ob mice. *Science* 269, 540-543.

Poggioli, R., Vergoni, A. V., and Bertolini, A. (1986). ACTH-(1-24) and alpha-MSH antagonize feeding behavior stimulated by kappa opiate agonists. *Peptides* 7, 843-848.

Porsolt, R. D., Bertin, A., and Jalfre, M. (1977a). Behavioral despair in mice: a primary screening test for antidepressants. *Arch Int Pharmacodyn Ther* 229, 327-336.

Porsolt, R. D., Le Pichon, M., and Jalfre, M. (1977b). Depression: a new animal model sensitive to antidepressant treatments. *Nature* 266, 730-732.

Qian, S., Chen, H., Weingarh, D., Trumbauer, M. E., Novi, D. E., Guan, X., Yu, H., Shen, Z., Feng, Y., Frazier, E., *et al.* (2002). Neither agouti-related protein nor neuropeptide Y is critically required for the regulation of energy homeostasis in mice. *Mol Cell Biol* 22, 5027-5035.

Qu, D., Ludwig, D. S., Gammeltoft, S., Piper, M., Pelleymounter, M. A., Cullen, M. J., Mathes, W. F., Przypek, R., Kanarek, R., and Maratos-Flier, E. (1996). A role for melanin-concentrating hormone in the central regulation of feeding behaviour. *Nature* 380, 243-247.

Rangwala, S. M., and Lazar, M. A. (2000). Transcriptional control of adipogenesis. *Annu Rev Nutr* 20, 535-559.

Read, N., French, S., and Cunningham, K. (1994). The role of the gut in regulating food intake in man. *Nutr Rev* 52, 1-10.

Refinetti, R. (1993). Laboratory instrumentation and computing: comparison of six methods for the determination of the period of circadian rhythms. *Physiol Behav* 54, 869-875.

Reizes, O., Lincecum, J., Wang, Z., Goldberger, O., Huang, L., Kaksonen, M., Ahima, R., Hinkes, M. T., Barsh, G. S., Rauvala, H., and Bernfield, M. (2001). Transgenic expression of syndecan-1 uncovers a physiological control of feeding behavior by syndecan-3. *Cell* 106, 105-116.

Ritter, R. C., Roelke, M., and Neville, M. (1978). Glucoprivic feeding behavior in absence of other signs of glucoprivation. *Am J Physiol* 234, E617-621.

Romeo, R. D., Mueller, A., Sisti, H. M., Ogawa, S., McEwen, B. S., and Brake, W. G. (2003). Anxiety and fear behaviors in adult male and female C57BL/6 mice are modulated by maternal separation. *Horm Behav* 43, 561-567.

Rutter, J., Reick, M., and McKnight, S. L. (2002). Metabolism and the control of circadian rhythms. *Annu Rev Biochem* 71, 307-331.

Sakurai, T., Amemiya, A., Ishii, M., Matsuzaki, I., Chemelli, R. M., Tanaka, H., Williams, S. C., Richardson, J. A., Kozlowski, G. P., Wilson, S., *et al.* (1998). Orexins and orexin receptors: a family of hypothalamic neuropeptides and G protein-coupled receptors that regulate feeding behavior. *Cell* 92, 573-585.

Salton, S. R. J., Hahm, S., and Mizuno, T. M. (2000). Of MICE and MEN: What transgenic models tell us about hypothalamic control of energy balance. *Neuron* 25, 265-268.

Saunders, R. (2001). Compulsive eating and gastric bypass surgery: what does hunger have to do with it? *Obes Surg* 11, 757-761.

Saunders, R. (2004). "Grazing": a high-risk behavior. *Obes Surg* 14, 98-102.

Schwartz, M. W., Dallman, M. F., and Woods, S. C. (1995). Hypothalamic response to starvation: implications for the study of wasting disorders. *Am J Physiol* 269, R949-957.

Schwartz, M. W., and Seeley, R. J. (1997). Seminars in medicine of the Beth Israel Deaconess Medical Center. Neuroendocrine responses to starvation and weight loss. *N Engl J Med* 336, 1802-1811.

Schwartz, M. W., Woods, S. C., Porte, D., Jr., Seeley, R. J., and Baskin, D. G. (2000). Central nervous system control of food intake. *Nature* 404, 661-671.

Scrocchi, L. A., Hill, M. E., Saleh, J., Perkins, B., and Drucker, D. J. (2000). Elimination of glucagon-like peptide 1R signaling does not modify weight gain and islet adaptation in mice with combined disruption of leptin and GLP-1 action. *Diabetes* 49, 1552-1560.

Shimada, M., Tritos, N. A., Lowell, B. B., Flier, J. S., and Maratos-Flier, E. (1998). Mice lacking melanin-concentrating hormone are hypophagic and lean. *Nature* 396, 670-674.

Shimomura, Y., Bray, G. A., and Lee, M. (1987). Adrenalectomy and steroid treatment in obese (ob/ob) and diabetic (db/db) mice. *Horm Metab Res* 19, 295-299.

Shimomura, Y., Harada, M., Goto, M., Sugo, T., Matsumoto, Y., Abe, M., Watanabe, T., Asami, T., Kitada, C., Mori, M., *et al.* (2002). Identification of neuropeptide W as the endogenous ligand for orphan G-protein-coupled receptors GPR7 and GPR8. *J Biol Chem* 277, 35826-35832.

Sims, E. A., and Horton, E. S. (1968). Endocrine and metabolic adaptation to obesity and starvation. *Am J Clin Nutr* 21, 1455-1470.

Smith, G. P., and Epstein, A. N. (1969). Increased feeding in response to decreased glucose utilization in the rat and monkey. *Am J Physiol* 217, 1083-1087.

- Smith, G. W., Aubry, J. M., Dellu, F., Contarino, A., Bilezikjian, L. M., Gold, L. H., Chen, R., Marchuk, Y., Hauser, C., Bentley, C. A., *et al.* (1998). Corticotropin releasing factor receptor 1-deficient mice display decreased anxiety, impaired stress response, and aberrant neuroendocrine development. *Neuron* 20, 1093-1102.
- Sokolove, P. G., and Bushell, W. N. (1978). The chi square periodogram: its utility for analysis of circadian rhythms. *J Theor Biol* 72, 131-160.
- Solomon, J., and Mayer, J. (1973). The effect of adrenalectomy on the development of the obese-hyperglycemic syndrome in ob-ob mice. *Endocrinology* 93, 510-512.
- Soukas, A., Cohen, P., Socci, N. D., and Friedman, J. M. (2000). Leptin-specific patterns of gene expression in white adipose tissue. *Genes Dev* 14, 963-980.
- Steckler, T., and Holsboer, F. (1999). Corticotropin-releasing hormone receptor subtypes and emotion. *Biol Psychiatry* 46, 1480-1508.
- Stunkard, A. J., Foch, T. T., and Hrubec, Z. (1986). A twin study of human obesity. *Jama* 256, 51-54.
- Stunkard, A. J., Harris, J. R., Pedersen, N. L., and McClearn, G. E. (1990). The body-mass index of twins who have been reared apart. *N Engl J Med* 322, 1483-1487.
- Sun, Y., Ahmed, S., and Smith, R. G. (2003). Deletion of ghrelin impairs neither growth nor appetite. *Mol Cell Biol* 23, 7973-7981.
- Tanaka, H., Yoshida, T., Miyamoto, N., Motoike, T., Kurosu, H., Shibata, K., Yamanaka, A., Williams, S. C., Richardson, J. A., Tsujino, N., *et al.* (2003). Characterization of a family of endogenous neuropeptide ligands for the G protein-coupled receptors GPR7 and GPR8. *Proc Natl Acad Sci U S A* 100, 6251-6256.
- Tartaglia, L. A., Dembski, M., Weng, X., Deng, N., Culpepper, J., Devos, R., Richards, G. J., Campfield, L. A., Clark, F. T., and Deeds, J. (1995). Identification and expression cloning of a leptin receptor, OB-R. *Cell* 83, 1263-1271.
- Taubes, G. (1998). Obesity: How Big a Problem? *Science* 280, 1364-1368.
- Tschop, M., Smiley, D. L., and Heiman, M. L. (2000). Ghrelin induces adiposity in rodents. *Nature* 407, 908-913.

- Uotani, S., Bjorbaek, C., Tornoe, J., and Flier, J. S. (1999). Functional properties of leptin receptor isoforms: internalization and degradation of leptin and ligand-induced receptor downregulation. *Diabetes* 48, 279-286.
- Vaisse, C., Halaas, J. L., Horvath, C. M., Darnell, J. E., Stoffel, M., and Friedman, J. M. (1996). Leptin activation of Stat3 in the hypothalamus of wild-type and ob/ob mice but not db/db mice. *Nat Genet* 14, 95-97.
- van Esseveldt, K. E., Lehman, M. N., and Boer, G. J. (2000). The suprachiasmatic nucleus and the circadian time-keeping system revisited. *Brain Res Brain Res Rev* 33, 34-77.
- Varshavsky, A. (1996). The N-end rule: functions, mysteries, uses. *Proc Natl Acad Sci U S A* 93, 12142-12149.
- Wadden, T. A. (1993). Treatment of Obesity by Moderate and Severe Caloric Restriction: Results of Clinical Research Trials. *Ann Intern Med* 119, 688-693.
- Walker, D. L., Toufexis, D. J., and Davis, M. (2003). Role of the bed nucleus of the stria terminalis versus the amygdala in fear, stress, and anxiety. *Eur J Pharmacol* 463, 199-216.
- Wallenius, V., Wallenius, K., Ahren, B., Rudling, M., Carlsten, H., Dickson, S. L., Ohlsson, C., and Jansson, J. O. (2002). Interleukin-6-deficient mice develop mature-onset obesity. *Nat Med* 8, 75-79.
- Wang, J., Liu, R., Hawkins, M., Barzilai, N., and Rossetti, L. (1998). A nutrient-sensing pathway regulates leptin gene expression in muscle and fat. *Nature* 393, 684-688.
- Willie, J. T., Chemelli, R. M., Sinton, C. M., Tokita, S., Williams, S. C., Kisanuki, Y. Y., Marcus, J. N., Lee, C., Elmquist, J. K., Kohlmeier, K. A., *et al.* (2003). Distinct Narcolepsy Syndromes in Orexin Receptor-2 and Orexin Null Mice. Molecular Genetic Dissection of Non-REM and REM Sleep Regulatory Processes. *Neuron* 38, 715-730.
- Winsky-Sommerer, R., Huitron-Resendiz, S., Sanchez-Alavez, M., Slaght, K., Henriksen, S. J., Criado, J. R., and de Lecea, L. (2003). Effect of the endogenous GPR7/8 ligand (neuropeptide W) on sleep/wakefulness. *Sleep* 26, A49-A49.
- Wise, A., Jupe, S. C., and Rees, S. (2004). The identification of ligands at orphan G-protein coupled receptors. *Annu Rev Pharmacol Toxicol* 44, 43-66.

Wright, P., and Turner, C. (1973). Sex differences in body weight following gonadectomy and goldthioglucose injections in mice. *Physiol Behav* *11*, 155-159.

Wu, W., Samoszuk, M. K., Comhair, S. A., Thomassen, M. J., Farver, C. F., Dweik, R. A., Kavuru, M. S., Erzurum, S. C., and Hazen, S. L. (2000). Eosinophils generate brominating oxidants in allergen-induced asthma. *J Clin Invest* *105*, 1455-1463.

Yang, X. D. W., Model, P., and Heintz, N. (1997). Homologous recombination based modification in *Escherichia coli* and germline transmission in transgenic mice of a bacterial artificial chromosome. *Nat Biotechnol* *15*, 859-865.

Yaswen, L., Diehl, N., Brennan, M. B., and Hochgeschwender, U. (1999). Obesity in the mouse model of pro-opiomelanocortin deficiency responds to peripheral melanocortin. *Nat Med* *5*, 1066-1070.

Zhang, Y. Y., Proenca, R., Maffei, M., Barone, M., Leopold, L., and Friedman, J. M. (1994). Positional Cloning of the Mouse Obese Gene and Its Human Homolog. *Nature* *372*, 425-432.

Zhou, Z., Yon Toh, S., Chen, Z., Guo, K., Ng, C. P., Ponniah, S., Lin, S. C., Hong, W., and Li, P. (2003). Cidea-deficient mice have lean phenotype and are resistant to obesity. *Nat Genet* *35*, 49-56.